

## Table of Contents

Appendix A: Wartsila 3rd Party OSV Information.....	2
Appendix B: VLCC maneuvering trials and modeling .....	8
Appendix C: Hose Length Calculations .....	59
Appendix D: ABS Guidance notes on Qualifying New Technologies .....	62
Appendix E: Detonation Arrester.....	90
Appendix F: Detonation Arrester on a CALM Buoy .....	92
Appendix G: USCG Policy Letter 2-16 .....	94
Appendix H: Modeling .....	99
Appendix I: Coast Guard Authorized Certifying Entities for Facility Vapor Control Systems.....	112
Appendix J: Texas GulfLink Deepwater Port Vapor Recovery Line Profile.....	119
Appendix K: Correspondence .....	121
Appendix L: Riverhead NY, United Riverhead Terminal Document.....	126
Appendix M: API Flame Arresters.....	130
Appendix N: TGL Operating Weather Limits.....	133
Appendix O: El Segundo Marine Terminal, CA – San Pedro Vapor Barge.....	135

# Appendix A: Wartsila 3rd Party OSV Information

REDACTED

REDACTED



REDACTED

REDACTED

REDACTED

# Appendix B: VLCC maneuvering trials and modeling



*Esso Osaka* during full left rudder turn; medium water depth site, Gulf of Mexico

## Maneuvering Trials of a 278 000-DWT Tanker in Shallow and Deep Waters

C. Lincoln Crane, Jr.,<sup>1</sup> Member

Maneuvering trials of the 278 000-dwt *Esso Osaka* were made in two shallow-water and one deep-water site in the Gulf of Mexico during July/August 1977 as a cooperative effort of the U. S. Maritime Administration, the U. S. Coast Guard, and the American Institute of Merchant Shipping. A principal objective of these trials was to develop data for improving the quality of computer simulations of shiphandling for training shiphandlers and for research and design. Other objectives were to provide data needed for the development of deepwater port safety zones and to aid in the development of maneuvering information for mariners aboard ship. The trials satisfied all of the objectives and demonstrated additionally that a typical VLCC can maneuver reliably and predictably under the realistic-type conditions that were tested. They also showed that industry and government, working together, can produce fruitful results toward improving navigational safety and protecting the environment.

<sup>1</sup> Engineering Associate, Exxon International, Florham Park, NJ.

Presented at the Annual Meeting, New York, N. Y., November 15-17, 1979, of THE SOCIETY OF NAVAL ARCHITECTS AND MARINE ENGINEERS.

The opinions expressed herein are those of the author and do not necessarily reflect those of the trial program sponsors or the contractor.

## Introduction

### Background

INTEREST in ship controllability has increased sharply in the past few years. While laymen mainly question the size and controllability of large tankers, experienced operators are equally concerned with the unique features affecting controllability of large container ships, liquefied gas ships and other vessels.

During the same few years, special facilities for analyzing and predicting ship controllability have been developed which apply to all types and sizes of vessels. Improvements of mathematical ship maneuvering models have resulted from accelerated work on maneuvering theory, captive model tests and calculation capabilities. Taking advantage of these developments, real-time shiphandling simulators, such as at Wageningen and Delft in The Netherlands, the Swedish State Shipbuilding Experimental Tank (SSPA) and CAORF,<sup>2</sup> have been built, permitting research studies of the interactions among the key parts of overall ship/waterway control systems, including human factors. However, most simulators are now dedicated to use as training devices for ships' officers and pilots. In other work, hydraulic models of segments of particular waterways have been built which incorporate manned self-propelled ship models. These also are used in both shiphandler training and in controllability studies such as at Grenoble, France; The Netherlands Ship Model Basin (NSMB); the University of Michigan, and Vicksburg. With these tools available, the complex relationships existing between vessel, waterway, environment, aids-to-navigation, shipboard navigation aids, operating rules and the shiphandler are now subject to study and better understanding.

Maneuvering mathematical models are based on Newton's equations of motion, and incorporate such physical factors as ship's mass and fluid forces acting on hull, propeller and rudder, together with wind forces and the influences of shallow water, channel sides and water currents ([1-4]<sup>3</sup> and similar sources). Because several of the complex factors affecting maneuvers are represented using scale-model data and theories containing assumptions, it is essential that mathematical models be validated through comparison of predicted results with carefully planned and executed full-scale maneuvering trials.

Unfortunately, in the case of shallow-water maneuvering, few data are available for this purpose [5, 6]. In view of this, and with the knowledge that the most important maneuvers of large ships such as tankers occur in shallow water, the U. S. Maritime Administration (MarAd), the U. S. Coast Guard and the American Institute of Merchant Shipping joined together to sponsor a comprehensive shallow-water maneuvering trial program in the Gulf of Mexico off Freeport, Texas. Appendix 1 lists contributing organizations. The trials were conducted under the management of Exxon International Company Tanker Department in late July and early August 1977, using the 278 000-dwt turbine tanker *Esso Osaka*. Other organizations assisting in the planning, execution and data processing are also listed in Appendix 1.

### Objectives

The objectives of the trials were:

1. To develop full-scale ship trial data which will provide a major improvement in the quality of simulations of ship maneuvering behavior, particularly in shallow water.
2. To develop information leading to a better understanding

of model scale effects on ship maneuvering predictions.

3. To improve the data upon which the size and configuration of deepwater port safety zones are based.

4. To provide data upon which to base shiphandling maneuvering information for ships' watchkeeping officers and pilots.

### Summary

The trials were conducted in shallow and deep waters providing 20, 50 and 320 percent bottom clearance, and showed the following main results: With 20 percent bottom clearance, turning-circle tactical diameter increased as much as 75 percent over the deepwater result. With 50 percent clearance, the increase was less than 20 percent, directionally confirming earlier model predictions. The ship's checking and counterturning ability was reduced in intermediate water depth, but was increased in shallow water.

The main shallow-water effect on stopping from slow speed was an increase in yaw rotation to the right as the ship came to a halt (increasing to almost 90 deg, with 20 percent bottom clearance). As expected, rudder control was eventually lost during stopping with sustained astern rpm, although heading could be controlled to some extent by early rudder action. In the "controlled" stop, where desired heading had priority over stopping distance, and rpm was controlled, the heading could be maintained almost constant, although this was at the expense of significantly increased stopping distance.

Perhaps the principal finding of the trials, in terms of maneuvering safety, was that steering control could be maintained in all three water depths at speeds as low as 1.5 knots, even with the engine stopped. This was demonstrated by the coasting turns and coasting Z-maneuvers; that is, checking and counterturning ability was preserved down to this slow speed in the coasting Z-maneuver. Accelerating turns quantified the advantage of "kicking ahead" with the engine to expedite a turn from stopped condition. The coasting maneuvers and the accelerating turns, taken together, confirmed what is already known by good shiphandlers, that is, that maneuverability is improved when rpm is quickly increased, and reduced when rpm is rapidly decreased. Because of this, a prudent shiphandler will navigate in tight quarters at the slowest safe speed. Then, if required to increase speed he will gain control, rather than risk losing it if required to slow down.

Other trial data covered the effects of speed of approach, propeller asymmetry and water currents. Very precise readings of selected additional maneuvers were also made for use in researching "systems identification" methods for determining hydrodynamic coefficients of the mathematical maneuvering model.

### Trial preparations

#### Ship selection

A very large crude carrier (VLCC) was selected for the maneuvering trials, recognizing the expected important model-to-ship scale effects due to large differences in Reynolds numbers (reflecting large differences in ratios of fluid inertial to viscous forces) and the modern and extensive navigation equipment found aboard VLCCs, often including double-axis Doppler sonar speed sensors. The latter was useful as part of the trial instrumentation. Other points in favor of selecting a VLCC were the anticipated construction of deepwater ports in the coastal waters of the United States, the large worldwide population of VLCCs, and the concern within some segments of the public over the ability of large single-screw VLCCs to

<sup>2</sup> Computer Aided Operations Research Facility, located at the U. S. Merchant Marine Academy at Kings Point, New York.

<sup>3</sup> Numbers in brackets designate References at end of paper.

maneuver reliably and predictably, especially in shallow water.

*Esso Osaka* satisfied all these requirements, and had the additional advantage of being scheduled for a lightering-type discharge in the Gulf of Mexico. It also had a hull cleaning and painting only three months before the trials. Principal characteristics and sketches are presented in Appendix 2.

### Trial agenda

The trial agenda given in Table 1 was designed to efficiently obtain information on normal operating requirements, ship response in the event of propulsion breakdown, and model-ship scale effects in the linear and nonlinear motion ranges.

Planning discussions were held among project sponsors and hydrodynamic and ship control experts coordinated through SNAME Panels H-10 and H-5. The water depths that were chosen provided water depth-to-draft ratios of 1.2 (shallow), 1.5 (medium) and greater than 4.2 (deep). The appearance of the *Esso Osaka*'s cross section in these depths is sketched in Fig. 1.

### Trial site selection

Factors entering the selection of the shallow- and medium-depth maneuvering trial sites included the needs for acceptable water depths, depth gradients and bottom smoothness. In addition, low water currents and high probability of good weather with low winds, waves and swell were sought, as were low vessel traffic, fishing effort and naval activity. Finally, a satisfactory location for trial vessel availability and logistical support was required.

The selection process was in two phases, covering a literature search of documented information from government, industry and academic sources, followed by a field confirmation of water depth, current and sea-floor bathymetry by precision survey. This work, described more fully in Appendix 3, resulted in selection of very satisfactory shallow, medium and deepwater trial sites in the Galveston area of the western Gulf of Mexico. The area is depicted on chart segments in Appendix Figs. 23 and 24.

### Measurements

Ship instrumentation design, installation and monitoring

Table 1 Trial agenda

TYPE OF MANEUVER OR CALIBRATION RUN	SPEED OF APPROACH TO MANEUVERS, knots		
	Depth/Draft 1.2	Depth/Draft 1.5	Depth/Draft 4.2
1. Maneuvers	Shallow	Medium	Deep
Turn, port, 35-deg L rudder	5, 7	7	7
Turn, stbd, 35-deg R rudder	5, 7	7	7, 10
Turn, accelerating, 35-deg R rudder	0+	0+	—
Turn, coasting, 35-deg R rudder	5	5	5
Z-maneuver, 20/20	7	7	7
Z-maneuver, 20/20 coasting	5	5	5
Z-maneuver 10/10	7	7	7
Biased Z-maneuver	7	7	7
Spiral	7	7	7
Stop, 35-deg L rudder	3.5	—	3.5
Stop, 35-deg R rudder	3.5	3.5	3.5
Stop, controlled heading	3.5	—	3.5
Stop, steering for constant heading	—	—	3.5
2. Calibration Runs			
Speed/rpm, taken during steady runs prior to chosen maneuvers	3.5, 6, 8.5	5, 7.5	7, 10
Total runs	17	12	15

were provided by the Full Scale Trials Branch of the David W. Taylor Naval Ship Research and Development Center (DTNSRDC). AMETEK, Straza Division, modified the ship's existing double-axis sonar Doppler docking and navigation system to obtain precision bottom clearance information. Decca Survey Systems, Inc. separately provided ship position information.

Most trial measurements taken by DTNSRDC were from existing ship's systems in the wheelhouse with careful calibrations, as described in Appendix 4. Test instrumentation installation commenced six days prior to the trials while the *Esso Osaka* was discharging Persian Gulf crude oil into smaller lightering vessels at a position about 50 miles south of Galveston, Texas.

Water current meters were fixed to their moorings by Sippican oceanographer/divers as soon as possible after arrival of the *Esso Osaka* in each trial area and they were removed shortly

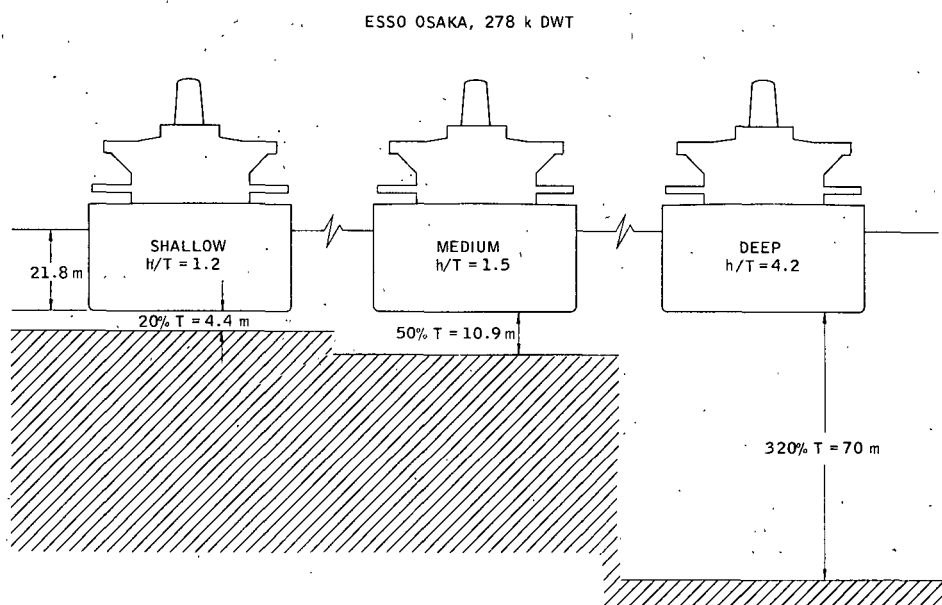
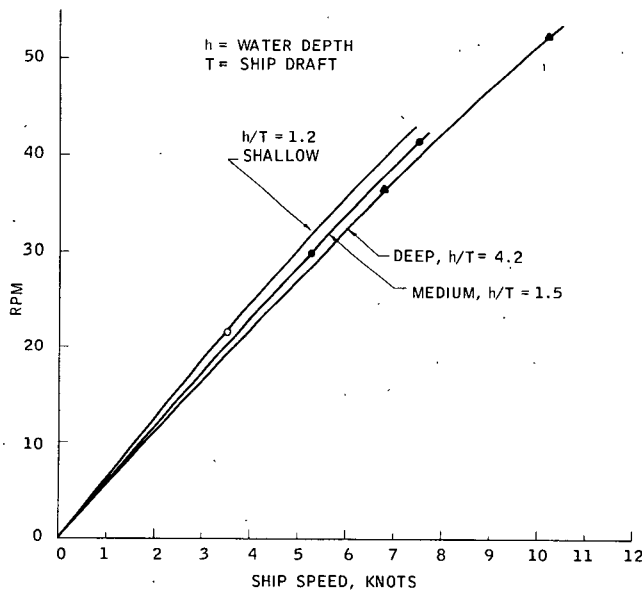


Fig. 1 Cross-sectional sketch of *Esso Osaka* relative to the three water depths of the trials



**Fig. 2** Speed versus rpm calibration curves in the three water depths, for ship's draft of 21.79 m (71.5 ft)

before departure. Current speed and direction were automatically recorded at 9.1-m (30 ft) and 21.3-m (70 ft) depths at each mooring location marked on Appendix Fig. 23. The measurement system and recorded data are presented in Appendix 5, which is paraphrased from Sippican's report [9]. In addition, a portable profiling current meter was used to obtain local current and temperature profiles versus depth at several locations, as also reported in Appendix 5.

The following quantities were measured:

**Automatically recorded:**

- Position, by Decca Survey Systems (antennae on radar mast).
- Ship's heading and rate of turn.
- Ship's longitudinal and lateral speed components, at bow and stern locations of sonar Doppler transducers.
- Bottom clearance at location of stern sonar Doppler transducer.
- Wind direction and speed.
- Rudder angle.
- Propeller rpm.
- Water current direction and speed at two depths at two different locations adjacent to each trial site (Sippican's moored current meters).
- Time.

**Measured and recorded by Ship's engineers** (on file with Exxon International Co., R&D):

- High- and low-pressure turbine steam pressure and temperature.
- Condenser vacuum and seawater temperature.
- Propeller shaft torque, horsepower and rpm.
- Time.

**Measured and recorded by oceanographer/divers:**

- Water current speed, direction and temperature vertical profiles by a hand-operated profiling current meter—periodically at given stations.

**Periodically measured and recorded by trial director and ship's crew:**

- Vessel drafts, forward, amidships and aft, and heel angle.

- Wave height, period and direction (estimated).
- Visibility.
- Visual observations of waterflow, wavemaking, etc.

**U. S. Coast Guard support**

Coast Guard support was received through Headquarters staff, Commander Eighth Coast Guard District staff, and from officers and crews of the USCG cutters *Durable* (210-ft medium-endurance cutter), *Point Monroe* (82-ft patrol boat), and *Blackthorn* (180-ft buoy tender).

Support included publication of a "Notice to Mariners," special notices to fishermen and contacts with fisheries experts. Immediately prior to trials, the *Blackthorn* assisted in establishing the Sippican-prepared current meter moorings at two stations bordering each trial site. The cutters *Durable* and *Point Monroe* alternated patrol duties throughout the trial, and assisted the oceanographer/divers in locating and successfully guarding moorings and current meters against theft or damage. Bird's-eye view photographs of the maneuvering *Esso Osaka* were taken by a USCG patrol aircraft from Air Station Corpus Christi on the first day of trials.

**Trial procedures**

**Preliminary**

Prior to entering the trial areas, the *Esso Osaka* discharged cargo and ballasted to a draft of 21.79 m (71.5 ft), fore and aft. Decca Hi-Fix receivers were carried to the ship by launch, tracking the launch's position from a known location to preserve lane counts. A Coast Guard patrol cutter preceded the *Osaka* into the shallow-water sites, warning away fishing boats and providing safety assistance to the oceanographer/divers as they fixed current meters to previously set moorings. The 2 by 5-mile (3.2 by 8 km) shallow-water trial site was entered via a surveyed access lane. The *Osaka* then made a slow run along the shallowest side while the master verified minimum surveyed water depths.

**Calibration runs**

A series of speed-versus-rpm calibration runs were completed prior to conducting the maneuvering trials at each site. These were required to allow equilibrium ship speed and propeller speed to be set quickly on approach runs within limited trial area dimensions. Each calibration point required three straight trial runs at the given rpm in alternating directions.

As expected, the resulting speed/rpm calibrations differed according to water depth under the ship. For example, at 35 rpm the *Osaka* attained a water speed of 6.55 knots at the deepwater site, 6.25 knots at the medium-water depth site and 5.90 knots at the shallow-water depth site. Calibration curves developed from these runs are shown in Fig. 2.

**Trial runs**

Most of the maneuvering runs were preceded by a minimum of two minutes steady approach during which baseline data were obtained. When the execute command was passed to the helmsman, a mark was entered on the recording medium to indicate the precise time of execution. Data collection then continued at two-second intervals until the end of run.

Several of the data channels, such as rpm and rudder angle, were continuously monitored via digital displays in order to facilitate the approach and execute procedure. The progress of each test was monitored by the printout of all data channels at 40-sec intervals.

Because of the limited site dimensions, it was necessary to maximize acceleration to achieve desired speed and rpm approach conditions. This was usually done by accelerating at



maximum maneuvering power on a parallel and reciprocal course from the desired approach, turning 180 deg near the end of the area and continuing the acceleration until approach speed was reached. The equilibrium rpm was then set using the feedback control and the "steady" approach commenced. Speed through the water was estimated by correcting measured speed-over-ground for longitudinal drift using whatever local water current data were available at that moment.

The sequence of maneuvering runs was chosen for maximum efficiency by linking runs together with the help of pretrial simulations. These pretrial studies were made by Hydronautics Inc., and sponsored by SNAME. Other steps taken to avoid delays included making accelerating turns from dead in the water as the first trial in the morning after drafts were read and the anchor heaved in. Stopping trials usually were made when coming to anchor at night. Except on a few occasions, the ship was not otherwise stopped.

Conventional turning circle, stopping and Z-maneuver trials followed well established procedures [10, 11] and will not be described in detail here. Definition diagrams of trial maneuvers are provided in Figs. 3 and 4. However, the accelerating turn, coasting turn, stopping while steering for constant heading, stopping with controlled heading, coasting Z-maneuver, spiral test and biased Z-maneuver all require some comment.

**Accelerating turn**—This trial begins from dead in the water. The rudder is set to 35 deg and the engine simultaneously ordered to 55 rpm ahead. The result is a turning path tighter than with the conventional turn.

**Coasting turn**—The coasting turn is similar to a conventional turning circle, except that the engine is ordered stopped at the instant the initial rudder execute command is given. Due to the initially slow approach speed and ship slowdown in the maneuver, it was not practical to continue this maneuver through more than a partial turn. Modified performance measures used are discussed under "Results."

**Stopping while steering for constant heading.** This is a conventional stopping maneuver with given astern rpm, except that the helmsman is ordered to hold course as closely as possible with rudder alone. In general, he will be unsuccessful after an interval as slower speed is reached. This speed depends upon the astern rpm that is ordered.

**Stopping with controlled heading**—In this trial, holding the original ship's heading has priority over minimizing stopping distance. To do this the shiphandler is given freedom to control both rudder angle and engine rpm as he sees fit. It is a subjective trial depending upon the skill and training of the shiphandler. In the absence of external disturbances, rudder angle alone will not suffice for heading control as the ship loses speed with constant astern rpm. Therefore, the engine will have to be periodically stopped or even run ahead for short intervals for heading control.

**Coasting Z-maneuver**—This trial is similar to the conventional Z-maneuver except that the engine is ordered stopped at the instant the first rudder execute command is given. The Z-maneuver is continued until the ship's heading no longer responds to rudder. In the present trials only two or three rudder commands were made before control was lost at very slow speed. Therefore, modified performance indices were used, such as maximum lateral deviation and corresponding advance at maximum lateral deviation. These are in addition to first yaw angle overshoot.

**Spiral test**—This is a specialized maneuvering trial which provides information on dynamic stability (that is, yaw and sway stability with controls fixed) in a small rudder angle range about amidships [2, 10, 12]. Only those special considerations required for the present trials are discussed here. For example,

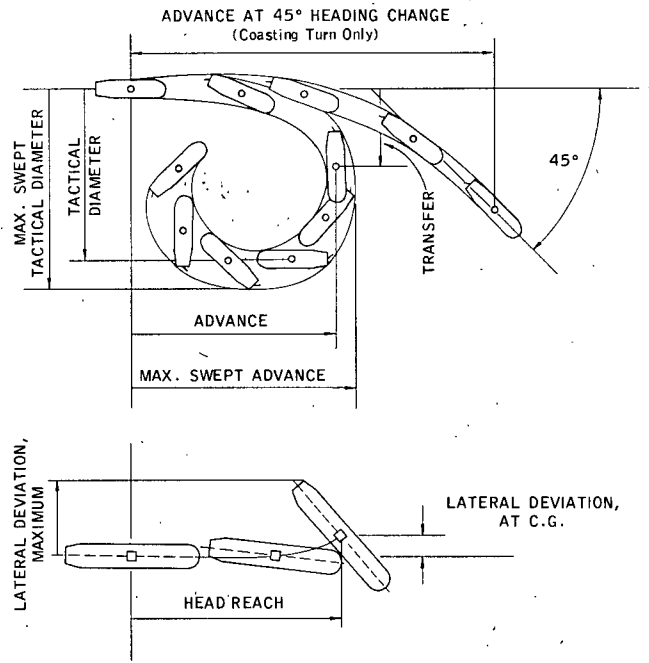


Fig. 3 Definition diagrams of turning circle and stopping maneuvers

a compromise between a direct spiral and the reversed spiral was used.

In the direct spiral test, the rudder is consecutively fixed at predetermined angles, and after sufficient time to achieve steady turning, the turning rate and ship speed are recorded. To expedite the trial, which may take three hours, the reverse spiral is sometimes substituted. A skilled helmsman then steers using smallest possible rudder angle changes to achieve predetermined turning rates (degrees per second). In the present trial, preliminary rudder commands were given by the trial director to approach the desired turning rate, after which a constant rudder angle was ordered. When turning rate and ship speed appeared constant, data were recorded. This modified procedure was used because most helmsmen are not experienced at steering ordered turning rates, and because long steadying periods would cause the limited dimensions of the

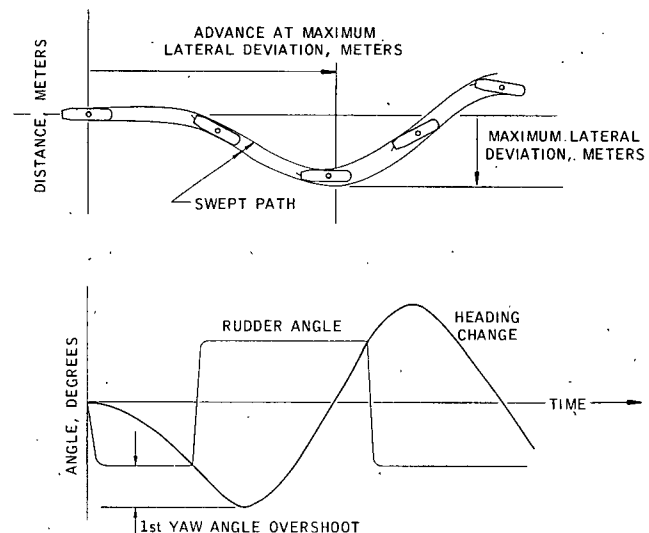


Fig. 4 Definition diagram of Z-maneuver

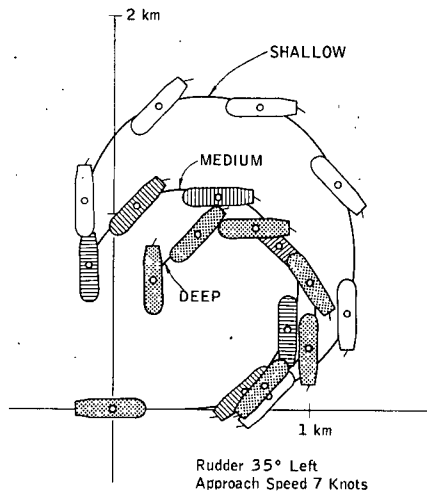


Fig. 5 Water depth effect on turning circle path. Depth/draft ratios of 1.2, 1.5, and 4.2

2 by 5-mile trial sites to be exceeded. Even with this procedure, it was not possible to do the spiral in a continuous run in the shallow-water site.

**Biased Z-maneuvers**—These maneuvers were made at MarAd's request to provide transient data in the nonlinear turning range as required for systems identification work being done at Massachusetts Institute of Technology (MIT). MIT provided steering procedures in a sequence of rudder angles and ordered time durations. Path traces approached as circles with somewhat flattened segments on perimeters. Data were provided directly to MIT by DTNSRDC and are not reported here.

## Results

### General

Trial results address the effects of shallow water, engine maneuvers, approach speed, propeller asymmetry, and water currents, in that order.

Although detailed time-history and path plots of most maneuvers were prepared and are included in reference [17], only one pair is shown in Appendix 6 due to paper length limitations.

Time histories were prepared for all trial maneuvers except the biased Z-maneuver, which was performed and recorded

(SEE FIGURE 3 FOR DEFINITION DIAGRAM)

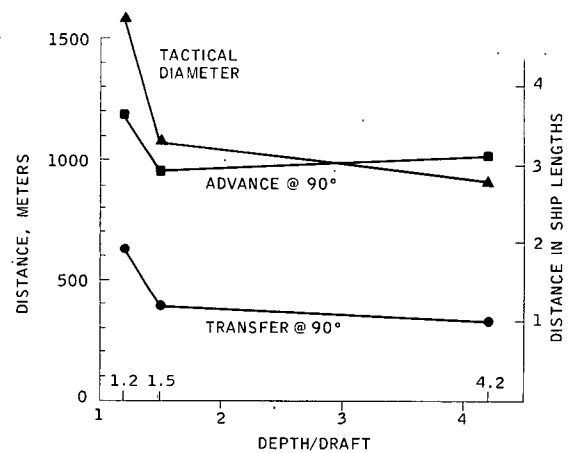


Fig. 6 Changes in turning circle indices with water depth

in detail as previously described. Time-history variables include rpm, forward speed, lateral speed at center of gravity (CG), rudder angle, rate of turn, change of heading and bottom clearance. Ship speed components were corrected to "through the water," by methods described in Appendix 5, together with the water current measurements.

Plots showing swept paths of the vessel were also prepared for all maneuvers except the Z-maneuvers, spiral tests and biased Z-maneuvers. Path plots were initially made as measured relative to ground. They were then corrected for set and drift to a nominal stillwater condition. Winds and seas were very mild throughout the trials and their effects are assumed negligible. See Appendix 7 for weather data.

Trial data were printed at 2-sec intervals and are retained by Exxon International. Original magnetic flexible disk records are retained by the DTNSRDC Full Scale Trials Branch, and those records will be transferred to 8-track magnetic tape during 1979.

### Shallow-water effects

**Conventional Turning Circles**—The large effect of water depth on the *Esso Osaka* entering a turn is shown in Fig. 5.<sup>4</sup> Turning circles were in most cases made through 540 deg, al-

<sup>4</sup> In this paper, depth-to-draft ratio is designated by  $h/T$ . Shallow water was nominally at  $h/T = 1.2$ , medium depth at 1.5 and deep water at  $h/T$  greater than 4.2.

Table 2 Turning circle results versus water depth, expressed using conventional indices

Rudder Angle	Depth ÷ Draft	AT 90-DEG HEADING CHANGE							AT 180-DEG HEADING CHANGE Tactical Diameter			
		Advance m	÷L	Δ*	Transfer m	÷L	Δ*	Speed Loss	m	÷L	Δ*	Speed Loss
35-deg left	4.2	1005	3.1	...	310	0.9	...	35%	895	2.75	...	56%
35-deg left	1.5	915	2.8	-9%	385	1.2	+24%	32%	1075	3.31	+20%	46%
35-deg left	1.2	1190	3.7	+18%	555	1.7	+79%	26%	1565	4.82	+75%	40%
35-deg right	4.2	1015	3.1	...	360	1.1	...	33%	925	2.85	...	58%
35-deg right	1.5	990	3.1	-2%	405	1.3	+13%	33%	1075	3.31	+16%	50%
35-deg right	1.2	1180	3.6	+16%	705	2.2	+96%	35%	1590	4.89	+72%	40%

#### NOTES:

Approach speed 7 knots.

Corrected for set and drift.

\* Percentage change from deepwater results.

though not indicated in path plots. Table 2 and Fig. 6 report conventional measures of turning circles and indicate that, at 35-deg left rudder, advance was reduced an average<sup>5</sup> 6 percent in the medium water depth compared with deep water, and in shallow water increased by about 17 percent.

Perhaps most significant to tanker operations are the extreme paths swept by the ship's hull. In this report, swept-path indices are measured from the extension of the approach path of the ship's center of gravity to the point on the hull which sweeps the widest path during the maneuver. Table 3 relates maximum swept advance and maximum swept diameter to water depth.

These data show that swept advance was reduced by an average of 8 percent in medium depth and increased by about 13 percent in shallow water, both relative to results in deep water. Maximum swept diameter increased by about 16 percent in medium depth and 61 percent in shallow water.

Transfer at 90-deg heading change increased an average of 19 percent in medium depth and by 88 percent in shallow water. Probably the most obvious water depth effect is on tactical diameter which, at 180-deg heading change, increased by 18 percent in medium depth and 74 percent in shallow water.

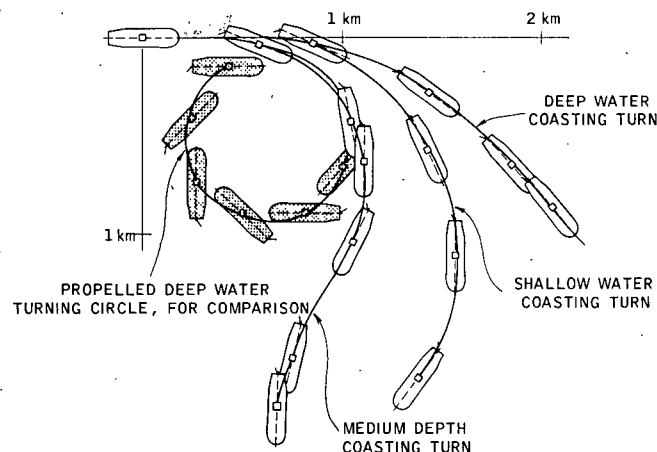
Taken together, these results show that normal modest course-changing maneuvers of a VLCC are not greatly affected by water depth, although the infrequent 180-deg course reversal maneuver is affected substantially.

Table 2 also shows that there is much less reduction of speed in a turn in shallow water than in medium or deep depths. At 180-deg heading change, speed loss from approach speed in deep water was roughly 57 percent. In the medium depth the speed was reduced by 48 percent and in shallow water by 40 percent.

**Coasting turns**—An interesting characteristic of shallow-water maneuvering is seen in the coasting turn. Results for the coasting turn to the right with 35-deg rudder are presented in Fig. 7, which also shows for comparison the conventional deepwater 35-deg rudder turn. Notice that initial turning is greatest in the medium water depth and least in deep water. In the shallow and deep cases, turning is consistently to the right, whereas in medium depth there is a slight reversal toward the end. As a performance measure for the coasting turn, we compare in Fig. 7 advance at 90-deg heading change with that in the conventionally powered turn. This shows how degradation of turning by coasting varies with water depth.

In deep water, coasting caused the advance in the turn at 45 deg heading change to increase by 170 percent.<sup>6</sup> In medium depth, coasting caused advance at 90 deg heading change to

	PROPELLED TURN, METERS $\div L$		COASTING TURN, METERS $\div L$		COASTING PROPELLED
DEEP*	706*	2.2	1906*	5.9	+170%
MEDIUM	990	3.1	1140	3.5	+15%
SHALLOW	1182	3.6	1616	5.0	+37%



\*Deepwater Turn Compared At 45° Heading Change

Fig. 7 Water depth effect on advance in the coasting turn, with propelled turn shown for comparison

increase by only 15 percent, and in shallow water it increased by 37 percent.

**Accelerating turns**—Accelerating turns were made in both medium and shallow water depths by building up from zero rpm to about 56 ahead, beginning with the ship dead in the water with rudder angle at 35 deg right. As shown in Fig. 8, the main water depth effect is seen in the changes in the tactical and maximum swept diameters. In shallow water the tactical diameter increased by 31 percent and the maximum swept diameter by 26 percent relative to medium-depth water.

**Stopping maneuvers**—Water depth effects on stopping from slow speed are most apparent in trials made with 35-deg right rudder and engine ordered to 45 rpm astern. Figures 9 and 10 show that headreach is roughly the same in the deep, medium and shallow water depths at 520, 575 and 550 m (1705, 1886 and 1804 ft), respectively. And as shown in the table on Fig. 9, had the approach speed of the deepwater maneuver been exactly the 3.8 knots of the medium and shallow maneuvers, instead of 3.5 knots, even closer results would have been obtained. The water depth effect is most strongly seen in the large heading change as the ship comes to a halt. Heading change varied from 18 deg in deep water to 50 deg in medium depth to 88 deg in shallow water, all to the right.

Lateral deviation of the ship's CG from the extended track-

Table 3 Turning circle results versus water depth, expressed using maximum swept-path indices

Rudder Angle	Depth $\div$ Draft	Maximum Swept Advance			Maximum Swept Tactical Diameter		
		m	$\div L$	$\Delta^*$	m	$\div L$	$\Delta^*$
35-deg left	4.2	1160	3.6	...	1040	3.2	...
35-deg left	1.5	990	3.1	-15%	1190	3.7	+14%
35-deg left	1.2	1270	3.9	+10%	1690	5.2	+63%
35-deg right	4.2	1100	3.4	...	1025	3.2	...
35-deg right	1.5	1080	3.3	-2%	1200	3.7	+17%
35-deg right	1.2	1280	3.9	+16%	1620	5.0	+58%

NOTES:

Approach speed 7 knots.

Corrected for set and drift.

\* Percentage change from deepwater results.

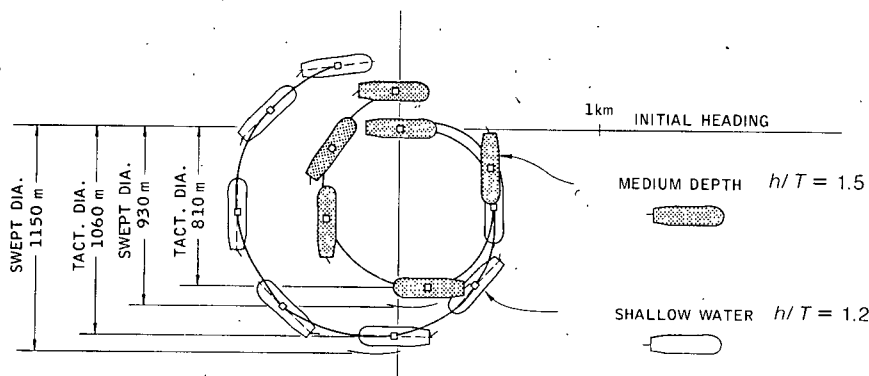


Fig. 8 Water depth effect on the accelerating turn; shallow-water versus medium-water depth conditions

line was small, varying from 20 m (65.6 ft) starboard to 50 m (164 ft) port to 35 m (115 ft) port for deep, medium and shallow depths, respectively. Obviously, maximum swept-path deviations are more pronounced, with the bow 90 m (295 ft) to starboard in deep water, and the stern 200 m (656 ft) to port in medium depth and 205 m (672 ft) to port in shallow depth.

**Z-maneuvers**—Z-maneuvers describe relative checking and counterturning ability in maneuvers about an initial heading. Table 4 and Fig. 11 provide values in the three water depths for the 20/20-deg Z-maneuver with initial 7-knot speed.

For port entry-type maneuvers, the first yaw angle overshoot and the resulting maximum lateral deviation (swept path away from original trackline) are significant. First yaw angle ov-

ershoots in the 20/20-deg maneuver varied from 9.5 deg in deep water to 11.2 deg in medium depth to 7.8 deg in shallow water. The maximum swept-path lateral deviation from trackline varied from 460 m (1509 ft) deep to 590 m (1935 ft) medium to 505 m (1656 ft) shallow.

In the 10-deg/deg Z-maneuvers the first yaw angle overshoots varied from 3.6 deg in deep water to 7.9 deg in medium depth to 6.2 deg in shallow water; there was some drift of rudder angles, however, as apparent from the time histories in Appendix 6.

**Coasting Z-maneuvers**—The effect of water depth on a ship's ability to continue maneuvering without propulsion power is shown by the coasting Z-maneuver. It is also useful

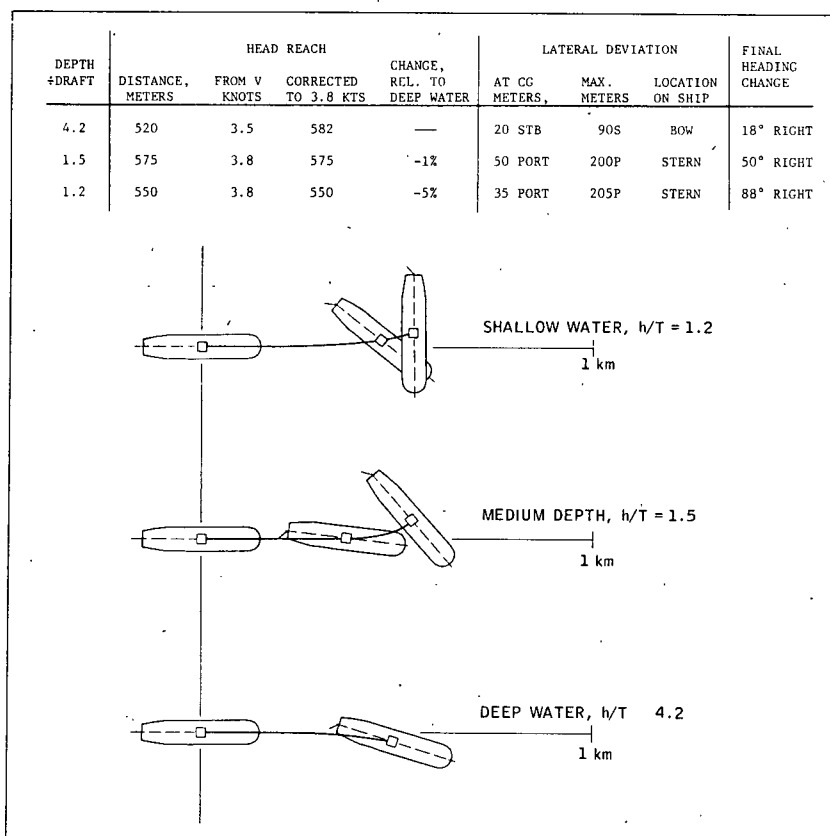


Fig. 9 Water depth effect on stopping path, with approach speed 3.8 knots, 35-deg right rudder and 45 rpm astern (about 50 percent of available astern power)

for determining a rough minimum maneuvering speed with engine stopped.

Again, first yaw angle overshoots, maximum lateral deviation and advance to that point are all informative. Figure 12 shows the effect of shallow water on the coasting Z-maneuver.

**Spiral test**—Spiral test results provide certain technical information on steady-state turning characteristics at small fixed rudder angles, that is, in the absence of active steering. However, they provide no direct information on maneuvering or coursekeeping ability with active steering; at least not in the case of large slow vessels such as VLCCs. In fact, spiral tests are not meaningful to the VLCC shiphandler unless unusual results are also obtained from the Z-maneuver, such as abnormally large overshoots.

A main purpose of the spiral test is to determine whether the resulting turning rate versus rudder angle curve contains a “hysteresis loop,” which would be associated with “dynamic instability.” It is important to understand, however, that the technical term “dynamically unstable,” as used in these paragraphs, relates to controls-fixed stability. It does not directly relate to acceptable “directional stability,” with use of the rudder, which is a required characteristic of every vessel.

The present spiral tests show interesting characteristics. From the records of turning rate in degrees per second (example segment in Fig. 30 of Appendix 8) together with working summary plots, Appendix 8 Figs. 31–33, smoothed summary dimensionless plots were prepared. These are shown compositely in Fig. 13. Comments are as follows:

- Deepwater spiral test: Turning rate versus rudder angle results of Fig. 13 and Appendix 8 suggest that the *Esso Osaka* is marginally dynamically stable in deep water; that is, no definite “loop” resulted, even though a very minor loop might have appeared if this particular trial was prolonged beyond the 2 hr-30 min used.
- Medium-depth spiral test: Results in Fig. 13 and Appendix 8 suggest that a narrow loop of perhaps 1-deg width exists, with a dimensionless height of about 0.4.
- Shallow-water spiral test: Results in Fig. 13 and Appendix 8 suggest that the vessel is probably dynamically stable, and probably has no loop. This interpretation ignores some of the plotted points and is based upon

- (a) Suspicion of points just to the left of the origin in Appendix 8 Fig. 33 because of the limited time they could be held for steady results. This was because of the restricted size of the 2 by 5-mile surveyed “safe” trial area.
- (b) Problems incurred in obtaining the points near the origin in piecewise fashion for the same reason as just given.
- (c) The tendency suggested by all points except those just to the upper left of the origin. A dashed line for the expected actual curve has been added to Fig. 33.

Taken together, the spiral test data in the three water depths suggest marginal dynamic stability in deep water, probable small instability in the medium depth, and stability in the shallow depth. Consistency of these results with the turning circle and Z-maneuver data are considered under “Discussion of results.”

Table 4 20/20-deg Z-maneuver indices versus water depth (approach speed 7 knots)				
	Deep	Medium	Change*	Shallow Change*
1st yaw angle overshoot, deg	9.5	11.2	+18%	7.8 -18%
Maximum lateral deviation, m	460	590	+28%	505 +10%
Advance, at maximum lateral deviation, m	1540	1650	+7%	1400 -9%

\* Relative to deepwater result.

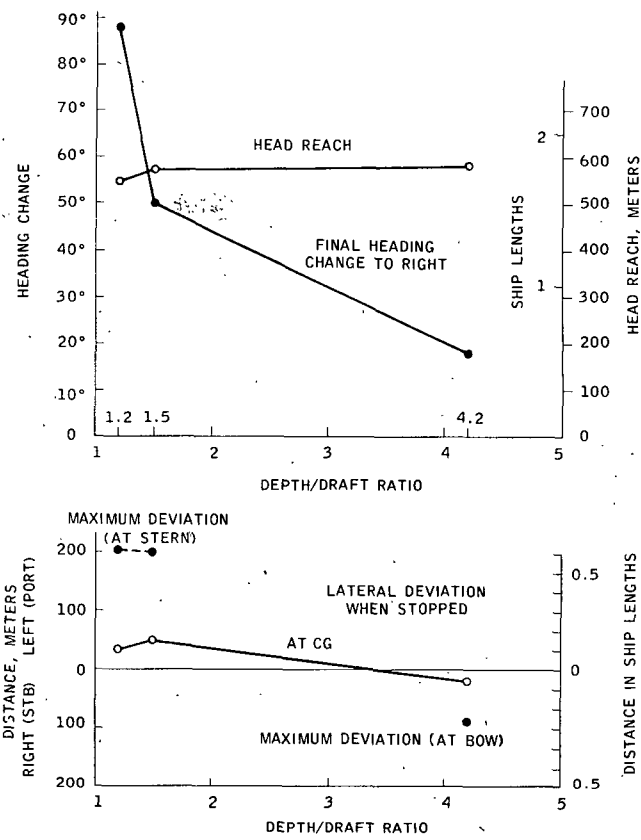


Fig. 10 Stopped position of ship as affected by water depth, with approach speed 3.8 knots, 35-deg right rudder and 45 rpm astern

Propeller rpm effects on heading control

The effects of the use of propeller rpm on maneuvering are shown by certain turning, stopping and Z-maneuver trials.

**Rpm effects on turning**—Turning of a single-screw single-rudder ship is strongly affected by use of propeller rpm.

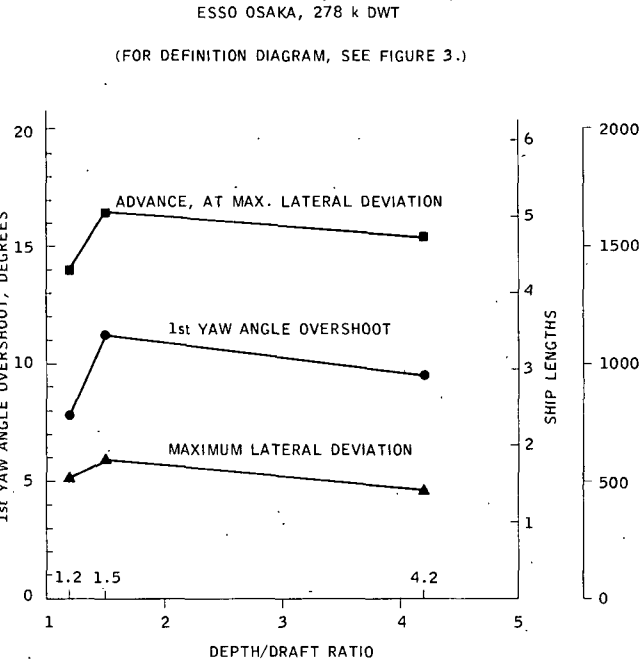


Fig. 11 20/20-deg Z-maneuver indices versus water depth

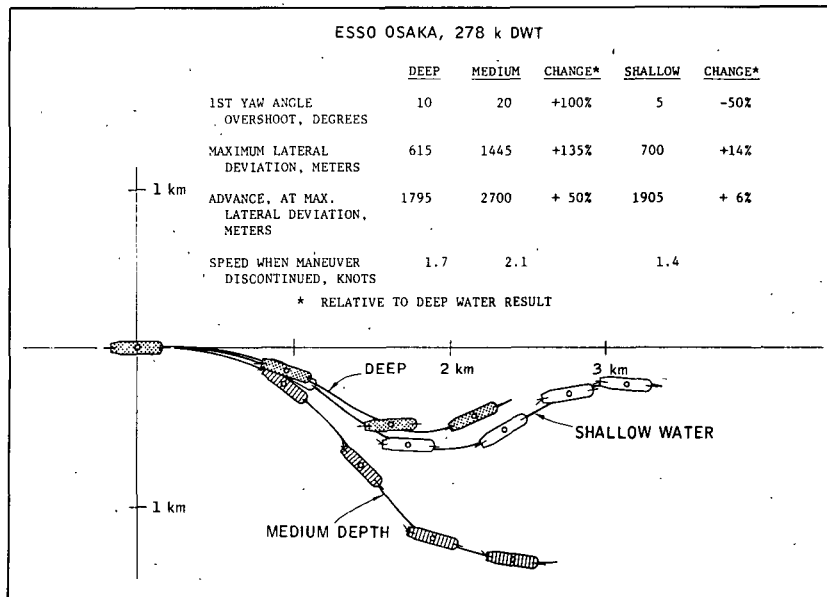


Fig. 12 Water depth effect on coasting 20/20-deg Z-manuever, from 5 knots

This is clearly shown in Fig. 14 for the case of water-depth-to-draft ratio 1.2. The conventional turning maneuver shown in Path A is diminished when the vessel coasts with propulsion power cut off, as in Path B. The accelerating turn, Path C, has a different approach condition, beginning from dead in the water and building up propeller speed to about 56 rpm from the moment the rudder is deflected to 35-deg right.

Similar rpm effect results were obtained in medium-depth water, as seen in Fig. 15.

**Coasting versus conventional Z-manuevers**—The relative ability to maneuver while "coasting" is seen in Table 5, which compares the coasting condition with the conventional Z-manuevers of Table 4. Figure 16 shows the variations of Z-manuever paths, coasting versus powered, for the three water

depths. Figures 17 and 18 show how water depth changes the effects of coasting on Z-manuever overshoot, maximum deviation and advance.

#### Effect of rudder and rpm control on stopping

**Rudder angle effect**—The stopping results reported under "Water depth effect" were for the 35-deg right-rudder case. The effects of applying instead 35-deg left rudder in the deep- and shallow-water cases can be seen in the combined Fig. 19, with paired left- and right-rudder stopping maneuvers. The tendency of the astern propeller rotation to move the stern to port is clearly preponderant in shallow water, whereas rudder angle was the controlling factor in deep water.

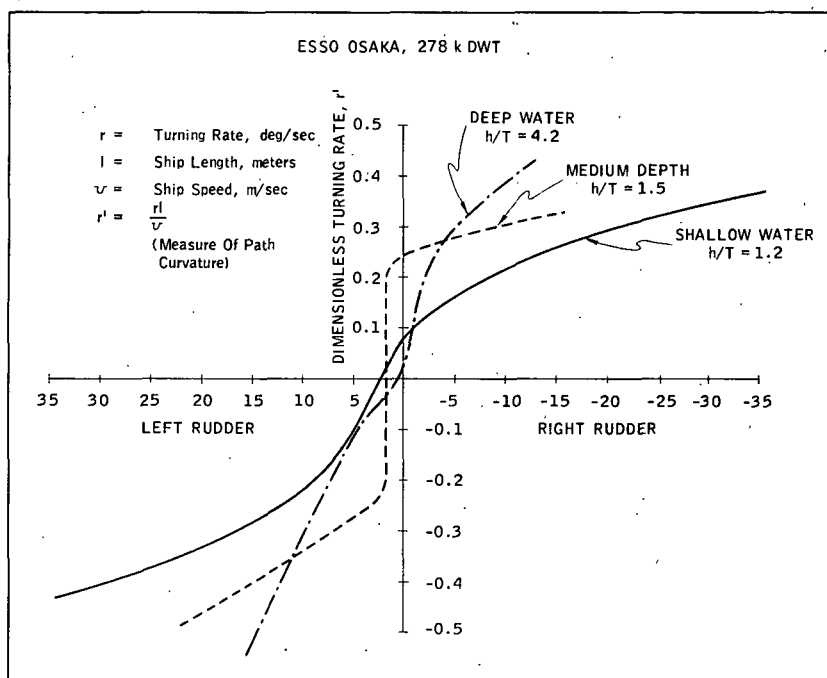


Fig. 13 Smoothed spiral test results, showing dimensionless turning rate versus rudder angle, from 7 knots

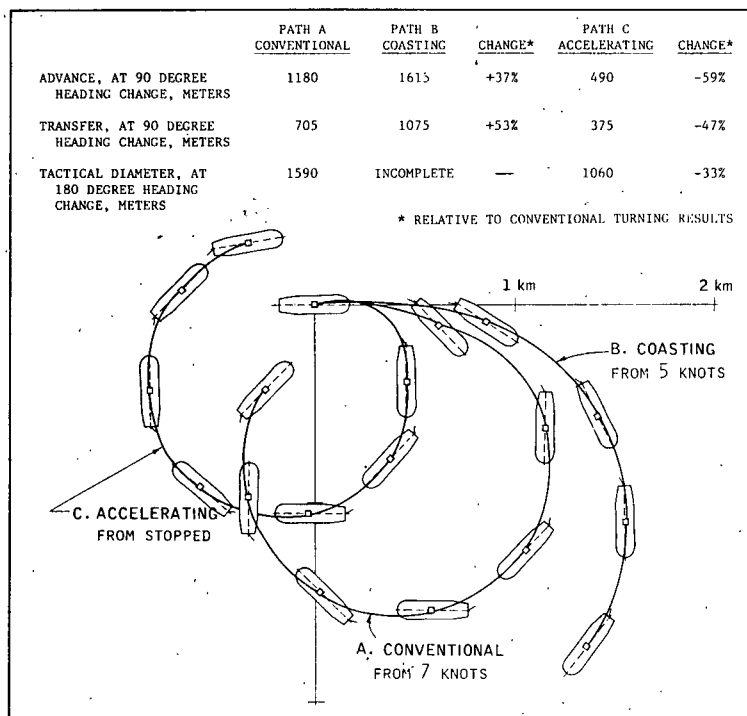


Fig. 14 Rpm effect on turning circle in shallow water, showing coasting, conventional, and accelerating turns;  $h/T = 1.2$

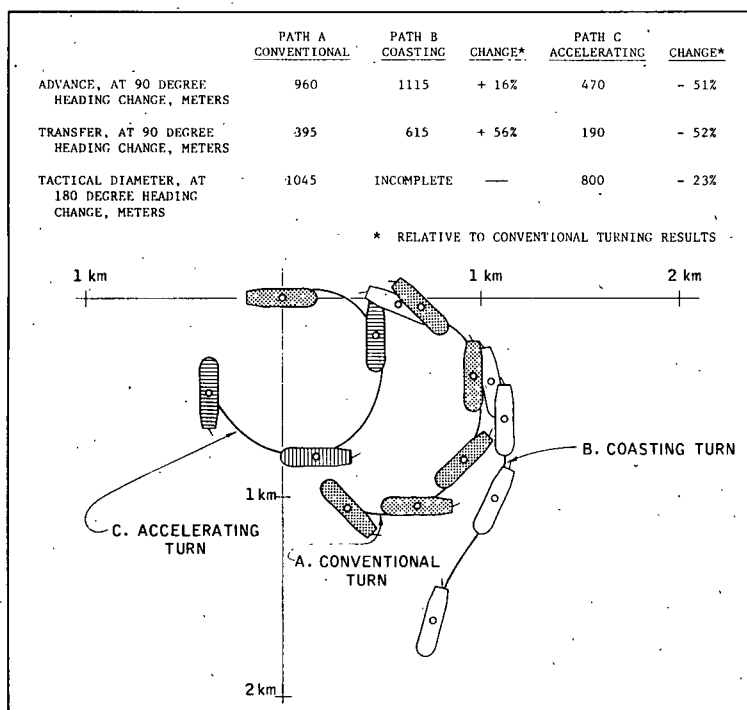


Fig. 15 Rpm effect on turning path in medium water depth, showing coasting, conventional, and accelerating turns;  $h/T = 1.5$

Table 5 Effect of coasting on 20/20-deg Z-maneuver in three water depths

	Deep		Medium		Shallow	
	Conventional	Coasting	Conventional	Coasting	Conventional	Coasting
1st yaw angle overshoot, deg	9.5	10	11.2	20	7.8	5
Maximum lateral deviation, m	460	615	590	1445	505	700
Advance, at maximum lateral deviation, m	1540	1795	1650	2700	1400	1905
Speed on approach, knots	7	5	7	5	7	5
Speed when maneuver discontinued, knots	4.5	1.7	4.8	2.1	5.1	1.4

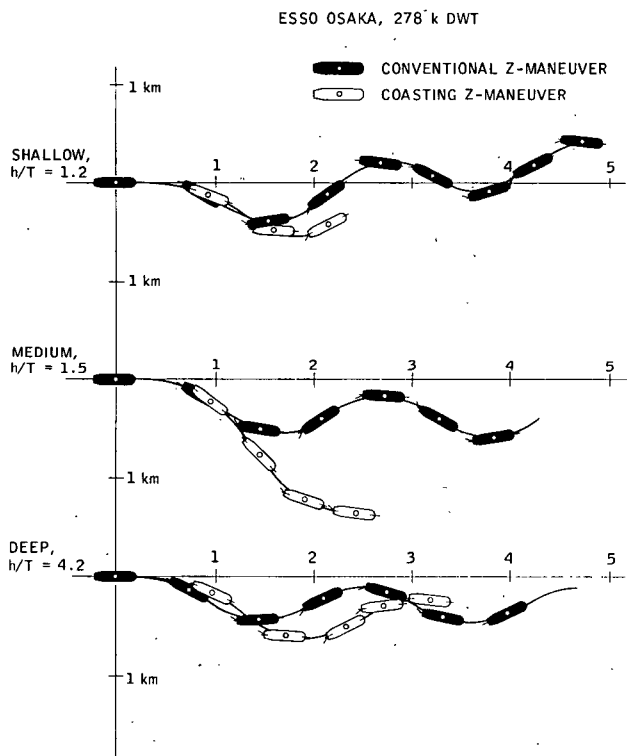


Fig. 16 Coasting effect on 20/20-deg Z-manuever path in three water depths

In deep water, special trials were made to show the value of steering and rpm maneuvers for maintaining constant heading while stopping. Results are shown in Fig. 20. The base case was a simple stopping maneuver with engine-ordered 45 rpm astern and rudder-ordered 35-deg right (top of Fig. 20), from an approach speed of 3.5 knots. Next, steering for constant heading was attempted, with engine ordered to a constant 45 rpm astern. The result, shown in the middle of the Fig. 20, indicates little change. Finally, the master was asked to stop

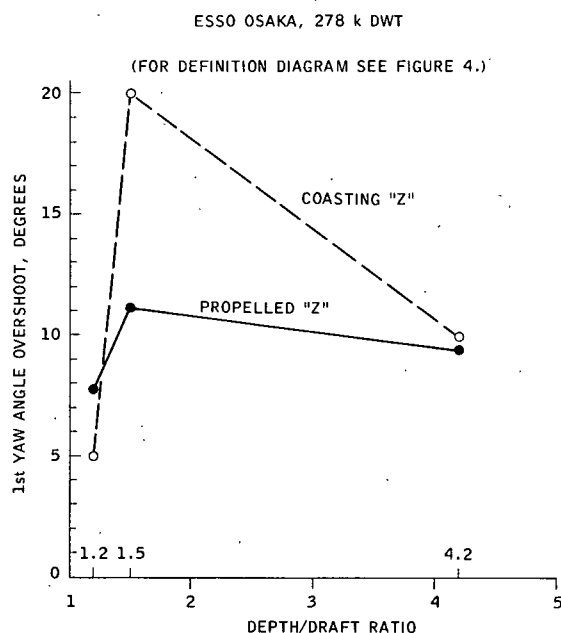


Fig. 17 Coasting effect on first yaw angle overshoot of 20/20-deg Z-manuever in three water depths

the vessel using both rudder and engine speed as he thought best to maintain the original heading, with stopping distance being a secondary objective. The resulting maneuver is shown at the bottom of Fig. 20, with a headreach of about three times that of the simple stop or the steering stop. Examination of the time history of the controlled stop showed that when 35-deg left rudder was found insufficient to hold the heading steady (at about 140 sec into the maneuver) the master alternately used rpm astern, ahead, and stopped to control the heading. Table 6 shows that, although the heading was held virtually constant, the vessel gradually drifted to the left a distance even greater than the maximum deviation of the stern swinging to port in the 35-deg right-rudder case.

A similar trial run was made in shallow water ( $h/T = 1.2$ ) without quite as much attention to maintaining heading. In that case, stopping distance, relative to the simple stop with 35-deg right rudder and no engine maneuvering, increased by about 80 percent (when normalized to 3.8-knots approach speed). However, ship's heading diverged as much as 17 deg to starboard and ended at 7 deg starboard when forward motion had stopped.

### Additional results

**Ship speed effects on rudder maneuvers with constant rpm**—The effect of ship speed on the path geometry of a large tanker is usually considered to be small. This is because tankers normally operate at relatively low Froude number, meaning that wavemaking and heeling are small. For this reason the hull, propeller and rudder hydrodynamic forces all vary roughly proportionally to the square of ship's speed through the water, and produce geometrically similar maneuvering paths.

Two trial runs of the present series were scheduled in an attempt to verify this. The first was a turning circle with 35-deg

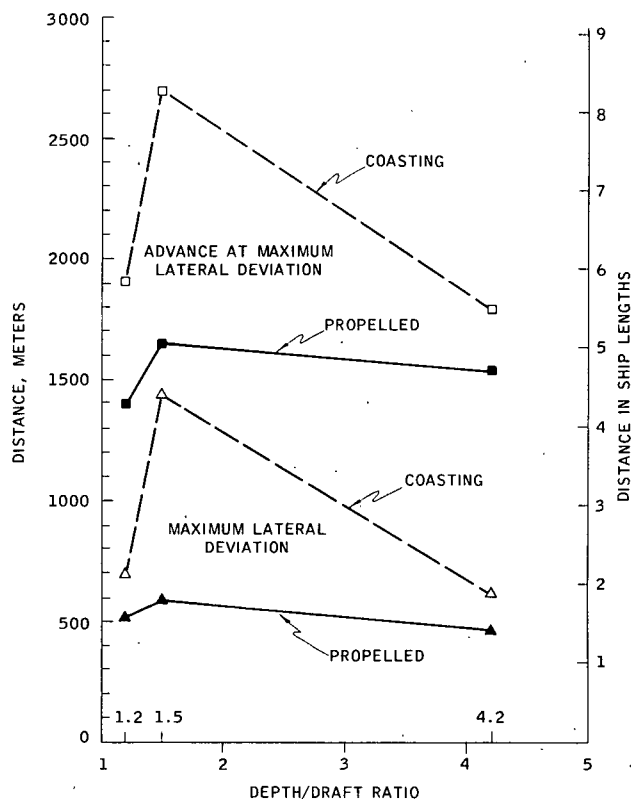


Fig. 18 Coasting effect on lateral deviation and advance of 20/20-deg Z-manuever in three water depths



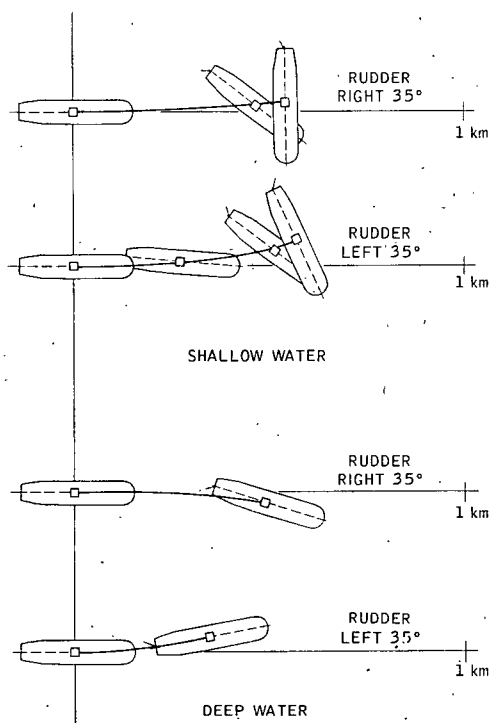


Fig. 19 Rudder angle effect on stopping in shallow water and deep water from 3.8 knots, with 45 rpm astern

left rudder from 5.0 knots in shallow water. This is compared with another run which is the same except for the approach speed of 7.0 knots. Unfortunately, the 5-knots approach speed (and slower in the turn) allowed significant path distortion due to water current set and drift. Also, the measured rudder angle in the 7.0-knot trial was 36 deg instead of 35-deg left. Nevertheless, the results show nothing that strongly contests the assumption that path geometry is independent of speed. Turning indices are summarized in Table 7.

The second comparison was made in a deepwater turn with

Table 6 Rudder and rpm control effect on stopping (deep water)

Rudder Angle	RPM Astern	Speed Approach, knots	Max Heading Change, deg	Head-reach m	Max Lateral** m
35-deg Right	45	3.5	18° Right	490	49 left
Steered*	45	3.4	16° Right	495	88 left
Steered*	varied	3.5	2° Left	1650	195 left

\* Mainly 35-deg left rudder.

\*\* Swept path, extreme.

Table 7 Speed effect on turning circle in shallow water ( $h/T = 1.2$ )

Rudder Angle	Approach Speed, knots	Advance at 90 deg, m	Transfer at 90 deg, m	Tactical Diameter at 180 deg, m
35-deg L	5.0	1197	668	1631
35-deg L	7.0	1189	555	1564

Table 8 Speed effect on turning circle in deep water ( $h/T = 4.2$ )

Rudder Angle	Approach Speed, knots	Advance at 90 deg, m	Transfer at 90 deg, m	Tactical Diameter at 180 deg, m
35-deg R	7.8	1017	361	924
35-deg R	10.0	1138	567	1001

35-deg right rudder, Table 8. One run was from an approach speed of 7.8 knots, a comparison run from 10.0 knots. Again the water current (0.73 knots in the 7.8-knot approach case) casts some doubt on the validity of the comparison, but the results do not seriously contest the assumption of path independence of ship speed. In fact, the tendencies are in the opposite direction from those of the previous comparison.

**Water current effects**—Although path plots of all maneuvers were "corrected" to a nominal stillwater condition, as described in Appendix 5, set and drift are a fact of life in slow-speed maneuvers. Shiphandlers must be skilled in adapting to non-uniform and time-varying currents for the same reason that current corrections cannot be accurately made even in controlled experiments such as these. The degree of water current nonuniformity in these trials is discussed in Appendix 5. Here

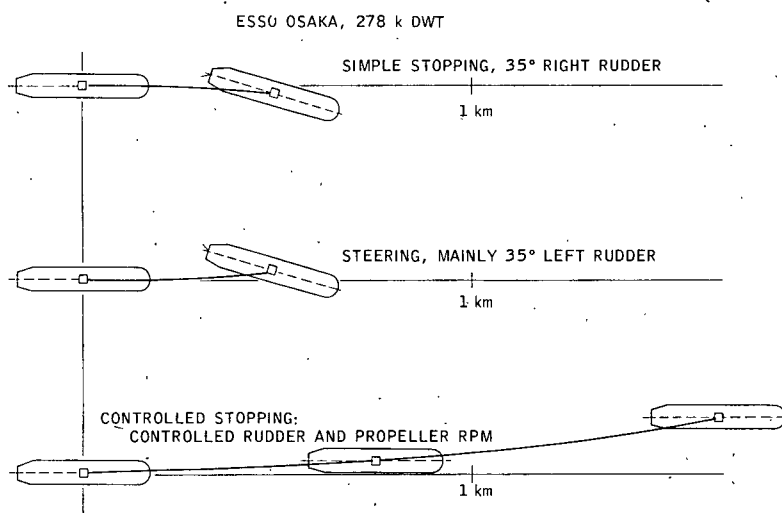


Fig. 20 Comparison of controlled, simple, and steered stops in deep water. Approach speed 3.5 knots, and engine speed 45 rpm astern except in controlled stop, where it was varied

**Table 9 Example of current effect on turning indices**

Condition	Advance, m, at 90 deg	Transfer, m, at 90 deg	Tactical Diameter, m, at 180 deg
Uncorrected	880	420	1007
Corrected for set toward 66.5 degrees T, 0.73 knot drift	1017	361	924
Error, relative to corrected value	-14%	+16%	+9%

**Table 10 Propeller asymmetry effects on turning circles**

Water Depth	Rudder Angle,	Advance, m, at 90-deg Heading	Transfer, m, at 90-deg Heading	Tactical Diameter, m, at 180-deg Heading
Shallow	36-deg L	1189	555	1564
Shallow	34-deg R	1182	707	1591
Difference		-1%	+27%	+2%
Medium	33-deg L	916	384	1073
Medium	36-deg R	990	407	1073
Difference		+8%	+6%	0%
Deep	35-deg L	1006	309	894
Deep	36-deg R	1017	361	924
Difference		+1%	+17%	+3%

we need only point out that the importance of current effects can, if desired, be assessed by comparing "as measured" and corrected path plots which can be found in reference [17].

A particular example is a deepwater turning circle where current speed is about 10 percent of the 7.8-knot approach speed to the maneuver. Approach heading was 272 deg, T. Had path results not been corrected for set and drift, the turning indices would have been affected as seen in Table 9. The results in Table 9 should be kept in mind when asking shipmasters to perform ad hoc maneuvering trials at sea. Of course, water current drift errors will be exaggerated in stronger currents unless ship speeds are correspondingly faster.

ESSO OSAKA, 278 k DWT

RUDDER ANGLE	ADVANCE AT 90° HEADING, m.	TRANSFER AT 90° HEADING, m.	TACTICAL DIAMETER AT 180° HEADING, m.
35° L	355	205	750
35° R	470	160	810
DIFFERENCE	+32%	-22%	+8%

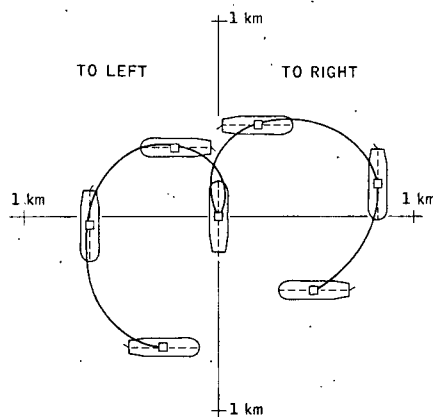


**Fig. 21** Propeller asymmetry effect on accelerating turn in medium water depth. Accelerating from zero ship speed with engine rpm rapidly increased from zero to 56. Rudder 35-deg right,  $h/t = 1.5$

**Propeller asymmetry effects**—The effects of propeller asymmetry of a single-screw ship were already seen in the data on water depth effects on turning and stopping maneuvers. The comparisons of Table 10 only summarize asymmetry effects on turning maneuvers made in different water depths. The degree by which the dimensions of right turns exceed those of left turns is shown below each pair.

Although the exact rudder angles desired for good comparisons were not always achieved, it is apparent that turning circles to the left required somewhat smaller areas than those to the right.

The accelerating turn shows a larger effect of propeller asymmetry, as seen in Fig. 21.

#### Visual observations during maneuvers

- **Heel in turning:** Limited bottom clearance in the shallow-water site caused particular attention to be paid to any dynamic heeling that might have brought the bilge closer to the bottom. However, no measurable heel was detected with the ship's existing pendulum inclinometer. Sightings were therefore made from a central point in the wheelhouse, using wheelhouse side window edges and the clear horizon as guides. This rough check, made in the medium-depth area, indicated that heel due to turning at 7 knots, with 35-deg rudder, did not exceed one-half degree. Also, heel was toward the center of the turn and not outboard as anticipated. This may have resulted from a higher dynamic water level on the outboard side of the ship which would have more than corrected the opposing inertial heeling moment.

- **Sinkage and trim:** Vessel sinkage and trim were not measured in the trials, although pneumatic draft gages installed in the *Esso Osaka* were observed several times during maneuvers. On no occasion was more than 15-cm (6 in.) trim aft indicated, including during a 35-deg rudder angle turn from a 7-knot approach speed with 4-m (13 ft) bottom clearance. These indications are not taken as reliable, as we do not know the characteristics of pneumatic draft gage readings as a function of ship speed or local drift angle. Regarding sinkage, according to a preliminary calculation, a total change of about 15 cm was expected with 4-m bottom clearance. However, even with good echo-sounding measurements it was not believed that the generally flat sea bottom was sufficiently uniform to measure sinkage.

- **Silt in wake:** Hard-packed gray clay was observed by divers on the sea bottom and was collected from the anchor chain on deck. In addition, there was evidence of a bottom layer of fine silt or sand. The ship's wake was observed during turning maneuvers, and showed a bright yellow path in the otherwise blue water. In fact the ship was observed to retrace its own path after completing more than 360 deg of 540-deg turning circles in the medium- and shallow-water sites. Coast Guardsmen on patrol cutters also reported observing the wake from straight course running some distance behind the ship, although this was not evident from onboard. Divers reported reduced visibility near the sea bottom, also suggesting a finely silted bottom.

## Discussion of results

### General

The trial results show clearly that distortions of flow about a ship's hull in shallow water significantly affect maneuvering motions. The sketches of Fig. 1 show why the cross-flow passing under a ship's bottom when maneuvering in deep water must, in very shallow water, be mainly constrained to pass around the ship's sides. In consequence, the combined effects of shallow water on side drift and turning in maneuvers greatly exaggerate the hydrodynamic side forces acting on a ship, and

shift the center of pressure aft toward amidships. Meanwhile, the relative effectiveness of the rudder is reduced because its center of pressure moves forward [12–16]. Also, the rudder's effective aspect ratio, due to the presence of the seabottom, is increased much less in shallow water than is that of the hull. Recall that a ship's hull has a very low aspect ratio in deep water.

With this brief physical picture, some trial findings are discussed.

### Turning, Z-maneuver and spiral test results

Changes in turning circle characteristics and Z-maneuver indices with water depth are loosely related to the changes in dynamic stability that are indicated by spiral test results.

According to theory [12–16] and the present trials, the dynamic stability of a ship's hull (that is, with controls fixed) first decreases when moving from deep to medium water depths and then increases again as water depth becomes very shallow. We therefore look for relationships between dynamic stability<sup>7</sup> and maneuvering in terms of turning ability and quickness of response, such as in checking a turn. In general, these appeared in the present trial results as follows.

The hull, with controls fixed, as interpreted from spiral test results, appeared to be marginally dynamically stable in deep water, slightly unstable in medium depth and stable in shallow water. Although dynamic (controls fixed) stability is not directly related to *directional* stability, it has some relationship to Z-maneuver and turning-circle behavior. For example, the first yaw angle overshoot in the Z-maneuver increased from 9.5 deg in deep water to 11.2 deg in medium depth, and then reduced to 7.8 deg in shallow water. Maximum lateral deviations, and advance at maximum lateral deviations also, changed consistently with yaw overshoots. This suggests that the minimum dynamic stability in medium water depth is associated with the maximum Z-maneuver overshoot in the medium water depth. Also, the maximum swept turning diameter increased only modestly in medium depth (14 percent); but greatly in shallow water (63 percent) compared with deep water.

Of course, not too much should be read into the relationship between dynamic stability and maximum turning ability, since dynamic stability indications from the spiral test refer mainly to steady turning motions with small rudder angles, while maximum turning with large rudder angle is highly nonlinear.

On the other hand, Z-maneuver results relate more closely to quickness of response as indicated by the spiral test results. And, in fact, the Z-maneuver results reflect the reversal trend of the spiral results much more faithfully than do the changes in maximum turning diameters.

### Propeller rpm effects on heading control

The accelerating turns made in the medium and shallow water depths confirm facts well known to shiphandlers, that is, that advance and tactical diameter can be reduced by "kicking ahead" with the propeller in a slow-speed turn. The reason is that water flow past the rudder is quickly increased, while the hull hydrodynamic forces aiding or resisting the turn are not.

On the other hand, the coasting turns showed a directionally predictable decrease in turning ability when the propeller discharge flow was removed from the rudder. Much of the rudder was then put in a separated flow region behind the idling propeller. But perhaps of greatest significance is that the single-screw VLCC, once predicted to be virtually unmanagable

in slow-speed maneuvers, was able to turn reliably at slow speeds, even with the engine stopped.

Taken together, the foregoing trial results emphasize that maneuverability is improved when rpm is increased and degraded when rpm is reduced. Knowing this, the prudent shiphandler will look for the slowest safe speed in certain critical maneuvering areas. If then required to speed up, maneuverability will increase instead of being degraded if unexpectedly required to slow down.

The coasting Z-maneuver gave further evidence that the trial vessel could maneuver reliably and predictably with engine stopped, even at speeds as low as 1.4 knots. In all cases it appeared that the ship was still responding to rudder commands when the maneuver was terminated.

The trends of response to the coasting 20/20-deg Z-maneuver closely follow those of the conventional 20/20-deg Z-maneuver, as shown in Table 4. Both follow the trends expected from the spiral tests based on what has been learned about dynamic stability in different water depths. The results with engine stopped were actually better than expected, since the water flow about the ship's rudder must have been greatly reduced with the propeller dragging.

### Rudder and rpm effects on stopping

In general the strongest observed effect of shallow water on stopping was the much greater tendency for the ship's stern to swing to port as it comes to a halt. A possible explanation is that the sea bottom tends to restrict the forward-directed propeller outflow (when stopping), causing more flow around the sides of the vessel, and therefore exaggerating the usual propeller asymmetry side-force effects.

Although subjective, one of the more interesting trials was the controlled stopping maneuver, that is, holding the heading constant throughout. It had been assumed that success would show a clear benefit of the controlled stop over simple stopping with constant astern rpm. Instead, the results showed that from a prudent slow approach speed, as is normally used in approaching a single-point mooring (SPM), the simple stop developed smaller lateral deviation, and a much shorter headreach. This suggests that the only advantage of the controlled stop from a slow approach is that the desired heading is maintained. However, if the trial maneuver had been designed to maintain a desired straight trackline instead of heading, the trackline probably could have been achieved with substantially less lateral deviation than that of the simple stop. The controlled trackline also corresponds more closely to actual operations in a channel or approaching an SPM. The gradual drift of the ship to the left during the controlled stop may be explained by the following considerations:

(a) With reversed propeller rotation, a side force to port develops, causing the stern to drift to port. To counter this, left rudder is used.

(b) If the sum of the side forces due to reversed propeller and left rudder are equal in magnitude, and have the same center of pressure, no lateral drift will result.

(c) Lateral drift to port did occur, however, even though no heading drift occurred. Therefore, although the yaw moments due to astern rpm and left rudder angle cancelled each other, their side force contributions apparently did not. A possible explanation is that the center of pressure of rudder force is further aft than the center of pressure due to astern propeller rpm. The rudder force acting to starboard could then be smaller than the propeller side force acting to port, and this would result in a small drift to port, as observed.

### Ship speed and water current effects

The corrected turning circle results from tests at different approach speeds show quite similar paths. This verifies that

<sup>7</sup> With controls fixed. See discussion under "Spiral test" in the section on results.

**Table 11 Comparison of *Esso Osaka* data with previous shallow-water results**

SHIP	Depth/Draft		Turning-Circle Tactical Diameter (ship lengths)	
<i>Esso Osaka</i> (Present trials)	1.2	1.5	4.9	3.3
<i>Magdala</i> (Ref. [6])	1.2	1.5	...	3.5
<i>Esso Bernicia</i> (Ref. [5]*)	1.2	1.6	...	2.8
<i>Esso Bernicia</i> (HY-A PMM model)	1.2	1.7	4.2	2.2
		deep		3.1
SHIP	Depth/Draft		Z-Maneuver 1st Yaw Overshoot (deg)	
<i>Esso Osaka</i> (Present trials)	1.2	1.5	7.8	11.2
<i>Esso Bernicia</i> (Ref [5]*)	1.2	1.6	...	22
<i>Esso Bernicia</i> (HY-A PMM model)	1.2	1.7	2.5	6
		deep		...

\* Speed of approach 14.7 knots.

there is little speed effect on turning geometry at low Froude numbers (below 0.10 in these trials). With water current present, however, the slow-speed maneuvers suffer much greater distortion than high-speed maneuvers because of the translation of the current. Wind, if strong enough to be important, would also affect maneuvers at slow speed much more than those at high speed. For a given ship configuration and draft, the ratio of wind speed to ship speed is important. These facts are well understood by shiphandlers as they judge minimum safe maneuvering speeds. For further discussion of variable water current effects, see Appendix 9.

#### Comparison with previous model and ship data

As indicated in the Introduction, previous model and full-scale maneuvering trial data in shallow water were not always satisfactory. To illustrate this, Table 11 provides comparative data from available shallow-water maneuvering trials of other VLCCs: *Esso Bernicia* [5] and *Magdala* [6]; and from predictions made of *Esso Bernicia* maneuvers by Hy-A Laboratory in Lyngby, Denmark (using planar motion mechanism model tests for hydrodynamic coefficients and computer calculations; unpublished).

The comparisons show that while the model-based predictions of tactical diameters do not differ greatly from the *Esso Osaka* or other full-scale results, the Hy-A Z-maneuver first yaw angle overshoot predictions for *Esso Bernicia* are much smaller than the results from the *Osaka*. Also *Bernicia* model and ship results do not compare very well, at least for the Z-maneuver in medium water depth.

Results of Hy-A model-based computer calculations of *Bernicia* spiral tests in different water depths predicted no loop in any of the depth-to-draft ratios tested: 1.2, 1.7 and 2.0. On the other hand, the *Bernicia* trials [5] show almost identical loops in spiral tests in shallow water (depth/draft = 1.4) and deep water. Although some differences should be expected due to somewhat different hull and rudder configurations, these comparisons support the original contention that insufficient shallow water maneuvering trial data existed at the outset of this program.

## Conclusions

1. The present trials provided a quantity of new information regarding the maneuvering characteristics of a ship in shallow water. Both research- and operational-type maneuvers keyed to large tankers were made. In the process it was found that the single-screw *Esso Osaka*, a 278 000-dwt tanker, was able to maneuver reliably and predictably in all tested water depths, even with engine stopped as when simulating maneuvers after a propulsion failure.

2. Distortions of the flow about the hull of a ship in shallow water were found to have an important effect on maneuvering motions. For example, trial measurements indicated that:

- In shallow water, turning circle tactical diameters will increase by as much as 75 percent with 20 percent underkeel clearance, while drift angle and related speed loss will reduce relative to turning in deep water. With 50 percent bottom clearance, the changes from deepwater turning are much less. The effects on turning circle diameter are significantly greater than expected, based on previous model predictions and full-scale trials.

- Checking and counterturning ability are reduced as water depth decreases to an intermediate depth (50 percent bottom clearance in the trials) and then, with 20 percent bottom clearance, these qualities increase to better than in the deepwater case. This is closely related to the apparent reversal in maneuvering dynamic stability (with controls fixed), as is suggested by the present spiral test results. Again, previous model and full-scale trials in shallow water failed to disclose this.

- The greatest effect of decreasing water depth on the stopping of a single-screw tanker, from slow speed, appears to be an increase in yaw rotation to the right as it comes to a halt. In the present trials the heading change increased from 18 to 50 to 88 deg in deep, medium and shallow water, respectively.

- Accelerating turns increased in diameter in shallow water, but to a lesser extent than did the conventional turns. On the other hand, coasting turns suffered a trend reversal. The widest coasting turn path was in the medium water depth and the least was in deep water.

3. Trials to show the effects of a shiphandler's control of propeller rpm during maneuvers provided useful insights. For example:

- Accelerating turns confirmed that "kicking" ahead the rpm when moving at reduced speed significantly increases turning ability.

- The coasting Z-maneuver demonstrated conclusively that the subject VLCC could continue maneuvering in response to rudder actions even with the engine stopped. It also showed that this very large vessel could continue maneuvering while coasting down to speeds less than 1.5 knots. This result should be encouraging to those concerned with the maneuvering safety of tankers. The magnitudes of yaw angle overshoots, although different from those with engine operating, showed directionally similar tendencies with respect to effect of water depth.

- As expected, rudder control of the single-screw vessel was eventually lost during stopping maneuvers with constant astern rpm, although the vessel's final orientation was to some extent affected by early rudder action. Although the ship's heading could be maintained constant during a "controlled" stop by using various engine orders, it was at the expense of increased stopping distance and greater lateral drift.

Taken together, the points of Conclusion 3 emphasize that maneuverability is improved when rpm is increased and degraded when reduced. Knowing this, the prudent shiphandler will usually look for the slowest safe speed in a critical maneu-

vering area. If then required to speed up, maneuverability will increase instead of being degraded if unexpectedly required to slow down.

4. Other technical conclusions, which are mainly confirmatory, are

- Speed of approach has a minor effect on the geometry of the conventional turning circle of a large tanker within the maneuvering speed range (5 to 10 knots).
- Asymmetry of maneuvers to the left and right-hand, caused by single-screw propeller rotation, is greatest when rpm ahead or astern is large relative to ship speed. This is the case in slow-speed stopping and in accelerating turns. It is minor in the case of conventional turns.

5. Technical data from the present trials should be adequate for validating model and analytical methods for predicting ship maneuvering in deep and shallow water under operational-type conditions at slow speeds, and for meeting all of the other objectives of the program.

### Recommendations

After comparing the results and conclusions of the present trials against the objectives, it is recommended that the sponsors encourage and support efforts to:

1. Validate present-day procedures for developing mathematical models by performing experiments with captive models, making computer predictions, comparing these with the present full-scale trial data and then, if necessary, improving the prediction techniques.

2. Establish the validity of large hydraulic models in applicable areas. These models, which include large self-propelled model ships, are being used under conditions where irregular side and bottom boundaries and water currents are believed important.

3. Determine to what extent full-scale trial data can be useful for developing maneuvering information for posting in the wheelhouse of vessels, as is recommended by IMCO and required by U. S. Coast Guard.

### Acknowledgments

The trial program reported here is the product of extensive industry/Government cooperation among the sponsoring organizations, advisory groups, and trial participants listed in Appendix I. Contributing individuals most directly involved were W. O. Gray of Exxon Corporation who, after realizing the need, drew together the sponsors; P. M. Kimon, who had overall Exxon responsibility for the program; Dr. P. D. Fitzgerald, who shared in the onboard direction of the trials; and Captain G. Gomez who acted as supernumerary captain. Outside of Exxon, grateful acknowledgement is given to Mr. R. Falls, Maritime Administration's technical representative, and CDR W. D. Snider, the Coast Guard's project monitor. Both gentlemen were closely associated with the trials from planning through execution.

Key persons among the subcontractors were Mr. L. L. Hundley, who headed the DTNSRDC Full Scale Trials Branch team, and Messrs. J. W. Feeney, W. E. Walsh, and R. Eustis of Sippican Corporation, who provided all oceanographic services, and personally carried out many long days of diving and current measurements from a small inflatable boat, with enduring humor. We acknowledge also the services of R. Boehme of AMETEK, Straza, who modified the ship's Doppler sonar for precision depth sounding and otherwise assisted, and Messrs. J. Carpenter and J. Webb of Decca Survey for their competent position-fixing services.

We acknowledge the excellent cooperation and skills of the master of the *Esso Osaka*, Captain I. Basterrechea, and his crew,

all of whom carried out their duties and our requests throughout the trials with good humor and with traditional good seamanship. Finally, the captains and crews of the assisting Coast Guard units are gratefully acknowledged.

### References

1. Eda, H. and Crane, C. L., Jr., "Steering Characteristics of Ships in Calm Water and Waves," TRANS. SNAME, Vol. 73, 1965.
2. Mandel, P., "Ship Maneuvering and Control," Chapter 8 of *Principles of Naval Architecture* (Revised), SNAME, 1967.
3. Crane, C. Lincoln, Jr., "Maneuvering Safety of Large Tankers: Stopping, Turning, and Speed Selection," TRANS. SNAME, Vol. 81, 1973.
4. SNAME Panel H-10, "Proposed Procedures for Determining Ship Controllability Requirements and Capabilities," SNAME STAR Symposium, Washington, D. C., 1975.
5. Clarke, D., Patterson, D. R., and Wooderson, R. K., "Maneuvering Trials with the 193,000 Tonne Deadweight Tanker *Esso Bernicia*," Trans. RINA, 1973.
6. de Lambilly, R., Arnand, F., and Jourdain, M., "Les Essais a la mer du Pétrolier de 213,000 tonnes *Magdala*."
7. The Sippican Corporation, "VLCC Shallow Water Maneuvering Site Selection," Report No. R-830 (submitted to Exxon International Co.), June 1977.
8. Feeney, James W. and Walsh, William E., "VLCC Shallow Water Maneuvering Sea Floor Survey," The Sippican Corporation, Report No. R-844 (submitted to Exxon International Co.), Sept. 1977.
9. Feeney, James W. and Walsh, William E., "VLCC Shallow Water Maneuvering Ocean Current Study," The Sippican Corporation, Report No. R-875, March 1978.
10. Gertler, M. and Gover, S. C., "Handling Quality Criteria for Surface Ships," First Symposium on Ship Maneuverability, David Taylor Model Basin, DTMB Report 1461, Bethesda, Md., 1960.
11. Wagner Smitt, L., "The Reversed Spiral Test," Hydro-Og Aerodynamisk Laboratorium, Report No. Hy-10, Lyngby, Denmark, 1967.
12. Fujino, M., "Maneuverability in Restricted Waters: State of the Art," University of Michigan, Department of Naval Architecture and Marine Engineering Report No. 184, Ann Arbor, Mich., Aug. 1976.
13. Tsakonas, S., Kim, C. H., Eda, H., and Jacobs, W. R., "Lateral Stability Derivatives of a Ship in Shallow Water," Davidson Laboratory, Stevens Institute of Technology, Report SIT-DL-77-1905, Hoboken, N. J., March 1977.
14. Hess, Felix, "Rudder Effectiveness and Course-Keeping Stability in Shallow Water: A Theoretical Model," University of Adelaide Report No. H-01, Adelaide, Australia, 1977.
15. Newman, J. N., "Talk on Ship Maneuvering in Shallow and/or Restricted Water," Joint Meeting of SNAME Panels H-5 and H-10 during planning of *Esso Osaka* Shallow Water Maneuvering Trial Program, at the David W. Taylor Naval Ship Research and Development Center, Bethesda, Md., 30 March 1977.
16. Hooft, J. P., "Maneuvering Large Ships at Shallow Water," Parts I and II, Netherlands Ship Model Basin, Wageningen, The Netherlands, 1973.
17. Crane, C. L., Jr., "Maneuvering Trials of the 278,000 DWT *Esso Osaka* in Shallow and Deep Waters," Exxon International Company, Jan. 1979.

### Appendix I

#### Sponsors, subcontractors, and participants

##### Sponsors

U. S. Government agencies:

U. S. Coast Guard, Department of Transportation  
Maritime Administration, Department of Commerce  
American Institute of Merchant Shipping, contributing members:

Amoco Shipping Company  
Chevron Shipping Company

El Paso LNG Company  
Exxon Company, U. S. A.  
Gulf Trading & Transportation Company  
Interstate and Ocean Transport Company  
Mobil Shipping & Transportation Company  
Shell Oil Company  
Standard Oil Company of Ohio  
Sun Transport, Inc.  
Texaco, Inc.

#### Contractor

Exxon International Company, Tanker Department

#### Subcontractors

David W. Taylor Naval Ship R&D Center, Full-Scale Trials  
Branch, Carderock, Maryland  
Sippican Corporation, Sippican Oceanographic Division,  
Marion, Massachusetts  
Decca Survey Systems, Inc., Houston, Texas  
AMETEK, Straza Division, El Cajon, California

#### Additional participants, advisors, etc.

Exxon Company, U. S. A., Baytown Branch, Marine Department  
Hydronautics, Inc.

Maritime Administration, Department of Commerce:  
Division of Maritime Technology  
National Maritime Research Center  
Massachusetts Institute of Technology, Ocean Engineering  
Department  
Stevens Institute of Technology, Davidson Laboratory  
The Society of Naval Architects and Marine Engineers:  
Panel H-10 (Controllability)  
Panel H-5 (Analytical Ship-Wave Relations)  
U. S. Coast Guard  
Headquarters Staff  
Commander Eighth Coast Guard District  
Cutters *Blackthorn*, *Durable* and *Point Monroe*  
Patrol Aircraft, Air Station Corpus Christi

Draft, molded, at trials	21.73 m	(71.3 ft)
Draft, extreme, at trials	21.79 m	(71.5 ft)
Trim in still water, at trials	0	0
Displacement at trials	319 400 mt	(314 410 LT)
Longitudinal CG at trials; forward of amidship	10.30 m	(33.8 ft)

#### Engine

##### Propulsion Machinery

Hitachi Impulse 2-Cylinder Cross-Compound Main Steam  
Turbine:

continuous full output, hp	36 000 at 82 rpm
service output, hp	35 000 at 81 rpm

##### Main Turbine Controls (Bridge Telegraph)

Operation	Program control	Revolution Feedback Control	Notes
ahead	yes	yes, below 60 rpm no, 60 rpm and above	rpm indicator inaccurate read rpm indicator
astern	yes	yes	read rpm indicator
crash astern	no	no	astern full revolutions quickly attainable

##### Propeller

Single, right-handed, 5 blades

diameter, m (ft)	9.1 (29.86)
propeller pitch, m (ft)	6.507 (21.35)
expanded area, m <sup>2</sup> (ft <sup>2</sup> )	44.33 (477.15)
projected area, m <sup>2</sup> (ft <sup>2</sup> )	37.22 (400.62)
disk area, m <sup>2</sup> (ft <sup>2</sup> )	65.0 (699.64)
pitch ratio	0.71505
expanded area ratio	0.682
projected area ratio	0.572
rake angle	4 deg 24 min

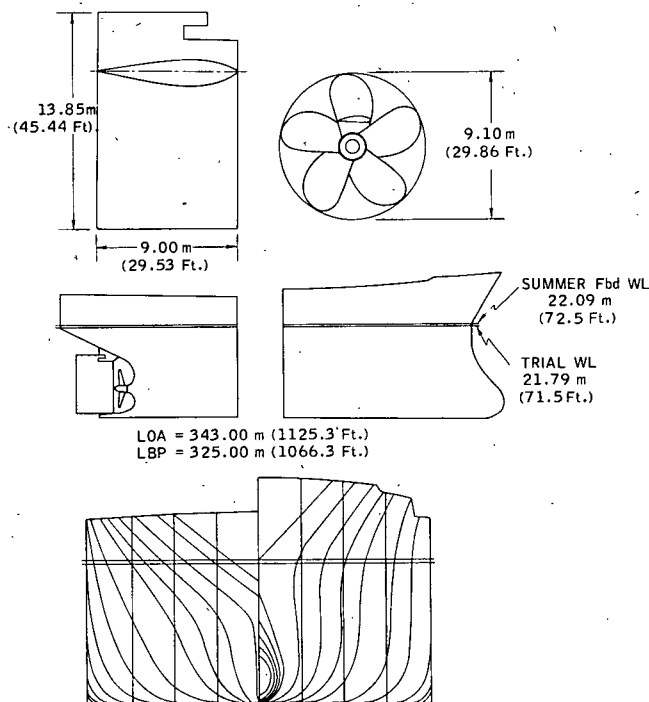


Fig. 22 Sketches of Esso Osaka rudder, propeller, hull end profiles, and body lines

## Appendix 2

### Esso Osaka particulars (Fig. 22)

#### Hull

Length overall	343.00 m	(1125.3 ft)
Length between perpendiculars	325.00 m	(1066.3 ft)
Breadth molded	53.00 m	(173.9 ft)
Depth, molded	28.30 m	(92.8 ft)
Designed load draft, molded	22.05 m	(72.3 ft)
Assigned summer freeboard draft, extreme	22.09 m	(72.5 ft)
Full load displacement at assigned summer freeboard draft	328 880 mt	(323 740 LT)
Block coefficient, summer freeboard draft	0.831	(0.831)
Bow	bulbous type	
Stern	transom type	
Number of rudders	one	
Rudder area	119.817 m <sup>2</sup>	(1289.67 ft <sup>2</sup> )

The trials were made at a slightly reduced draft, altering draft related figures as follows:

## Appendix 3

### Trial site selection

Selection and surveys of sites for the shallow, medium and deepwater trials that would satisfy all requirements listed in the main text were made in two phases:

Phase I was a literature search of documented National Ocean Surveys and other bathymetry, oceanographic and meteorological data. This included discussions with university and oil company oceanographers, fisheries experts, and fishermen. The search centered on the Galveston, Mobile, Panama City, and Suwanee areas of the Gulf of Mexico and an ocean area off Georgia. This work and later survey and trial oceanographic measurements were done by oceanographers and divers of Sippican Corporation.

Phase I resulted in the preliminary selection of shallow- and medium-depth trial sites in the Galveston area within the limits of the planned Seadock deepwater port survey area, as shown in Figs. 23 and 24.

Phase II was a field confirmation of water depth, current, and sea floor topography by a precision survey of the shallow- and medium-depth sites [8]. Soundings and side-scanning sonar continuously mapped the sea floor and assured that no bottom obstruction existed. This was done just three weeks before the trials to minimize the possibility of a new obstruction arising in the interim.

These data also gave the ship's master confidence when maneuvering in shallow water in an area not usually visited by large tankers. Reference [8] also describes and illustrates the construction and deployment of 12 expendable Sippican current drifters used to check water current drifts at two depths during the bottom survey.

The criteria for the deepwater trial site were the same except that the water depth criterion was to exceed only four times the ship's draft, but be within reach for water current meter moorings. The area used was about 20 miles (32 km) south of the medium water depth area. References [7] and [8] report details of the site selection process.

Details of site selection Phases I and II were reported in detail by Sippican, and can be made available [7, 8].

## Appendix 4

### Trial instrumentation

Ship's heading was obtained from the gyro repeater circuit normally used to drive the starboard wing heading indicator. This circuit was connected to a step motor brought onboard for the trials. This motor receives 70-V pulses from the gyro-compass in response to heading changes in increments of 1/6 of a deg. The shaft of the step motor was coupled to an ac synchro which controlled a solid-state synchro converter to provide a dc signal proportional to ship's course.

Rudder angle was obtained by paralleling the ship's rudder angle indicator on the bridge. This ac synchro signal was input to a solid-state synchro converter, producing a dc voltage proportional to rudder angle. A rudder angle calibration was performed using the ship's quadrant as a reference. This calibration, plus checks made during the course of the trials, indicated that the data recorded were within  $\pm 0.4$  deg relative to the quadrant position.

Propeller rpm was obtained from the output of a tach generator geared to the main shaft. The rpm signal, equal to 0.1 V per rpm, was input to a high-impedance operational amplifier to avoid affecting the ship's indicating system. Calibration

of the rpm signal was accomplished by counting shaft revolutions for one-minute intervals while on a steady course. Repeated checks on this signal indicated an rpm accuracy of better than  $\pm 0.2$  rpm.

Ship's ground speed components were obtained from the ship's MRQ2036C sonar Doppler speed indicator. The 0.25-V-per-knot signal was coupled to the recording system via an operational amplifier to avoid changing the normal operation of the Doppler system. Bow and stern lateral speeds were also obtained from the Doppler instrument. Since the lateral speed data are present only in digital form and each speed reading consists of three digits and a polarity indication, a total of 27 data lines was required to obtain these two signals. Additionally, three control lines were necessary to insure that valid data were available when the Doppler was sampled. The recording system initiated a "handshake" procedure when speed data were requested. A gate signal was transmitted to the Doppler that caused the Doppler to complete its current update cycle and hold. When the current update was completed, a flag signal was generated causing the data to be transferred to the recording system. The Doppler system was then allowed to return to its own sample rate. The gate/flag handshake cycle required less than one millisecond (ms) for completion.

Depth under the keel was obtained by modifying the Doppler sonar. The modification, accomplished by an Ametek-Straza engineer, resulted in the repetitive generation of an additional electrical pulse at the aft Doppler transducer. The time difference between this pulse and its echo was indicative of the time required for the pulse to traverse to and from the sea bottom. The recording system automatically converted each interval measured to depth in feet by allowing for the 30-deg angle of pulse travel made with the vertical and the speed of the pulse through the water on its round trip. A period of 5.47 ms, for example, would be converted to a depth of 12 ft (3.6 m). The Doppler modification performed quite well, with a valid return signal being obtained about 98 percent of the time. A larger percentage of false returns occurred during parts of the shallow-water trials when the water was clouded by large amounts of silt stirred up from the ocean floor, such as with astern rpm at very slow ship speeds.

The output of the ship's turning rate indicator was recorded, in addition to the output of a rate gyro purchased specifically for these trials. Rate gyro No. 2, with a range of  $\pm 3$  deg per second, was purchased from Condor Pacific Industries as a backup for the ship unit because of the importance placed on this measurement. Measurements obtained during the trial indicated larger turning rates by the carefully calibrated Condor unit. The rate of turn, checked by derivation from the time rate of change of heading signal, indicated that the ship's turning rate indicator is in error; reading too low.

Wind velocity was measured using a DTNSRDC anemometer installed on the ship's radar mast. It was not deemed feasible to obtain wind velocity from the ship's wind measurement system since the ship's wind transmitter is a dc selsyn motor. These motors are somewhat rare in the United States and attempts to locate one were futile.

Ship position was obtained by a Decca Hi-Fix tracking system. Two Decca Survey Systems engineers operated their own equipment. Due to problems encountered attempting to interface to the Decca system, the position data were recorded on a different medium than the data obtained by the main recording system. The update rate of the tracking system was, however, controlled by the main recording system, thus providing a common time base.

### Recording instrumentation

The recording speed and the number of data channels specified for these trials resulted in selection of the Hewlett-



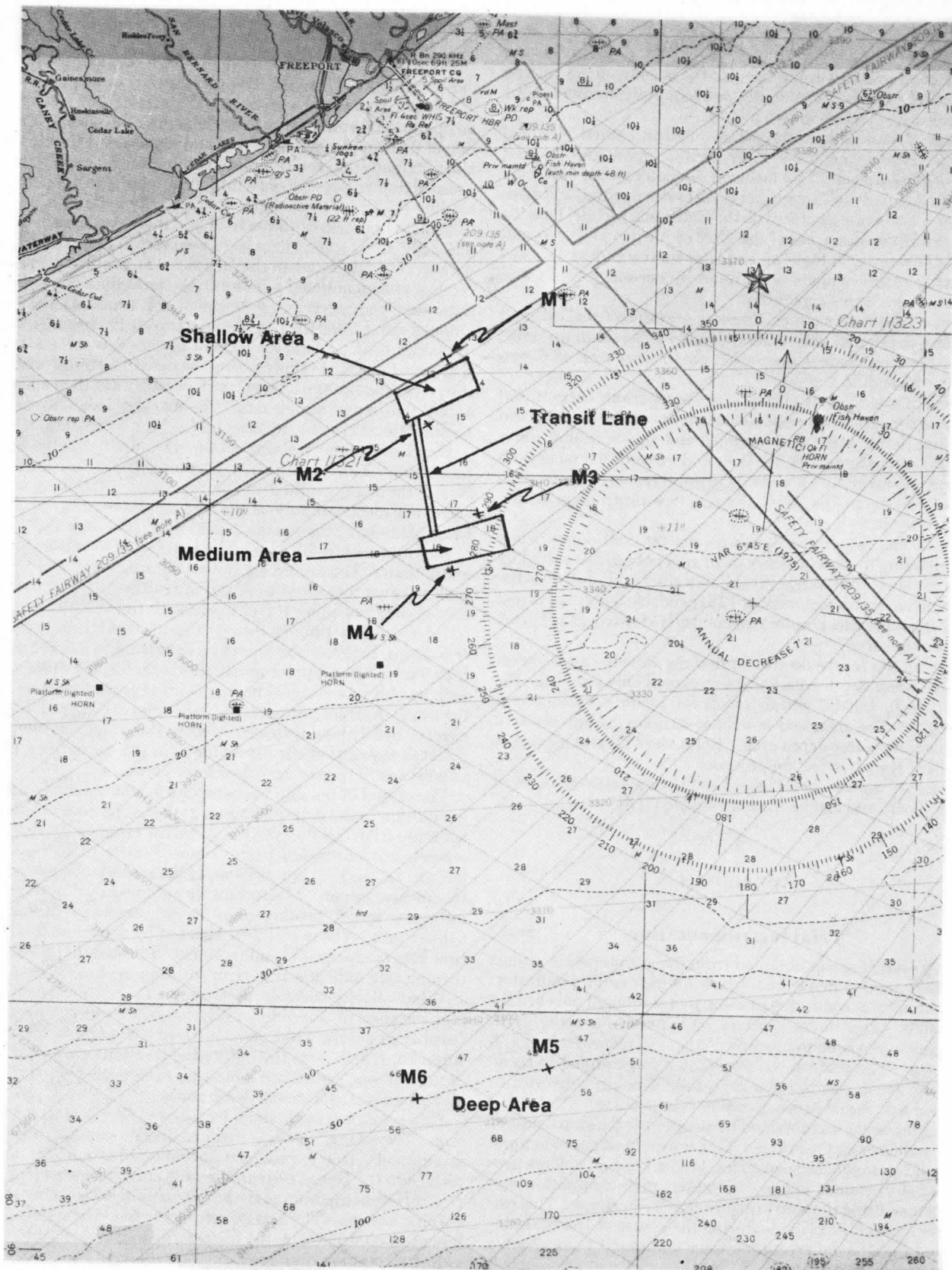


Fig. 23 Shallow, medium, and deepwater trial sites, and moored current meter locations



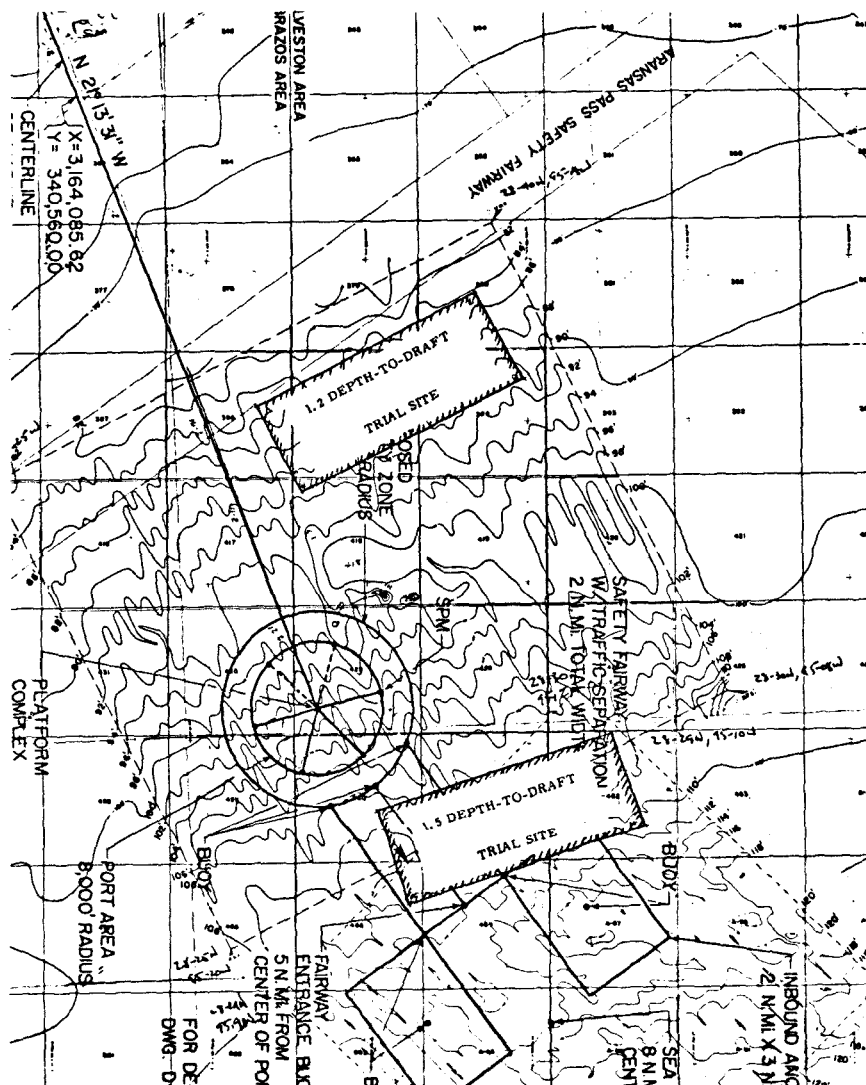


Fig. 24 Shallow and medium-depth sites selected within the 1974 Seadock survey area

Packard 9825A Desktop Computer as the controller for the recording system. The various analog and digital signals were coupled to the controller via the Hewlett-Packard 6940B Multi-programmer. The multiprogrammer was wired to collect the required data in addition to controlling the input devices via the "handshake" procedure previously described.

The permanent recording medium was a flexible disk drive. The disk drive is a random-access mass storage device with a capacity of up to 58 560 data points per diskette. With a sampling rate of once every two seconds, each diskette could contain over two hours of data.

In order to spot check the validity of all data channels during the trials, a sample of the data being recorded was printed every 40 sec on a high-speed thermal printer. This output provided a quick look at the response of the ship for the various maneuvers. By this means any suspect data channels could be quickly spotted. At the conclusion of a run additional data could be printed by accessing a special data output program.

In addition to the previously discussed data channels, time of day (hours, minutes, seconds), an event marker, and a scan interval count were also recorded during each run. The event marker provides a method of locating precise execution points of the run, such as Start Run, Execute, or End Run. The data

scan number allows immediate determination of the number of times each data channel was sampled.

Installation of all equipment went smoothly with the exception of the Decca interface problem previously mentioned. No ship system malfunctions were noted as a result of the external test connections. The additional equipment and personnel in the wheelhouse did, however, cause the ambient temperature to become unbearable. This problem was solved prior to start of the trial with the installation of a household-type window air-conditioning unit on each side of the wheelhouse. The addition of these units created a comfortable working environment for the wheelhouse personnel, and in all probability prevented instrumentation breakdowns.

## Appendix 5

### Water current measurements, and set and drift corrections

#### General

Water current measurements are difficult to make and to describe when variabilities or incoherencies in water motion



**Fig. 25** Endeco Type 105 current meter being leveled by a Sippican diver

exist and measurements are limited in space and time. The problem, difficult even in open ocean where currents are influenced primarily by winds and sloping density surfaces, is compounded in shallow water by such influences as transient winds, tidal phenomena, boundary currents and rapidly changing bottom topography.

Because of this, the physical oceanography of the continental shelves region adjacent to the major land masses out to a water depth of approximately 600 ft (183 m) has been largely neglected in favor of the deep ocean regions and the resolution of basic problems in general circulation.

Based on the high variability of currents encountered during the brief Phase II drifting buoy survey of the present program, it was decided to continuously monitor currents during the maneuvering trials of the *Esso Osaka*. Evaluations were made of the type and number of current measurements, the locations of current meter moorings and the logistics of the current measurement operation. The complete report by Sippican Corporation [9] discusses these considerations in detail. All decisions were made with an eye toward maximizing useful information while minimizing cost.

### Instrumentation and procedures

**Current meters and mooring system**—Currents were measured using Eulerian current meters fixed to mooring systems. This was done because of the time variability, and the difficulty of continuously plotting drifting buoy tracks.

Endeco Type 105 current meters were chosen (Fig. 25). The meters are approximately 2.5 ft (0.76 m) in length, and the ducted impeller (fan-shaped section) is approximately 1.5 ft (0.45 m) in diameter. The meters translate impeller revolution into current speed and record the data on photographic film at half-hour intervals. Current direction is obtained from an internal magnetic compass and is recorded on photographic film at the same time as the speed data. As recorded, the current speeds constitute cumulative averages over the half-hour measurement cycle, while the directions are instantaneous and correspond to the exact time that the data are recorded on the film. The manufacturer's stated speed accuracy is  $\pm 3$  percent of full scale or approximately 0.1 knots for the speed range used during the maneuvering trials. Directional accu-

racy is stated as being on the order of 10 deg of the compass.

The mooring configuration used is fairly standard for shallow-water current installations and incorporates several important features. The current meters were tethered to the stainless steel mooring cable at depths of 30 and 70 ft (9 and 21 m).

The current meters used had no provision for on-scene data readout. To obtain the data record, the photographic film was processed and decoded by the manufacturer. In order to provide for some real-time current input to the maneuvering trials, an Endeco Type 110 remote reading profiling current meter was also employed. Although less accurate than the permanently moored meters, it is useful when immediate knowledge of the currents is necessary. It is also a useful device for testing point-to-point variability across an area. The profiling meter contains a pressure/depth sensor and a temperature sensor in addition to the current speed and direction sensors. To obtain a data record from the profiling meter, it is lowered from an anchored vessel using an electromechanical cable connected to an on-deck instrument panel. Readings of ocean temperature, current speed and current direction are then taken at the desired depths.

During the trials the profiling current meter was employed in both the shallow and the medium-depth areas where it was practical to anchor a small boat. The profiling meter proved a valuable supplement to the permanently moored meters and enabled collection of temperature profiles. The temperature profiles were useful in the water current data analysis because of the stratification displayed.

**Mooring locations**—One of the disadvantages of dealing with fixed-point measurement devices is the difficulty of relating measurements at the fixed point to the mean motion, especially in shallow-water areas. Knowledge of the currents over an area of approximately 10 mile<sup>2</sup> (26 km<sup>2</sup>) was of interest in both the shallow and the medium-depth sites and over a somewhat larger area at the deep site.

Precise knowledge of the currents over the areas in question would have required many moorings of several current meters each. As a compromise, moorings were located as shown in Fig. 23. Two moorings per area were located one-quarter mile (0.4 km) from the area boundaries in both the shallow and the medium-depth areas. Adjacent to the deep area the two moorings were located on the 50-fathom (91.44 m) curve and separated by approximately five nautical miles.

The current meters were deployed and recovered by Sippican divers, who took the meters to the appropriate depth and attached them to the stainless steel mooring cables using the manufacturer's clamp-and-swivel arrangement.

After maneuvering trials were completed in a given area, the meters were recovered and moved to the next area. Because of the time required for recovery and redeployment, it was often impossible to have all four current meters in place by the time maneuvering trials recommenced in a new area, but monitoring time missed was minimal.

A small, 14-ft inflatable rubber boat with a 20-hp (14.9 kW) motor was used as a diving platform. However, nearly constant support in locating the moorings and in protecting the moorings from shipping traffic was provided by Coast Guard vessels assigned to the maneuvering trials.

During the maneuvering trials two of the original moorings were lost completely and two others were at least tampered with, probably by fishing vessels. Spare mooring material was carried and jury-rig replacement mooring systems were made. No mooring with current meters attached was lost, due to the diligent efforts of the cutters *Durable* and *Point Monroe*, which maintained a continuous watch on the moorings when outfitted with current meters.

All current meters were recovered, and 100 percent data recovery was achieved for the emplacement period.

## Data presentation and analysis

**Profiling data**—Figure 26 shows an example of profiling data collected during the maneuvering trials. Because the small boat had to be anchored when using the profiler, no profiling data were collected in the deepwater area. A total of 21 current and temperature profiles were collected from the shallow and medium-depth areas. During the trials real-time data were radioed to the tanker bridge as they became available. The following general comments can be made concerning the profiling data:

- Changes in the current structure usually corresponded well with changes in the thermal structure.
- Current speeds usually decreased with depth; however, this was not universally true.
- The shallow-water area was generally stratified into two thermal layers, the transition point occurring at 50 to 70 ft.
- The medium-depth area was generally stratified into three thermal layers, the transition points occurring at 20 to 50 ft and 60 to 80 ft.
- On a given day, correlation of current speeds and directions across the areas was good, particularly in the upper layer.

The use of the profiling current meter proved valuable in providing real-time data and allowing for thermal analysis of the areas. Based on the spatial variability revealed by the profiling data, interpolation between current meter moorings for estimates of the currents at other points in the areas is reasonable.

**Moored current meter data**—The most reliable current data gathered during the maneuvering trials were the moored data, because of the method of collection, that is, continuous sampling by the moored current meter system.

Digital records as decoded by the instrument manufacturer are contained in reference [9]. Data were also inspected in other formats for ease in data interpretation. Figure 27 is an example of bar graphs keyed to 45-deg sectors of the compass. This approach was used as one method of examining cross-area and shallow/deep directional correlations among current meters. The bar graphs are plots of data from the shallow M3S versus the deep M3D meters on Mooring M3, showing the generally poor directional correlation that was typical with depth.

In the Phase I site selection an analysis was made of the expected currents, using data reported in a NOAA report on the South Texas Outer Continental Shelf. In that report a comparison was made between currents measured in the Shell Oil Company Buccaneer field and currents measured at the Seadock site. [Both the shallow and medium trial areas were within the Seadock site boundaries, while the Buccaneer platform was some 30 miles (48 km) distant.] As reported in reference [9], similar scales of variability were observed in speed, while directional variability is more marked at the Buccaneer platform.

In reference [9] and [17] the current meter data are presented in various formats, both graphical and tabular.

**Current speed and direction estimates**—In order to apply the current meter data to the tanker maneuvering data, a need existed for estimates of current speed and direction, not at the current meter locations, but at the location of the tanker within the maneuvering areas. Sippican was asked to provide their best estimates of current conditions at 32 positions and times corresponding to average tanker positions during 32 maneuvering runs. The estimates provided are included with those by other methods in Table 12.

The water current estimates are essentially interpolations

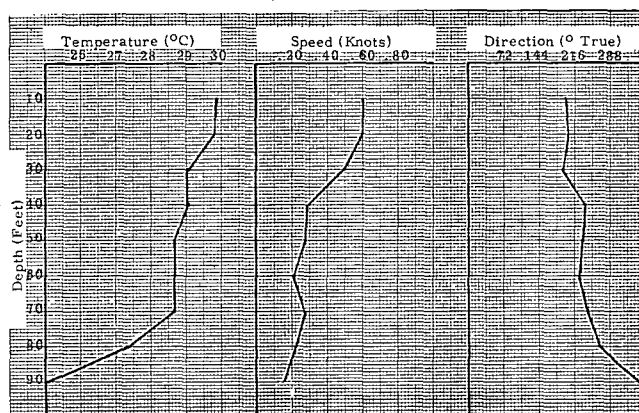


**Fig. 26** Example current velocity and temperature profiles at one location and time during the trials. Medium-depth area, 29 July, 1040 hr

among current meter moorings or profiling data, or both, where appropriate. Subjective confidence estimates have been given based upon current meter accuracies, number of current meters operating, spatial coherence, distances from the moorings, etc. Estimates were not possible for all runs, because some took place before current meters were in the water.

**Diver's observations**—During the deployment and retrieval of the current meters and moorings, the oceanographer/divers frequently entered the water for diving operations. They observed the following:

- Thermoclines measured with the profiler were physically sensed.
- Visibility was excellent, often on the order of 50 to 75 ft except within 10 ft of the bottom, where visibility was reduced to 10 ft.
- The bottom material in both the shallow and medium-depth areas was a hard-packed gray clay.

## Set and drift corrections

Three methods were used to estimate set and drift caused by water currents during the trial maneuvers. These were:

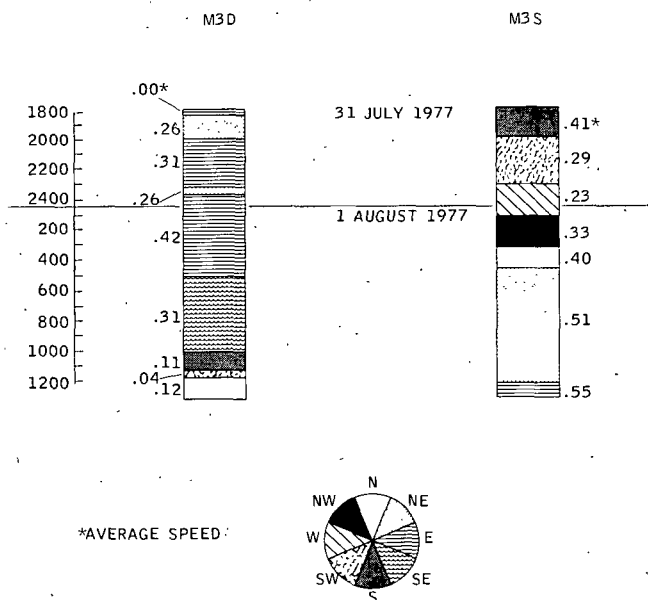


**Fig. 27** Shallow and deep current meter data at Mooring Location M3, showing variation with time at deep (M3D) and shallow (M3S) depths

Table 12 Set and drift values estimated by three methods

WATER CURRENT ESTIMATES; SOURCES AND DATA													
Run No.	Maneuver Code (See Note)	Water Depth	Approach Speed (Nominal)	Sippican Meters				DTNSRDC Circle Data		Doppler Data		Correction Selected	
				V <sub>c</sub>	Shallow Direction	V <sub>c</sub>	Deep Direction	V <sub>c</sub>	Direction	V <sub>c</sub>	Direction	V <sub>c</sub>	Direction
4712	TL	S	7					0.34	104	0.51	055	0.34	104
4512	TL	S	5					0.34	119	0.36	050	0.34	119
4711	TL	M	7					0.43	083	0.08	163	0.43	083
4713	TL	D	7	0.60	065	0.29	116			0.52	074	0.52	074
3722	TR	S	7					0.35	126	0.31	305	0.35	126
3512	TR	S	5					0.32	120	0.27	027	0.32	120
3711	TR	M	7	0.48	102	0.30	055	0.30	086	0.28	038	0.30	086
3723	TR	D	7	0.28	096	0.35	069	0.73	067	0.63	109	0.73	067
3213	TR	D	10	0.68	077	0.73	080	0.29	076	0.55	092	0.29	076
7012	ATR	S	0	0.50	060	0.29	113					0.50	060
7011	ATR	M	0	0.42	172	0.26	047					0.17	134
7021	ATL	M	0	0.57	054	0.25	133					0.33	076
5512	CTR	S	5	0.34	113	0.38	052			0.79	049	0.34	113
5511	CTR	M	5							0.43	243	0.17	134
5513	CTR	D	5	0.42	075	0.62	086			0.52	246	0.52	082
13712	Z20	S	7	0.48	063	0.19	113			0.20	245	0.48	063
13711	Z20	M	7	0.40	196	0.26	054			0.18	060	0.13	156
13713	Z20	D	7							0.61	097	0.66	066
6512	CZ20	S	5	0.37	035	0.18	091			0.27	123	0.37	035
6511	CZ20	M	5							0.30	086	0.30	086
6513	CZ20	D	5	0.71	082	0.92	059			0.63	076	0.80	069
										0.50	094		
12712	Z10	S	7	0.52	068	0.18	068			0.32	098	0.42	068
12711	Z10	M	7	0.37	224	0.43	073			0.20	077	0.10	132
12713	Z10	D	7	0.49	112	0.60	071			0.93	070	0.51	089
9512	SL	S	3.5	0.35	080	0.54	029					0.42	045
9513	SL	D	3.5	0.42	121	0.56	077					0.42	096
8512	SR	S	3.5	0.72	051	0.11	097					0.40	057
8511	SR	M	3.5	0.53	042	0.21	073					0.36	051
8513	CS	S	3.5	0.34	077	0.47	102					0.34	077
11512	CS	S	3.5	0.27	097	0.42	049					0.27	097
11513	CS	D	3.5	0.39	110	1.01	083					0.68	090
10513	SS	D	3.5							0.54	072	0.54	072

Maneuver code:

T = turn  
AT = accelerating turn  
CT = coasting turn

Z20 = 20/20 Z-maneuver  
Z10 = 10/10 Z-maneuver  
S = stop

CS = controlled stop  
SS = steered stop  
L = left  
R = right

Maneuver code:

T = turn  
AT = accelerating turn  
CT = coasting turn

Z20 = 20/20 Z-maneuver  
Z10 = 10/10 Z-maneuver  
S = stop

CS = controlled stop  
SS = steered stop  
L = left  
R = right

1. *Conventional turning-circle method, by DTNSRDC*—This method was applied to turning circles made through 540 deg. It requires the assumption that an almost circular path is swept by the ship after turning 180 deg. The estimated set and drift values are those which must be assumed to provide a corrected path which is a continuation of the circular path defined between the headings of 180 and 360 deg.

2. *Current meter method*—This method assumes that the resultant set and drift of the ship are identical to the water current speed and direction. This is exact only in the ideal case of a uniform current with respect to both time and space, and with no other disturbances. In the case of a temporally and spatially varying current, this method provides only an approximate set and drift. This is the case in the present trials. Furthermore, it is expected that even if the only nonuniformity had been the speed in the boundary-layer gradient near the sea bottom, it could cause a nonuniform set and drift. The reason is that at each different heading the speed gradient might have a different effect on the unbalanced hydrodynamic force and moment components acting on the ship.

Taking due regard of the foregoing, it is believed that if the current variations are not extreme, the estimated average current should provide a reasonably accurate estimate of set and drift.

### 3. Doppler ground speed versus speed/rpm calibration

*method*—Comparisons of measured longitudinal and lateral ship's ground speed components against the speeds derived by rpm calibration (in the same water depth) can provide components of set and drift. This determination requires an accurate speed/rpm calibration as well as steady ship motion conditions on straight path, with negligible lateral drift due to other factors (wind, propeller asymmetry, etc.). The longitudinal component of drift equals the difference between forward speed over ground measured by the Doppler log and speed "through the water" by rpm calibration. The lateral drift is then the observed Doppler lateral speed over ground.

*Comparison of methods and values used*—Table 12 compares set and drift values estimated by the foregoing three methods, and flags those values used for correcting the measured maneuvering data to a nominal "no current" condition. Large differences among data is the rule. Probable reasons for the discrepancies are:

1. Set and drift do not necessarily correspond to water current direction and speed, as just discussed.

2. Current meters were just outside the trial site boundaries, and not at the center of the maneuvers.

3. Doppler data accuracy depends on that of the speed/rpm curves, and how close the vessel speed and rpm are to equilibrium on the approaches.

Despite the relatively large discrepancies, the average current speeds were low.

## Appendix 6

### Example time-history and path plots of *Esso Osaka* maneuvers

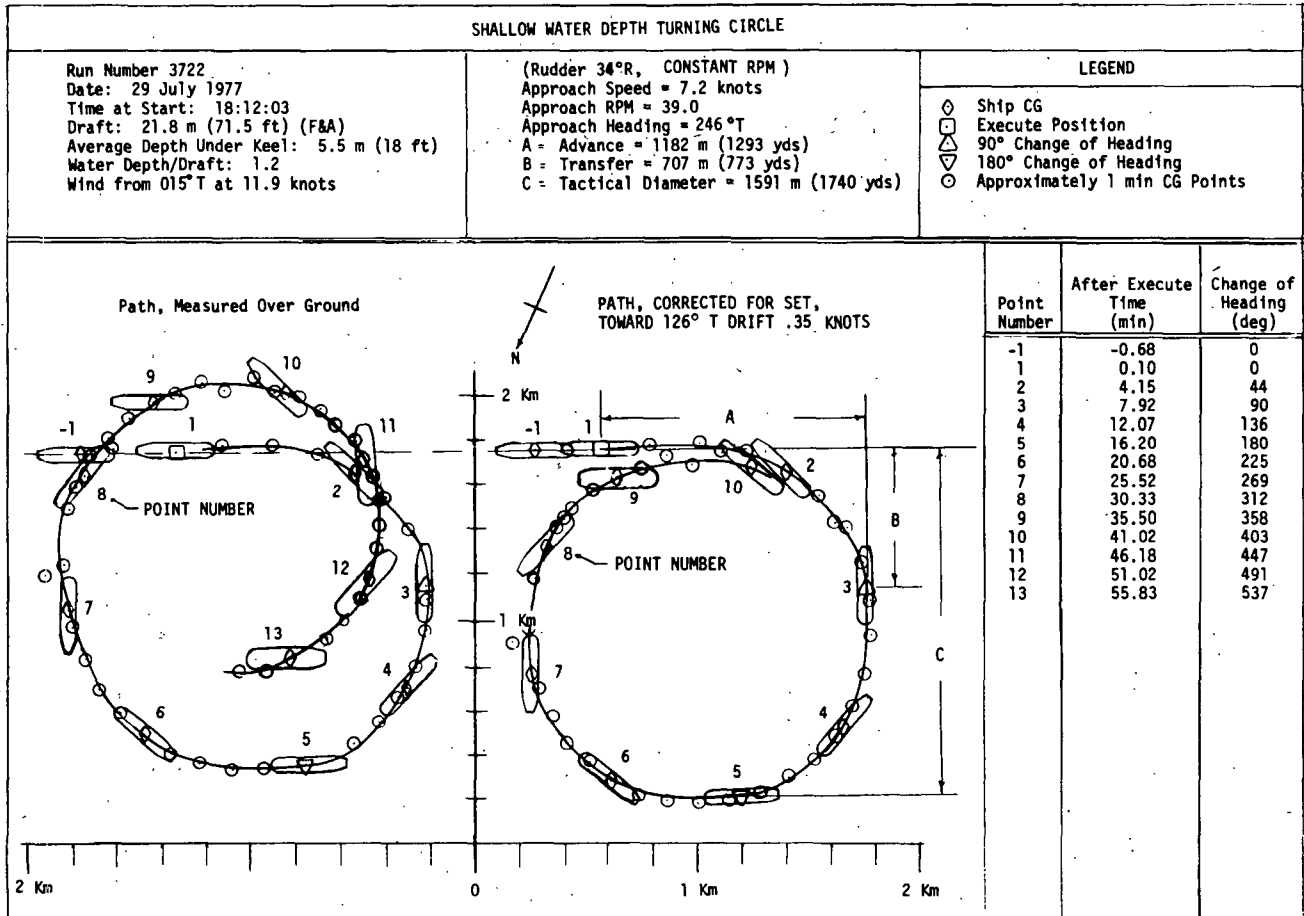
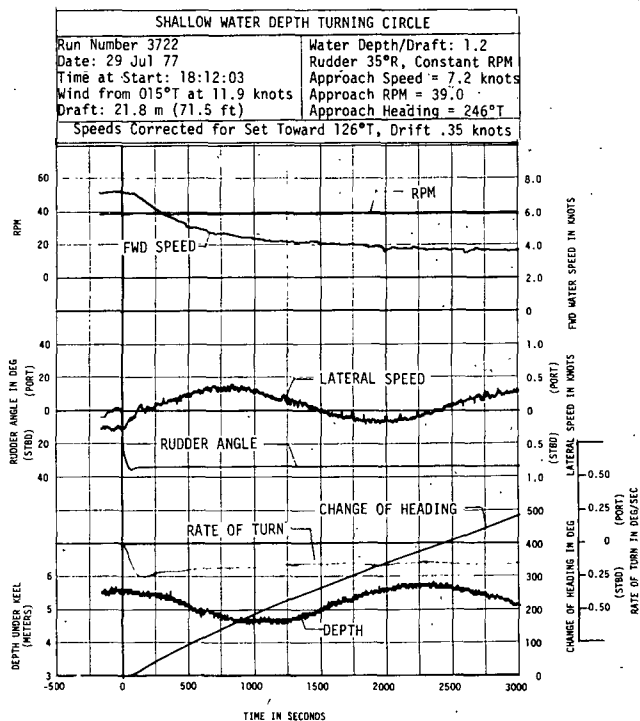


Fig. 28 Shallow water depth turning circle

Fig. 29 Shallow water depth turning circle



## Appendix 7

### Weather and other trial conditions

Date	27 July 1977-3 Aug. 1977
Sea state	0-1
Water specific gravity	1.025
Days out of dock	115
Average water temperature, deg F (deg C)	86 (30)
Average air temperature, deg F (deg C)	88 (31)

### Wind Conditions

Date	Water Depth	Average True Wind Speed (knots)	Average True Wind Direction (deg)
7/27/77	medium	7.4	081
7/28/77	shallow	7.3	176
7/29/77	shallow	10.9	205
7/30/77	shallow	9.7	198
7/31/77	shallow	9.8	221

(continued)

# Wind conditions (continued)

7/31/77	medium	8.9	191
8/01/77	medium	8.5	225
8/01/77	deep	7.3	208
8/02/77	deep	9.1	257
8/03/77	deep	8.8	052

## Appendix 8

### Spiral test record plots

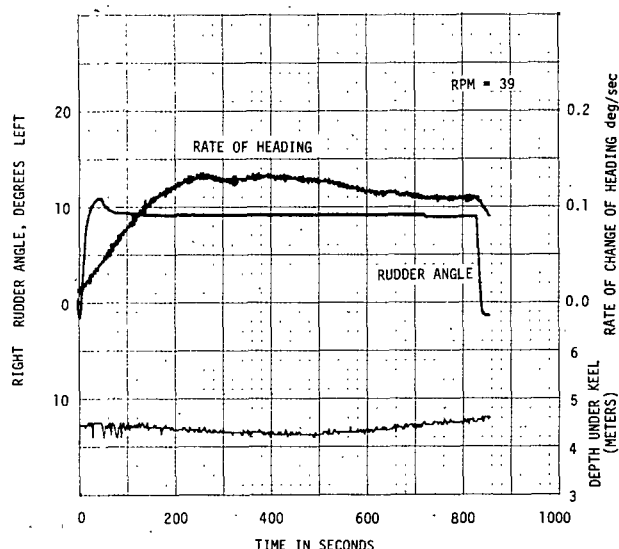


Fig. 30 Example segment of a spiral test record in shallow water, showing time histories of rudder angle, turning rate, and depth under keel

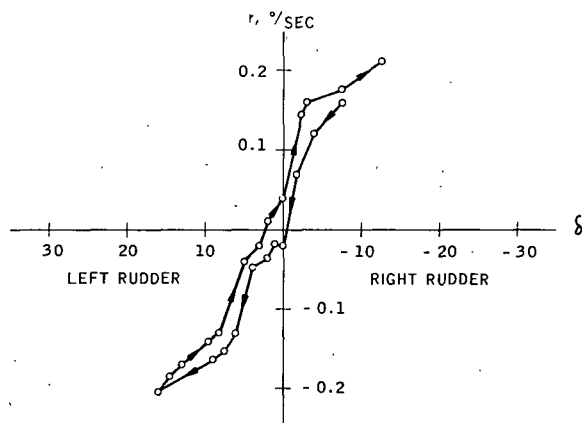


Fig. 31 Spiral test data in the deepwater site ( $h/T = 4.2$ ), showing turning rate,  $r$ , versus rudder angle

## Appendix 9

### Water current effects on maneuvering

Effects of a uniform water current on ship maneuvers are not difficult to determine. A more difficult problem is to under-

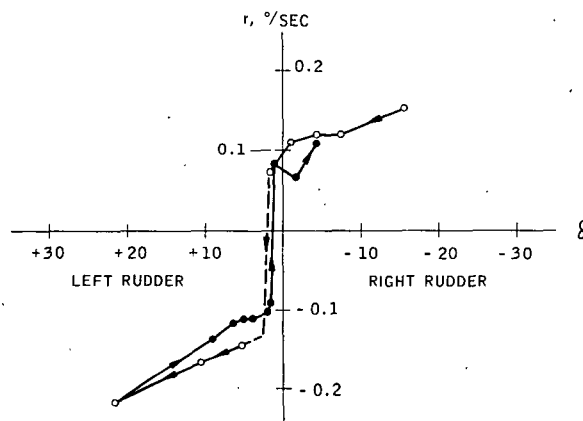


Fig. 32 Spiral test data in the medium-depth site ( $h/T = 1.5$ ), showing turning rate,  $r$ , versus rudder angle

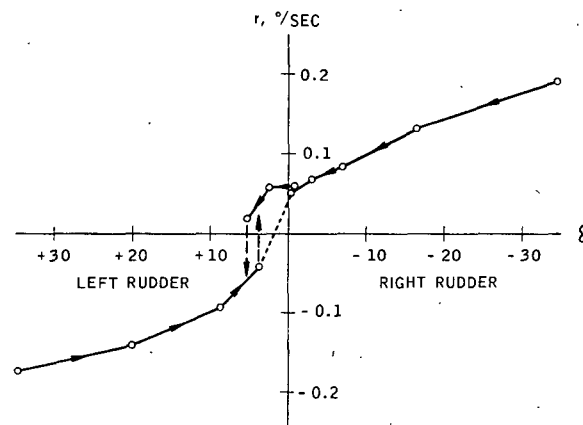


Fig. 33 Spiral test data in the shallow-water site ( $h/T = 1.2$ ), showing turning rate,  $r$ , versus rudder angle

stand the effects of water currents that vary in time and space, such as generally exist in waters restricted in depth and width. As described in Appendix 5, water current surveys were made before and during the present trials, and these showed both time and space variability. In normal maneuvering, time variability is not usually a problem for a shiphandler because of the relatively short time required for individual maneuvers. But space variability can be very difficult to assess even if current diagrams are available, as they are for several waterways along U. S. coasts.

Appendix 5 shows that variability of both water current speed and direction existed with respect to depth in the present trials. How this affected ship maneuvering motions is not fully understood, and further analysis of the present trial results may be desirable. However, the corrections made in this report appear adequate for the purpose of showing the effects of main parameters.

For examples of variability, consider the water current and temperature profiles of the medium depth area shown in Fig. 26 for 29 July at 10:40 a.m. At 3-m depth (10 ft) the current direction was toward 198 deg true and the speed was 0.60 knots. But at a depth about equal to ship's draft of 21.8 m (71.5 ft) current direction was 238 deg and the speed was 0.33 knots. This means that the vessel's speed and direction relative to water

were somewhat different at different depths.

Rigorous predictions of the effects of variable water current on maneuvering are outside the present state of the art. If current speeds are weak relative to ship speed, however, an estimated "average" water current value should suffice, as was used for correcting the present trial data. A more difficult problem in maneuvering is to predict the effects of a sudden

shear current of large magnitude on a vessel moving slowly ahead in a constraint waterway.

In the present trials, an excessive number of current meters would have been required to provide a good understanding of the current environment. Both the cost and the interference they would have caused with trial maneuvering were considered unacceptable.

## Discussion

### David Clarke,<sup>8</sup> Visitor

The author is to be congratulated on the overall presentation of this paper, where he has compressed an enormous amount of valuable information into a relatively small space and still managed to keep his treatment of the subject lucid and comprehensible.

The enormous number of maneuvers performed and the great wealth of data recorded will undoubtedly make this ship and these trials into the mathematical modeler's test piece for years to come, probably taking over the role of the *Compass Island*. Although a great deal of information is made available here, the author will agree that the actual time-histories of the various system states, yaw rate, sway velocity, rudder angle, and so on are what the mathematical modeler would require to be able to make the best use of all the trial data. While I realize that space precludes such data being included here, I would ask if this detailed information may be made available to other interested agencies at a later stage, as well as to those quoted in the paper, for modeling and system identification purposes. That this full-scale input to mathematical modeling is required is shown in Table 11, where the PMM model prediction shows the *Esso Bernicia* to have its smallest turning circle at a depth-draft ratio of 1.7. This is at variance with the three full-scale trial results cited in Table 11.

I was particularly impressed with the data acquisition system installed on board the ship for these trials. Having performed many maneuvering trials myself and having progressed, over the years, from a paper-and-pencil system through paper tape and magnetic tape and eventually to a floppy disk system, I know only too well from bitter experience the pitfalls of this type of exercise. Success can be ensured only by painstaking detailed planning, and I cannot stress firmly enough how much I appreciate the efforts of the author and his many colleagues in this area.

I was reassured, however, to find that the method which I favor myself for tidal drift correction, and which I used in the analysis of the *Esso Bernicia* turning circles [5], was found here to be still the most reliable technique. While performing several of the turning circles on *Esso Bernicia* in the shallow-water location, we also observed seabed sand or silt being drawn to the surface and marking the wake very clearly indeed.

The publication of this wealth of detailed data is extremely timely, since they adequately quantify the maneuvering behavior of a VLCC. Several regulatory bodies around the world are considering standards of maneuverability for various ships and they should study these data at great length. They describe clearly what a typical VLCC can and cannot do, and may prevent unrealistic rules being drafted in the future. It is my belief that once the size and geometry of a ship have been decided upon, then most of its maneuvering characteristics are inherent in it. Changing the rudder size and shape thereafter can alter the situation, but only to a limited degree.

<sup>8</sup> The British Ship Research Association, Tyne and Wear, England.

### J. Sommet,<sup>9</sup> Visitor

1. The program of trials carried out with the *Esso Osaka* forms part of an intensive and continuous study effort in recent years aimed at characterizing the ability of large ships to perform harbor approach maneuvers. The contribution made by these trials is original in two respects: First, numerous trial runs were effected in particularly shallow water ( $h/T = 1.2$ ), and second, the trial maneuvers were designed specifically to relate to harbor maneuvering conditions. The results obtained will be beneficial both in improving the reliability of mathematical simulation models in shallow water and in providing seamen with information directly applicable to the handling of their ships.

2. In the latter respect we note that a new factor, of great importance for the shiphandler, was taken into account in these tests, namely, the propeller bias effect with engine astern. The stopping tests underlined both the importance of the turning moment thus applied to the ship and the fact that this moment is significantly increased in shallow water. Of course the shiphandler must bear in mind that this effect can be attenuated or even reversed by the configuration of the seabed (slight slope, shoal, etc.). It is common practice to use the propeller bias effect to turn a single-propeller ship on the spot, by successive maneuvers of the engine full ahead (with rudder completely to starboard) and full astern (about 50 rpm), the ship having practically no headway. It would be interesting to define the optimum procedure for such a maneuver, as well as its duration and the dimensions of the turning area concerned.

3. Another very important aspect of the tests is that they confirm the peculiarity of behavior of a ship over depths of around  $h/T = 1.5$ . This means that the VLCC pilot must not be surprised if rudder response differs from that in deep water for depths of this order. Such depths are encountered especially in the approaches to shallow-water channels, in areas where the destabilizing effect of waves on the stern can combine with the shallow-water effect to increase the difficulty of maintaining the heading.

4. With regard to low-speed stopping distances, the trials did not confirm the tendency which seemed to be revealed by the *Magdala* tests, that is, a reduction of stopping distances over medium depth. With the *Esso Osaka*, the variation of stopping distance with depth was insignificant, and we can agree on the range of 1.8 to 2.5 ship lengths for a VLCC stopping from 4 knots. However, the trajectory corresponding to this maneuver (Figs. 9 and 19) performed with the normal procedure clearly demonstrates the risks it involves close to a pier and justifies a final berth approach by the stern rather than by the bow, so that any last-minute deceleration can be effected by a maneuver with the engine ahead, enabling the ship's heading to be controlled. With reference to Fig. 9, could the author indicate the duration of the maneuvers?

5. I would like to lend my support to Mr. Cranes's suggestion that verification tests be carried out in the large ship model

<sup>9</sup> Sogreah, Inc., Grenoble, France.



testing stations under conditions similar to those of the *Esso Osaka* tests.

Finally, we must show our gratitude to Exxon for having made available the results of this very important trial program in the shortest possible time.

**John H. Lancaster, Member**

[The views expressed herein are the opinions of the discussor and not necessarily those of the U. S. Coast Guard.]

I should like to commend Mr. Crane not only for the excellence and timeliness of this paper but also for the competence of his efforts and those of his company in directing the development and accomplishment of these trials, carrying out the objectives which the American Institute of Merchant Shipping, the Maritime Administration, and the Coast Guard had agreed upon. Success in a complex project of this nature is highly dependent upon quality of detailed planning and vigor of execution as well as thorough, professional knowledge.

The subject of safe passage of ships in confined and congested waters has become in recent years a subject of considerable international as well as national interest, particularly with respect to vessels carrying hazardous cargoes. This paper contains important, relevant findings. Of particular interest is the principal finding of the trials, set forth in the third paragraph of the Summary, that steering control could be maintained in all three water depths as low as 1.5 knots, even with the engine stopped. It was further noted that maneuverability is improved when rpm is quickly increased (kicking ahead) and reduced when rpm is rapidly decreased. The last two sentences which follow deserve to be memorized: "Because of this, a prudent ship handler will navigate in tight quarters at the slowest safe speed. Then if required to increase speed he will gain control, rather than risk losing it if required to slow down."

It is recognized that significant beam and quartering winds and currents normally require additional ahead vessel speed to reduce a vessel's deviation in heading with respect to its intended course. These values are readily calculated and allowed for. The important question of how much speed is required to maintain steering control of a large tanker driven by a fixed-pitch propeller has now been answered.

It should be noted that the results of the trials of the *Esso Osaka* are conditioned particularly by its propeller type and propulsion machinery characteristics. The steam turbine, reduction-gear, fixed-pitch propeller propulsion system permitted operation at any desired low speed with minimum interruption of flow to the rudder. A variable-pitch propeller system could be expected to produce somewhat different results. Fixed-pitch propeller systems with various diesel and gas turbine drives inherently are incapable of continuous operation at low power and consequently must resort to intermittent operation or tug assistance where low vessel speed is required. Caution should therefore be exercised in applying the results of the *Esso Osaka* trials to other tankers which do not have the same type of propulsion system.

Mr. Crane, Exxon International, the companies, agencies, and persons who supported and participated in these trials have made a valuable contribution to the fields of hydrodynamics and marine safety.

**Ronald W. Yeung, Member**

This is a fine and timely paper on a subject of much common concern and controversy: the safe operation of VLCCs in shallow water. The author is to be commended for coordinating successfully a full-scale program of such a magnitude involving sponsors of such a multitude. Results from these full-scale trials will no doubt provide the much-needed data to validate existing computer models as well as to develop

guidelines for the safe operations of tankers in shallow water. Of course, one must bear in mind that this paper discusses primarily the overall response of the vessel. Much analysis remains to be done in order to extract meaningful hydrodynamic coefficients from the trial data so that a tanker-handling simulator can be developed and future vessel and control-system design may be improved.

The effect of water depth on the dynamic stability of a tanker is a well-discussed topic in the recent literature. It seems fair to conclude that the trend reversal at medium water depth, as observed from these trials, conforms well with that predicted by experiments on tanker-type hulls (for example, Fujino [18]). (Additional references follow this discussion.) Thus it will be of interest if the author can compare the present trial data that are indicative of the dynamic stability of the vessel with either pretrial predictions based on model experiments directly or predictions using model-based computer simulation. The author has noted that such comparisons were not satisfactory for the case of *Esso Bernicia*. Is this the case for *Esso Osaka* or not?

It is gratifying to see that, as the water depth varies, the spiral-test and Z-maneuver results display trends consistent with each other. The author has expounded well on this point in relation to dynamic stability. To this discussor, it seems that an equally if not more revealing observation can be made from the coasting-turn results (Fig. 7). With the propeller shut off, the effect of the rudder is downplayed; the higher initial turning rate in medium depth compared with the other depths suggests an increase in maneuverability, thus a decrease in dynamic stability. Indeed, as the vessel slows down, the rudder develops so little lift that a "control fixed" situation is practically realized. The heading reversal toward the end is indicative of the presence of dynamic instability.

The final point this discussor would like to make is in regard to the author's recommendation that the effect of irregular boundaries and bottom on a vessel's maneuverability be studied by the use of large hydraulic models. This is a well-established route but is also known to be prohibitively expensive. It is worthwhile to call attention to the fact that analytical tools not available heretofore are now available for evaluating the effects of irregular boundaries. Figures 34 and 35 accompanying this discussion show the calculated unsteady hydrodynamic interaction between a tanker hull and a circular obstacle. The three-dimensional analytical model used is described by Yeung [19]. The effects of the hull geometry and the keel clearance are imbedded in the theory. Figure 34, taken from Tan [20], shows the time-history of the suction force and yaw moment experienced by a vessel as she moves near a circular island. The keel clearance to water-depth ratio  $\delta$  is 0.1. These results show that as the diameter of the island approaches the ship length, the maximum suction force is almost the same as that for a straight bank located at the same separation distance. The transient bow-out moment in fact could be 40 percent higher than the steady-state value corresponding to the case of a straight bank. Figure 35 shows how sensitive the force and moment patterns are to the curvature of the obstacle. As the circular "island" thins out to a finite-length breakwater, the bow-out moment changes to a bow-in moment during the approach, followed by a strong repulsion and a bow-out moment as the midship passes the obstacle. It is obvious that the aforementioned interaction phenomenon is highly relevant to ship operation in areas with submerged shoals where problems of ship control and accidents are known to be common. With the advent of such powerful tool of analysis, it seems fitting that they should be adopted and improved in parallel with the more classical means proposed by the author. The computation cost for the two figures shown here totals less than the cost incurred at an average commercial testing basin in half a day.



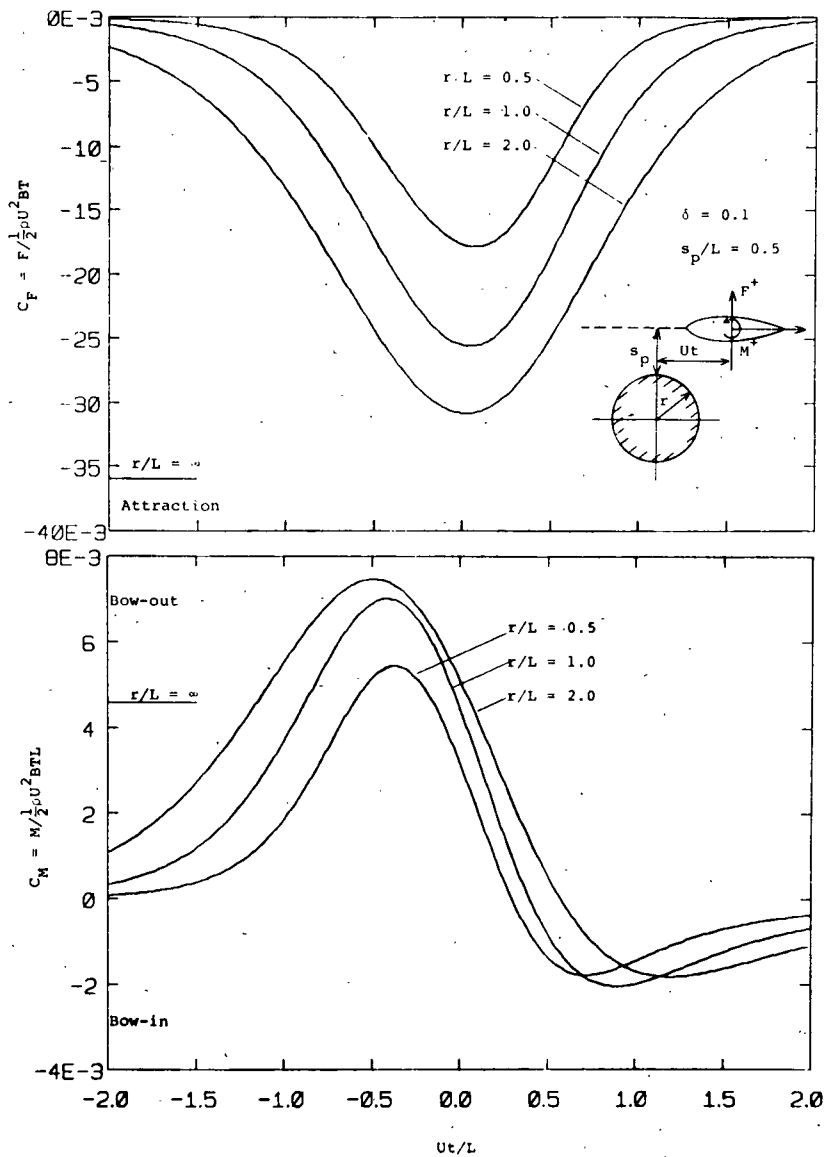


Fig. 34 Force and moment coefficient for interaction with a circular island

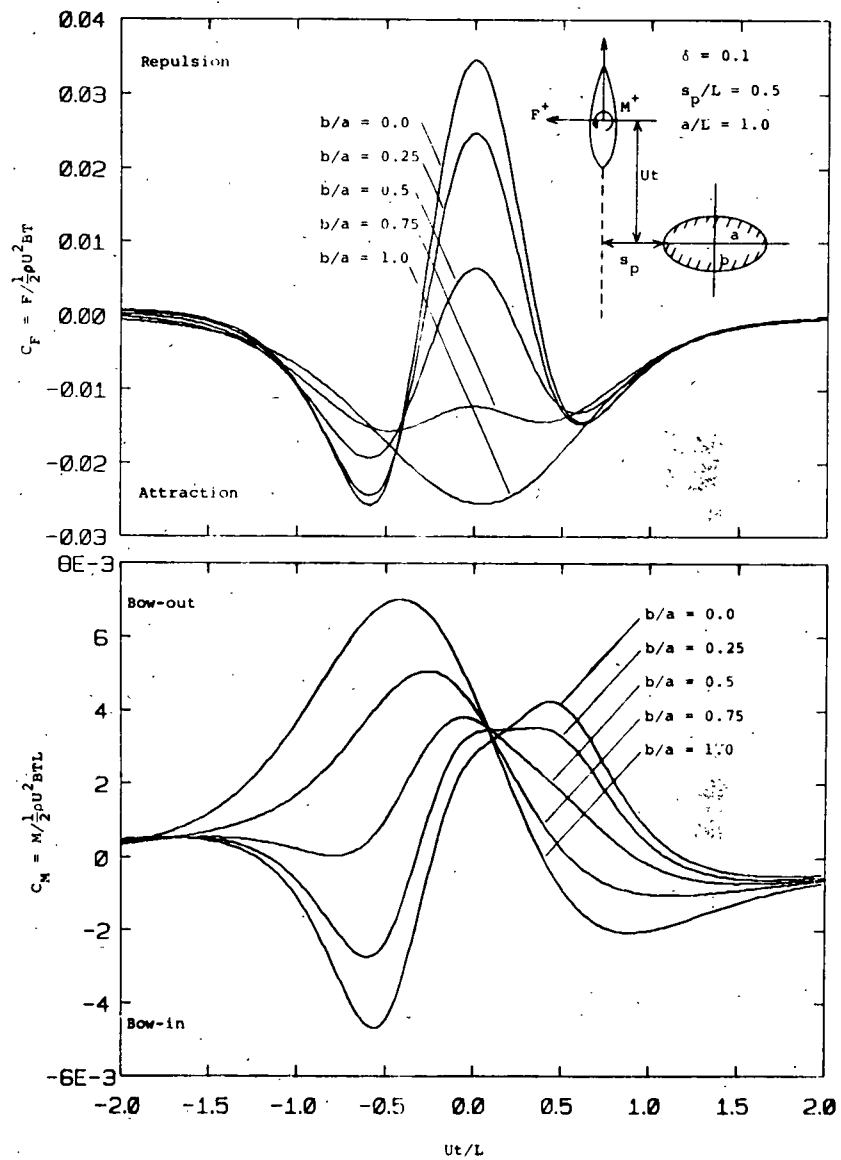


Fig. 35 Force and moment coefficient for interaction with an elliptical island perpendicular to path

## Additional references

- 18 Fujino, M., "Experimental Studies in Ship Maneuverability in Restricted Waters," *International Shipbuilding Progress*, Vol. 15, 1968, p. 168, and Vol. 17, 1970, p. 186.
- 19 Yeung, R. W., "On the Interactions of Slender Ships in Shallow Water," *Journal of Fluid Mechanics*, Vol. 85, Part 1, 1978, pp. 143-159.
- 20 Tan, W. T., "Unsteady Hydrodynamic Interactions of Ships in the Proximity of Fixed Objects," M.S. Thesis, Department of Ocean Engineering, Report 79-4, M.I.T., Cambridge, Mass., May 1979.

Nils H. Norrbin,<sup>10</sup> Visitor

This paper deserves the interest and appreciation of everybody in the profession, and especially of those of us who are concerned with scale-model testing and computer predictions of ship behavior in confined waters. For the first time we now have access to what appears to be reliable and consistent full-scale data. The discussor would certainly welcome an arrangement by which the *Esso Osaka* trials could be duplicated by free-sailing as well as captive tests with a large model in the new Maritime Dynamics Laboratory (MDL) at SSPA.

As a matter of interest it may be mentioned that the main dimensions of the Exxon tanker are very close to those of the *Svealand*, for which shallow-water model results were presented at the 1978 Delft Symposium on Aspects of Navigability and in the *International Shipbuilding Progress Journal*. A comparison of nondimensional turning circle data is given in Table 13 of this discussion. The blank spaces should be filled in with data from further tests with free-sailing models.

In particular the *Esso Osaka* trials do support earlier findings from model tests on the existence of a range of depths of water in which the dynamic stability is lowered. The trend toward a larger hydrodynamic damping with a reduction of underkeel clearance is still unique. In computer simulation the aforementioned phenomenon may well be included provided the nonlinear variations of forces with depth are properly described. This description requires tests with captive models.

Since the advent of screw propulsion, mariners have made use of the stern-to-port effect of a backing right-handed propeller. Due to the relatively small diameter and thrust of the propeller and the large inertia of a VLCC, that same effect will here only appear at low speeds or late in a stopping maneuver. The lateral thrust interference will be enhanced, again, by the two-dimensional flow conditions in shallow water, as proved by the *Esso Osaka* trials.

The Exxon trials showed that a controlled-heading stop required significantly increased distance to zero speed, and that lateral deviation still became a problem. From recent SSPA real-time simulations of controlled and tug-assisted stopping

of tankers in shallow water and canals, we may conclude that lateral control may sometimes be achieved at less expense in distance. It is only fair to admit, however, that the mathematical models for controlled-stopping maneuvers may still be improved. Full-scale experience such as here conveyed by Mr. Crane is of the utmost value.

J. N. Newman, Member

The material which is summarized in this excellent paper has been awaited eagerly by workers in the field of ship maneuvering. The successful execution of these trials is a tribute not only to the author, but to all of the individuals and organizations which participated.

Ship maneuvering in shallow water has received a substantial amount of theoretical attention during the past decade, supported in large part by several grants from the National Science Foundation and promoted by discussions in SNAME Panel H-5. The review of that work in reference [15] has been supplemented by a more recent survey [21] (below).

There is an encouraging degree of agreement between theoretical predictions and the results in this paper. The increased characteristic time scale of ship maneuvers in shallow water is readily predicted by the theoretical model, which, simply stated, predicts the characteristic time to increase in shallow water in proportion to the length/beam ratio. The increased turning radius in shallow water has been predicted by Hess [22], and the very steep increase of this theoretical radius in very shallow water appears to be consistent with the sparse experimental data in Fig. 6. On the other hand, the theory is unable to account for nonlinear effects and, as a consequence of the neutral stability at an intermediate depth, the turning radius cannot be satisfactorily predicted in this regime.

The "apparent reversal" of dynamic stability noted in the spiral tests is consistent to some extent with the theory of Hess, but even more so with the analysis of Fujino [12] based on captive model tests. This represents a modest exception to the author's claim that this effect has not been observed in prior work.

The small decrease in headreach also is consistent with the increased longitudinal added mass which is predicted in shallow water, but this is a weak effect in view of the dominant role of the ship's own mass.

I would welcome some comments from the author regarding the practical implementation of these results. The increased turning diameter and response time in shallow water can be factored into simulation, but what can be done beyond this level? It is reassuring to find that the *Esso Osaka* could be maneuvered at speeds as low as 1.5 knots. On the other hand, the collision in deep water off Tobago last July was the most serious reminder of the fallibility in VLCC operations. Our

<sup>10</sup> Swedish Maritime Research Centre (SSPA), Göteborg, Sweden.

Table 13 35-deg right rudder turning circle data (in metres)

	Advance at 90-deg Heading Change $h/T =$					Tactical Diam at 180-deg Heading Change $h/T =$				
	4.2	2.3	1.5	1.3	1.2	4.2	2.3	1.5	1.3	1.2
TT <i>Esso Osaka</i> trials $L_{pp}$ 325.00 m $B$ = 53.00 m $T$ = 21.73 m	1015		990		1180	925		1075		1590
MT <i>Svealand</i> trials $L_{pp}$ = 321.56 m $B$ = 54.56 m $T$ = 21.67 m	1160		—		—	990		—		—
MT <i>Svealand</i> SSPA model (free-sailing 5-m model in MDL)		1005		1110			1120		1530	

profession must intensify its efforts to minimize the probability of such casualties.

#### Additional references

21 Newman, J. N., "Theoretical Methods in Ship Maneuvering," Symposium on Advances in Marine Technology, Trondheim, Norway, June 13-15, 1979.

22 Hess, F., "Rudder Effectiveness and Course-Keeping Stability in Shallow Water: A Theoretical Model," *International Shipbuilding Progress*, Vol. 24, 1977, pp. 206-221.

#### J. B. Hooft, Member

The Netherland Ship Model Basin, like, I presume, many other organizations working on navigation studies, is indebted to the Society's responsive project mentioned in this paper. I would like to congratulate the author for the excellent discussion of this fantastic project and the skillful presentation and analysis of results he made.

Exact information on the real-life maneuvering performance of a tanker for a range of environmental conditions being now available, it will be possible to judge the results of the ship's maneuverability as described by several mathematical simulations. In this respect, I would like to emphasize that with the use of full-scale measurements the applicability of the mathematical model can be seriously considered. Not only have full-scale trials been performed of which most mathematical models are in reasonable agreement, but also such trials have been executed which define the ship's maneuverability much more accurately while supplying better criteria than have been supplied by existing mathematical models. I think this is one of the most important reasons why the project described is of such high value.

I disagree with the idea, expressed occasionally, that a mathematical model simulation can be developed by means of, for instance, system identification techniques, when a full description of the ship's maneuvers is at one's disposal. I especially dislike this approach since a very fine description of available maneuvers will be reached, possibly, while it may be doubted that such a description is applicable to other maneuvers since no proof of the extrapolation of the description is provided.

I therefore would recommend the development of a mathematical description based on all relevant hydrodynamic phenomena which play a role in those groups of maneuvers which have to be described by the mathematical simulation. The applicability of such a mathematical model has to be proved by comparing its results with the results attained from the full-scale measurements.

Also, I would like to join with the author in a study of the conditions of the maneuvers. He has at his disposal the results that have to be simulated and compared with the mathematical model. We will provide him the results of our calculations with the mathematical model available.

As a final remark, I would like to express my high estimation of the fiscal explanations with the very specific aspects of ship maneuverability in shallow water as presented by the author.

#### Eugene R. Miller, Jr., Member

This paper presents the results of a carefully conducted and successful set of full-scale maneuvering trials carried out under ideal conditions. The author and the sponsoring organizations are to be congratulated on their success. It is particularly noteworthy that the trial agenda included not only the normal definitive maneuvers, but also maneuvers which demonstrate the importance of hull, rudder, and propeller interactions which affect realistic operational maneuvers.

This discussion concerns the first recommendation of the paper. That is that the results of the trials be used to validate

present-day procedures for developing maneuvering mathematical models by means of model tests with captive models. This is of great importance to us at Hydronautics, Incorporated since we routinely develop such mathematical models by captive model tests using a large-amplitude horizontal planar motion mechanism. As a result, we offered to conduct a complete series of captive-model tests in the three water depths, carry out computer simulations, and make the results available if the Maritime Administration would provide for the construction of a model. In due time this offer was accepted and we have built and just finished testing a model of the *Esso Osaka*. The model is built of fiberglass to a scale ratio of 44.78, which results in a model length of 23.81 ft (7.25 m). A model of the propeller was also constructed. This relatively large model size was chosen so that the hull, propeller, and rudder interactions would be free from overwhelming scale effects. It is our understanding that MarAd will make this hull and propeller model available to other laboratories interested in conducting similar tests.

We have just completed the tests and have not yet carried out a final set of simulations of all of the trial maneuvers. Some preliminary comments about the test results can be made. The stability derivatives from model tests show the same effects of water depth on directional stability as the trials; that is, a high degree of directional stability at a  $H/T$  of 1.2, a small degree of directional instability at  $H/T = 1.5$ , and neutral stability in deep water. The asymmetric force and moment due to propeller rotation in stopping maneuvers were observed to increase significantly with reduction in water depth and these data when used in simulations of stopping maneuvers produced predictions in good agreement with the trials. The results of the simulations of the deepwater turning and Z-maneuvers, which are most complete at this time, show remarkably good agreement with the trial results. At the shallowest depth, the tactical diameter in a simulated 35-deg rudder turn was less than 10 percent larger than the trial result. The largest differences found so far between simulation predictions and the trial results is a tendency of the simulations to underpredict the first overshoot angle in the Z-maneuver at the shallowest water depth. Thus our preliminary conclusion is that captive-model tests with large models and the associated computer simulations give good qualitative agreement with the trial results and apparently acceptable quantitative agreement. The type and extent of corrections for scale effects, if such corrections are required, are not yet clear.

In any event, the results of these trials provide an outstanding opportunity to validate the procedures used to develop maneuvering mathematical models, and I am sure the laboratories involved in this type of work will not pass up the chance.

#### Haruzo Eda, Member

I would like to congratulate the author for completing such an extensive full-scale trial program in deep and shallow water. The results of the trials have an important impact on further development and improvement of computer simulation models to represent realistic ship maneuvering behavior.

We have been developing computer simulation capabilities of ship motions in deep and shallow water, mainly on the basis of captive model tests. Accordingly, I would like to point out an example of correlation between full-scale trials and computer simulation results. Let us compare the turning trajectories obtained in ship trials shown in Fig. 5 of the present paper (page 256) with those obtained in computer simulations for the case of the 80 000-dwt tanker shown in Fig. 3 of the preceding paper (page 231). There is an encouraging correlation of the shallow-water effect on the turning trajectory as demonstrated in these two figures. A substantial increase in turning diameter is shown in these figures for very shallow water depth ( $D_w/H$

= 1.2) relative to deep water. The rate of increase of turning diameter is slightly less than two times relative to that in deep water.

One difference in these figures, I notice, is the magnitude of drift angle in shallow-water turning. Since course-stability characteristics are increased and turning performance reduced in shallow water, relative to those in deep water, we expect much smaller drift angle in shallow water—as shown in Fig. 3 of the preceding paper. It appears to me that the drift angle shown in the shallow-water turning trajectory in Fig. 5 of the present paper is somewhat large. I wonder if the author can give us any comments regarding this point.

**Thomas Sartor, Member**

I appreciate Mr. Crane getting so many of these papers out—bringing a lot more theoretical material of value to us who are operating ships.

We recently were out running sea trials on the *Nostra Pioneer*. Bethlehem Steel was very cooperative with us on this, and we were trying to determine two things which relate to Mr. Crane's work.

First of all, I notice all the excellent detail he had to check his current situation. On our turning circles, we did not. We requested and Bethlehem agreed to give us three complete circles on each of our turning circles, and the results, which were done by Radist, are now under evaluation. The intent was that the difference between these second and third loops in a circle could be utilized as a correction factor for the first loop in determining the drift, wind factor—things of that nature.

The second thing we did—and once again the results are not yet complete—was to utilize the sea data to compare with the Radist data. We wanted to determine whether the Loran-C data are sufficiently accurate for and (for ships that are already in operation) will enable us to run with, at a convenient time, at-sea trials, whenever the master finds it convenient to do so.

So these are two practical steps pertaining to turning circles that we are hoping for, but which we do not yet have answers for.

Once again, I certainly appreciate this opportunity to tell the author of the little thing we have done in comparison with the big thing he has done.

**A. D. Fletcher,<sup>11</sup> Visitor**

This latest paper from Mr. Crane provides yet another valuable contribution toward filling the gap in our knowledge of the maneuvering characteristics of ships in shallow water, and I would like to congratulate him and all those associated with the trials.

As one representative of users of the data and equations published by Mr. Crane and others working in this field, I would like to comment on our particular requirements, which are related largely to the operational specifications and expressions of effectiveness of aids to navigation.

Our approach to such problems is a probabilistic one and it involves the need to express such probabilities as a ship's ability to maneuver within certain physical constraints, such as a channel or the constraint depth contours off a hazard. We are, therefore, concerned with establishing the possible effective beam (Fig. 1.) and maneuvering envelope for each of a number of classes of ships operating under extreme environmental conditions. We need to be able to put numbers and probabilities on all the factors which contribute toward the evaluation of the effective beam in both shallow ( $h/T = 1.1$ ) and deeper ( $h/T = >4$ ) water.

Two parameters which we have found to be of value in this

<sup>11</sup> Manager-Maritime Projects, EASAMS Limited, Camberley, Surrey, England.

work are Advance to 10° Change of Heading and Advance to 0° Yaw Angle at the stern following the application of rudder, and I look forward to the possibility of comparing our earlier evaluations with the results of these trials.

## Author's Closure

Mr. Clark has pointed out the importance of having time-histories of system states throughout maneuvers. The full report of the present trials includes charts of these for most of the maneuvers, and data on magnetic disks are retained. I do not anticipate any problem in obtaining these upon request to the Maritime Administration. Certainly we encourage any work that might be done toward improving mathematical model-to-ship correlations. In view of Mr. Clark's extensive experience with high-quality full-scale trials, his comments are indeed appreciated.

Mr. Sommet has suggested that we are now in a position to define the optimum procedure for certain maneuvers such as "back and fill" as are done in a turning basin. I agree, but must add that this may still be most easily done using a comprehensive mathematical model, possibly in a shiphandling simulator, or a large manned physical model. In either case, an important prerequisite is a good scale-effect study through careful comparisons of model and full-scale data.

Mr. Sommet's second point, regarding making the final approach to berth stern-first, to allow a strong corrective rudder action control if it should subsequently be necessary to go ahead, is well appreciated. This practice is, of course, now used with VLCCs and ULCCs in ports such as Cape Antifer (Le Havre). Again, such maneuvers are best optimized using a comprehensive mathematical model or large models after their validation.

With regard to the stopping maneuvers of Fig. 9, their durations were 10.7 min in shallow water, 8.9 min in medium depth, and 8.7 min in deep water.

Mr. Lancaster has gone directly to the operational significance of the paper. For example, he emphasizes points about very slow-speed maneuvering, both with and without rpm, and warns that vessels with other configurations will have somewhat different responses. Certainly, his caution about a slow-speed diesel VLCC having a higher minimum maneuvering speed is very appropriate.

I must, of course, agree with Professor Yeung's point that analytical tools are now available which can handle irregularities in bottom and side boundaries. I feel, however, that as with the large hydraulic model, these mathematical tools can also be quite expensive to develop. This is especially true if taken to the degree necessary to treat the nature of irregularities that large hydraulic models easily handle. Also, as boundary conditions become more complex, the degree of difficulty in correlating analytical results with full-scale trial data becomes greater. Therefore, at this point we will be happy even to see simple correlations regarding maneuvers in uniform shallow water.

Professor Norrbin shares the project sponsors' interest in having the trial results duplicated with predictions based on captive-model tests. In this connection, we are aware of the excellent results presently being obtained at SSPA in the area of the effects of side boundaries on ship maneuvers. In general, however, we believe that those organizations that are most active in developing model and analytical techniques should, if possible, take the initiative in this important correlation work.

Professor Newman asked for comments regarding practical implementation of our results. In fact, from the tanker operator's point of view, the most important present implementation

will be in validating the comprehensive maneuvering math models that are the basis for modern shiphandling training simulators. It is only through such correlations that the necessary degree of confidence in the simulations can be given to the shiphandler trainees. Presently there is a continuous flow of deck officers through the several real-time simulator facilities dedicated to increasing the safety of ship maneuvers and reducing the possibility of casualties. In addition, the mathematical models which these trials are aimed at improving are the basis of shiphandling studies used in the design of approach channels, in the development of bridge maneuvering information, etc. All of these can in some way be considered practical implementation of the trial results.

As usual, I agree with Dr. Hooft's comments and here I especially appreciate the interest he expresses in joining the study of scale effects and mathematical modeling of maneuvering and coursekeeping in general.

I am very happy to hear from Mr. Miller that the correlating captive-model and computer simulations of the *Esso Osaka* maneuvers are underway and apparently producing encouraging results. In this respect, it is important that both the water depth and rpm maneuver correlations be carried as far as possible. We cannot expect perfect agreements of predictions and full-scale trial results any more than we can expect direct model tests of resistance and propulsion to produce perfect answers. In both cases, logical corrections are required, and an exchange of details regarding these will help everyone.

Dr. Eda has noted some apparent disagreement between the sketches showing drift angles in the turning circle figures and

in his own simulations of these maneuvers. I should note that, to date, no attempt has been made to analyze the drift angles in the *Esso Osaka* trials, and that the sketches are not precise in this regard. After receiving Dr. Eda's comment, I did calculate the drift angle by using the Doppler-measured forward and lateral speed in two of the turning trial maneuvers. These showed very low drift angles in the shallow water cases, as Dr. Eda has predicted. In the recommended correlations between model and full-scale studies, I would certainly hope that detailed checks of important parameters such as drift angle would be made.

Mr. Sartor noted that in recent Farrell Lines trials, three complete circles were made in turning maneuvers. While this will give a good indication of mean set and drift due to water current in deep water, it is not certain that uniform set and drift will occur in shallow water as the ship heads at different angles to the current. Also, as shown by the current meter readings in the present trials, it is possible, especially in shallow water, that the water currents will be quite different at different depths. Finally, the type of correction made for turning circles cannot be made directly in the case of Z-maneuvers. We can intersperse turning trials with other trials, however, in an attempt to get some benefit from the turning circle correction data.

Regarding Mr. Sartor's comments on the use of Loran-C, I would note that local calibrations of Loran-C can make it accurate enough for use in maneuvering trials. The first step is to determine the accuracy of coordinate transformations in the existing Loran-C system, locally.

# Maneuvering in Shallow and Confined Water

Marc Vantorre<sup>1</sup>, Katrien Eloot<sup>1,2</sup>, Guillaume Delefortrie<sup>2</sup>, Evert Lataire<sup>1</sup>,  
Maxim Candries<sup>1</sup>, and Jeroen Verwilligen<sup>2</sup>

<sup>1</sup>*Ghent University, Ghent, Belgium*

<sup>2</sup>*Flanders Hydraulics Research, Antwerp, Belgium*

1	Maneuvering in Shallow Water	1
2	Bank Effects	4
3	Effect of Muddy Bottoms	7
4	Ship–Ship Interaction	10
	Nomenclature	15
	Glossary	16
	References	16

## 1 MANEUVERING IN SHALLOW WATER

### 1.1 Introduction

A ship's maneuverability depends on the water depth  $h$  of the navigation area in relation to the draft  $T$  of the vessel. PIANC (1992) makes a rather arbitrary distinction between deep ( $h/T > 3.0$ ), medium deep ( $1.5 < h/T < 3.0$ ), shallow ( $1.2 < h/T < 1.5$ ), and very shallow water ( $h/T < 1.2$ ). The effect of depth restrictions is noticeable in medium deep water, is very significant in shallow water, and dominates the ship's behavior in very shallow water. In dredged channels giving access to maritime ports, the ship's under-keel clearance (UKC), defined as  $(h - T)/T$  and expressed as a percentage of draft, typically takes values of 10–20% in sheltered areas and 15–40% in areas subject to waves and swell (PIANC, 2014), which implies that navigating in medium

deep, shallow, and very shallow water is a common practice in ports and their access channels. In such navigation areas, characterized by limited depth and width, sea-going vessels are often confronted with completely different environmental conditions compared to navigation at sea for which most ships are designed and optimized. Besides the effects of the restricted depth, a ship also has to deal with the vicinity of banks, the presence of other shipping traffic, currents, speed restrictions, and so on. In such situations, the advice of a pilot with thorough knowledge of the local situation is often required in order to guarantee a successful operation.

For inland vessels, on the other hand, waterways with limited depth and width can be considered as a natural habitat. According to the Dutch waterway guidelines (Rijkswaterstaat, 2011), the depth of an inland waterway for commercial navigation with normal profile must be at least 1.4 times the draft of the reference ship, to be reduced to 1.3 for waterways with a narrow or single-lane profile.

### 1.2 Effect of limited water depth on standard maneuvers

Water-depth limitations will change considerably the pressure distribution around a moving vessel and will mostly cause an increase of the hydrodynamic forces due to the ship's motion through the water. Besides an increase of the ship's resistance, water-depth restrictions in general result in a decrease of her maneuverability, manifesting itself in the results of standard maneuvers. However, most ships perform such maneuvers only during the trials, which are always executed in deep water. Information about trials in limited water depth is therefore mostly based on simulations or model tests. Full scale test results are very rare; the

most famous exception is the *Esso Osaka* test program (Crane, 1979). In 1977, maneuvering trials were conducted with this 278,000 ton deadweight crude oil carrier in the Gulf of Mexico, at UKCs of 320%, 50%, and 20% of draft.

Compared to deep water, the characteristic dimensions of the turning circle in general monotonically increase with decreasing water depth, as illustrated in Figure 1 (left). Apparently, the dependency of the maneuverability in the lower UKC range is very significant: a small decrease in UKC results in a huge increase of the turning circle dimensions. As a result, larger bend radii are required in shallow navigation channels. Figure 1 (left) also reveals a decreased drift angle in a steady turn compared to deep water, resulting in a narrower swept path and a relatively smaller decrease of the ship's forward speed in the bend.

Water depth also has an effect on the course-checking ability of a ship: in (very) shallow water, overshoot angles during zigzag tests are considerably smaller compared to the deep water case. In spite of this apparently beneficial effect (Figure 1, right), the trials have a much longer duration as the yaw rates are significantly lower in the case of shallow water.

However, maneuvering characteristics of certain ship types may deviate from this general pattern in medium deep water. In the case of the *Esso Osaka* at 50% UKC, for instance, the advance is slightly smaller compared to deep water. Moreover, the overshoot angles observed during zigzag tests may increase in the medium water depth range. This behavior is generally observed for full ship forms. In exceptional cases, the turning circle may even become smaller with decreasing water depth; a ship with wide beam (small  $L/B$ ) and small draft (small  $T/B$ ) appears to turn easier

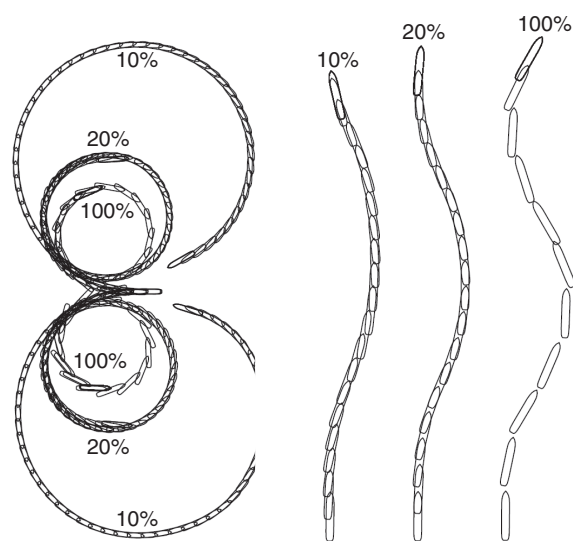


**Figure 1.** Turning circles and 20/20 zigzag tests with a ship model (confidential) at 10%, 20%, and 100% UKC, performed at BSHC, Varna, Bulgaria, on behalf of FHR, Antwerp, Belgium.

in shallow than in deep water (Yasukawa and Kobayashi, 1995).

Water-depth limitations also influence the straight-line stability. While a UKC decrease initially may have an adverse effect on directional stability (as was observed in case of the *Esso Osaka* at 50% UKC), in shallow water the dynamic stability increases with decreasing water depth.

Summarized, a ship's directional stability and maneuverability change considerably as a function of the available UKC. Especially in natural waterways (rivers, estuaries) where the water depth may vary significantly, both over the length of the channel and over the tidal cycle, a ship's maneuvering characteristics may be subjected to important changes during a transit through the channel.

### 1.3 Effect of limited water depth on hull and rudder forces during maneuvering

#### 1.3.1 Hull forces

The dynamic equilibrium of a moving ship requires a balance between the inertial forces and moments and the hydrodynamic actions on the ship's hull, propeller(s), and rudder(s). For a maneuvering vessel, the kinematics and dynamics in the horizontal plane are of main concern, although the six degrees of freedom are not independent. This implies that the study of maneuvering focuses on lateral forces and yawing moments.

The lateral force ( $Y$ ) and yawing moment ( $N$ ) acting on a ship's hull caused by the hydrodynamic reaction to the relative motion of the ship with respect to the water can be considered as functions of the ship's velocity through the water in the horizontal plane, decomposed in a longitudinal ( $u$ ) and a lateral ( $v$ ) velocity component in a ship-fixed coordinate system and a yawing rate ( $r$ ), and the corresponding accelerations  $\dot{u}$ ,  $\dot{v}$ , and  $\dot{r}$ . The most important acceleration-dependent force and moment, often denoted  $Y_{\dot{v}}\dot{v}$  and  $N_{\dot{r}}\dot{r}$ , respectively, amplify the ship's mass inertia terms.  $-Y_{\dot{v}}$  is referred to as the *added mass for sway*,  $-N_{\dot{r}}$  as the *added moment of inertia for yaw*, see also article **Maneuvering and Coursekeeping Characteristics**. While in deep water, the added mass for sway is typically somewhat less than the ship's mass, its value may increase with a factor 4–5 in very shallow water, as illustrated in Figure 2. As a result, a ship's inertia increases significantly at reduced UKC, which results in a more sluggish behavior.

A similar trend is valid for the sway and yaw velocity-dependent forces and moments. Due to its shape in the horizontal plane, a ship hull can be interpreted as a lift-generating profile with chord  $L$  and thickness  $B$ . The aspect ratio of this profile is very low: in deep water, the effective value can be considered as  $2T/L$ , where the



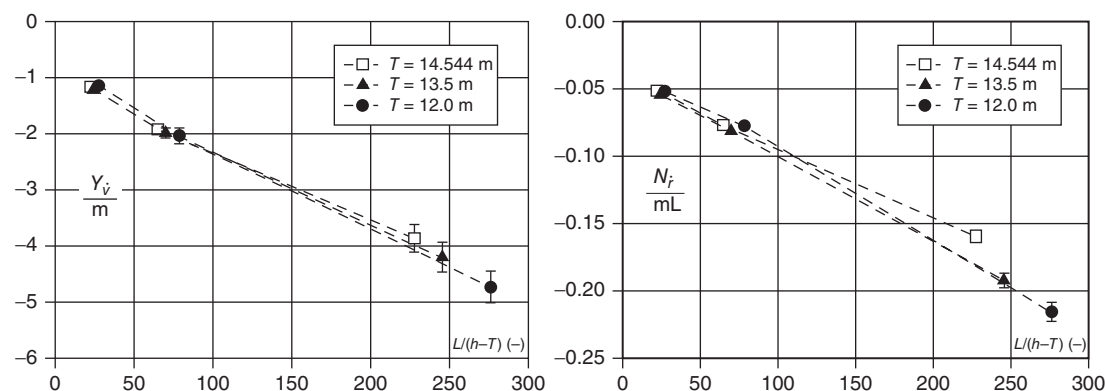


**Figure 2.** Nondimensional sway-added mass and yaw-added moment of inertia as a function of nondimensional UKC for a 1/80.8 scale model of an 8000 TEU container carrier. (Reproduced with permission from Eloot, Vantorre, and Delefortrie, 2006. © International Marine Simulator Forum, 2006.)

factor 2 is due to the presence of the free water surface. With decreasing UKC, the cross-flow between both sides of the ship is increasingly obstructed, the effect of which is equivalent to an increase of the aspect ratio. In the limit case  $h/T = 1$ , where no cross-flow is possible, the equivalent aspect ratio can be considered as infinite and the flow around the hull as two-dimensional.

As a result, the hydrodynamic lateral force and yawing moment acting on a ship moving at constant speed under a drift angle will increase significantly with decreasing UKC, as is illustrated in Figure 3.

Similarly, the yaw velocity-induced yawing moment gradually increases with decreasing UKC. A pure yaw motion also causes a hydrodynamic lateral force, which in deep water is practically negligible compared with the centrifugal inertia force ( $-mur$ ). In shallow water, however, this hydrodynamic lateral force is increasingly important

and is observed to counteract the centrifugal inertia force; the resultant of the hydrodynamic and inertial forces may even become centripetal at very low UKC.

### 1.3.2 Control forces

The forces on the rudder itself in general do not vary significantly with UKC. The flow toward the rudder is nevertheless affected by UKC limitations: the increased wake reduces the inflow, while on the other hand, the higher propeller loading increases the propeller-induced velocity. Both effects counteract each other, which almost results in a status-quo in most cases.

A rudder action induces an asymmetric flow that results in an asymmetric pressure distribution on both sides of the rudder and which eventually generates a lateral force on the rudder, which, expressed in the ship's coordinate system, is

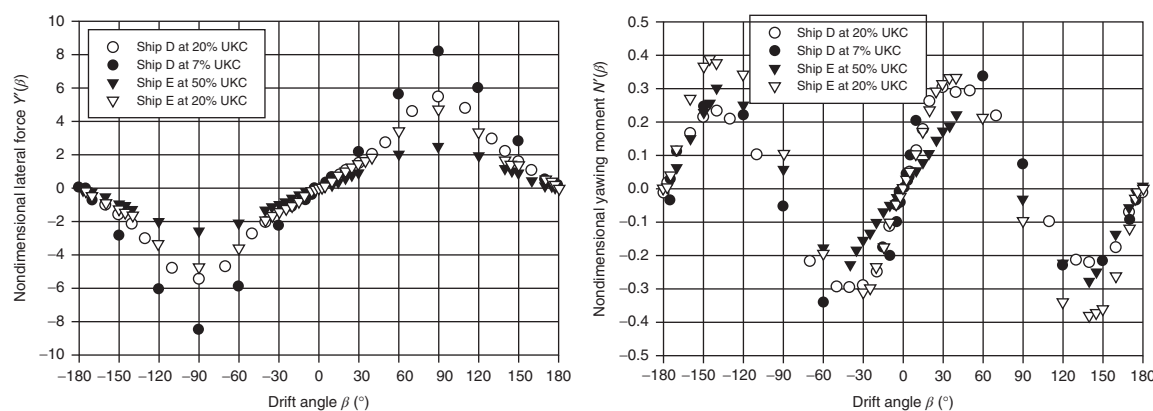


**Figure 3.** Nondimensional lateral force and yawing moment as a function of the drift angle  $\beta = \tan^{-1}(-vu^{-1})$  for two ship models (*D*: container carrier and *E*: tanker) at different UKC. (Reproduced with permission from Eloot, 2006. © Katrien Eloot, 2006.)



denoted  $Y_R$ . The asymmetry of the pressure field is not only restricted to the rudder, but extends over the aft part of the ship's hull. Integration of the pressures induced by rudder action over the hull therefore results in a lateral force, which can be formulated as a fraction  $a_H Y_R$  of the force on the rudder. In deep water,  $a_H$  is rather small, and the application point of the rudder-induced hull force is located near the ship's stern. With decreasing UKC, however, the magnitude of this force increases significantly; as its application point moves farther forward, the effect on the yawing moment is less important and can even have an adverse effect on the control actions when the rudder-induced hull force applies fore of midships.

## 2 BANK EFFECTS

### 2.1 Introduction

In restricted waters, a ship's behavior is affected by the lateral limits of the navigation area, such as banks and quay walls. These restrictions may influence the flow and pressure field around a ship and, therefore, the hydrodynamic forces and moments acting on the ship hull.

Different types of effects are distinguished, based on the relative motion of a ship with respect to the waterway boundary (ITTC, 2002):

- *Bank effects* are defined as the forces and moments acting on a ship due to a motion that has a mainly parallel orientation with respect to the bank.
- *Cushion effects* occur when a ship is moving laterally toward a solid boundary, typically resulting in an increase of the lateral hull force with decreasing bank clearance (e.g., berthing at a quay wall).
- Lateral restrictions influence a ship's frequency domain characteristics and, therefore, hydrodynamic *memory effects* occur in case of large accelerations or decelerations (e.g., contact of a berthing ship with fenders).

The following will concentrate on bank effects, which mainly occur when a ship is under way in a navigation area that is asymmetric with respect to the trajectory she is following. A ship navigating along the axis of a canal with a constant, symmetric cross-section will not experience any lateral force or yaw moment, but only an increase in resistance. If a ship is moving on an eccentric course, however, or if the navigation area is asymmetric, the flow around the ship will cause an asymmetric pressure field, resulting in a lateral force and a yawing moment.

In general, the relative water velocity at the side of the nearest bank will be increased compared to the open side. Due to Bernoulli's law, the pressure and, therefore, the water level will decrease more on the side of the nearest bank than on the open side. The resulting force will therefore (mostly) push the ship toward the nearest bank; for this reason this phenomenon is often called *bank suction*. As the water level depression is larger near the stern, while the bow wave may even result in an overpressure near the bow, this lateral force is accompanied by a yawing moment that moves the ship's bow away from the closest bank (*bow-out* moment). The vicinity of a bank also induces an increased ship resistance, as well as a modified squat and trim behavior.

### 2.2 Parameters determining bank effects

#### 2.2.1 Overview

Ship-bank interaction forces and moments depend on several parameters (ITTC, 2002):

- *Distance between Ship and Bank*. In general, the interaction effects increase with decreasing bank clearance, although the yawing moment may in some cases decrease for very small clearances.
- *Ship Speed*. As bank effects are dominated by Bernoulli effects, they are generally proportional to the square of the ship speed, although in shallow water, forces and moments increase even more than quadratic.
- *Water Depth to Draft Ratio*. The ship-bank interaction yawing moment increases monotonically with decreasing UKC and becomes spectacularly large in very shallow water. The lateral force is directed toward the nearest bank in medium deep water and shallow water; however, tank tests with towed ship models have shown that in the very shallow water range, the water level between the ship's side and the nearest bank appears to rise, so that a repulsion from that bank occurs if  $h/T$  is less than a critical value in the range 1.1–1.25.
- *Propeller Action*. The propeller-induced velocity modifies the pressure distribution near the stern, resulting in an additional attraction force between the stern and the bank, which reinforces the bow-out moment. At very low  $h/T$ , the bank repulsion effect observed for towed models mentioned above is changed into bank attraction for self-propelled models due to this effect.
- *Bank Geometry*. An arbitrary distinction can be made between vertical banks (quay walls), sloped (surface-piercing) banks, and submerged banks (e.g., dredged channels).

Most of these parameters and their influence on bank effects are not independent from each other.

### 2.2.2 Ship–bank distance and bank geometry

While the distance of a ship's side to a vertical wall can be defined in an unequivocal way, it is less obvious how to define the distance to a sloped or submerged bank. For this reason, several authors have formulated expressions for an equivalent ship–bank distance or for the effect of bank geometry on the ship–bank interaction forces.

In the 1970s, with the arrival of very large crude carriers, Norrbin (1974) executed captive force measurements and free-response trajectory tests with a tanker model along different banks with the aim to develop an analytical formulation for the lateral force and yawing moment due to the presence of a vertical bank as functions of  $h/T$  and a nondimensional ship–bank distance  $\eta_0$  (Figure 4(a)). For sloping banks, a multiplication factor was formulated as a function of the slope factor  $k$ , as well as an attenuation factor  $e^{-2(h_1)/(h-h_1)}$  for flooded banks (Norrbin, 1985). The analytical models of Norrbin, although only based on one ship model, are often used in ship maneuvering simulation, thanks to their straightforward formulations and the easy determination of the bank distance parameter.

In canal sections, the banks at port and starboard sides have a counteracting effect; Ch'ng, Doctors, and Renilson (1993) extended Norrbin's research based on model tests with

different ship types and developed generalized mathematical models, and introduced a nondimensional ship–bank distance parameter  $y_{B3}$ , based on the distances to each bank measured at half draft (Figure 4(b)):

$$y_{B3} = \frac{B}{2} \left( \frac{1}{y_{p3}} + \frac{1}{y_{s3}} \right) \quad (1)$$

In order to account for more complex, even arbitrary channel cross-sections, an equivalent nondimensional distance to bank (d2b) parameter was developed by Lataire and Vantorre (2008), based on a weight-distribution function  $w(y, z) = e^{-a|y| - b|z|}$  in the ship-bound coordinate system (see Figure 4(c)), which can be considered as an extension of the factor introduced by Norrbin (1985):

$$\frac{1}{d2b} = \frac{\chi_{\text{ship}}}{2} \left( \frac{1}{\chi_{\text{stb}}} - \frac{1}{\chi_{\text{port}}} \right) \quad (2)$$

$\chi$  being the integral of the weight-distribution function over the area mentioned in the subscript: “ship” refers to the ship's cross-section, and “stb” and “port” to the part of the channel cross-section at starboard and port side, respectively, of the symmetry axis of the ship's cross-section.

### 2.2.3 Ship speed, water depth, and bank geometry

As already mentioned in Section 2.2.1, bank-induced lateral force and yawing moment are observed to increase more

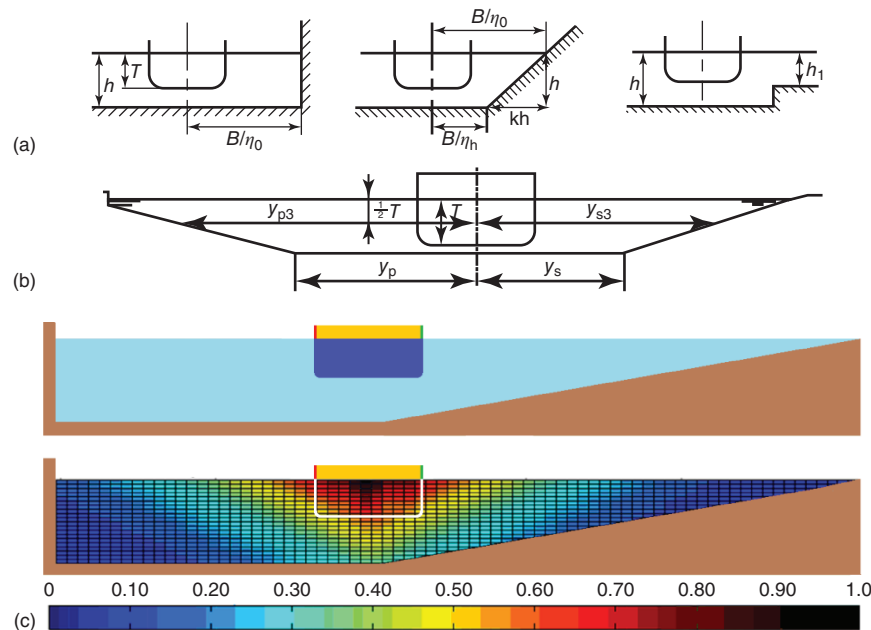


**Figure 4.** Ship–bank distance parameters. (a) Bank configurations considered by Norrbin (1974, 1985). (Reproduced from Norrbin, 1974. US Navy/Public Domain document.) (b) Definitions by Ch'ng, Doctors, and Renilson (1993). (Reproduced with permission from Ch'ng, Doctors, and Renilson, 1993. © IOS Press BV, 1993.) (c) Weight distribution function defined by Lataire and Vantorre (2008).

than proportional to the square of the ship's speed. On the basis of the comprehensive model-test series, Lataire (2014) concluded that bank effects are proportional to

$$\frac{V^2/V_{\text{crit}}^2}{\sqrt{1 - (V^2/V_{\text{crit}}^2)}}$$

$V_{\text{crit}}$  is the critical speed of the ship in the waterway, which is a function of the blockage factor  $m$  and the average water depth in the channel (Briggs *et al.*, 2009):

$$V_{\text{crit}} = \sqrt{gh_{\text{avg}}} \left( 2 \sin \left( \frac{\text{Arcsin}(1-m)}{3} \right) \right)^{3/2} \quad (3)$$

The proportionality is valid for subcritical speeds up to about  $0.84V_{\text{crit}}$ . As an alternative for the classical definition for the blockage factor  $m$ , that is, the ratio between the ship cross-section and the channel cross-section, an alternative equivalent blockage factor  $m_{\text{eq}}$  can be defined, accounting for the weight-distribution function introduced in Section 2.2.2. This allows account to be taken of the eccentric position of the ship in the channel, as well as arbitrary bank geometries.

### 2.3 Controllability of a ship navigating parallel to a bank

In order to maintain an eccentric lateral position in a channel, a rudder action directing the bow toward the closest bank is required to compensate the bank-induced yawing moment. Such a situation may occur in a two-way channel; prior to meeting, the vessels are lined up along their meeting lines. For a specific ship in a given loading condition with a specified UKC, the rudder angle required to compensate for bank-induced forces depends on the ship's speed, the applied propeller rate, and the ship–bank distance. For a specified engine setting, the required rudder capacity to counteract the bank effect can be calculated for each combination of speed and lateral position.

As an example, a typical panamax container carrier meeting a similar ship in the Gaillard Cut, the narrowest reach of the Panama Canal, is discussed. At this location, a ship preparing for a meeting will leave a clearance of about  $1.5B$  to the buoy line. Figure 5 illustrates the influence of the propeller rate on the controllability of the ship. For instance, the ship, sailing on her meeting line with a speed of 6.5 knots, requires 38% of the rudder capacity to counteract bank effects with propulsion *slow*, increasing to 70% at

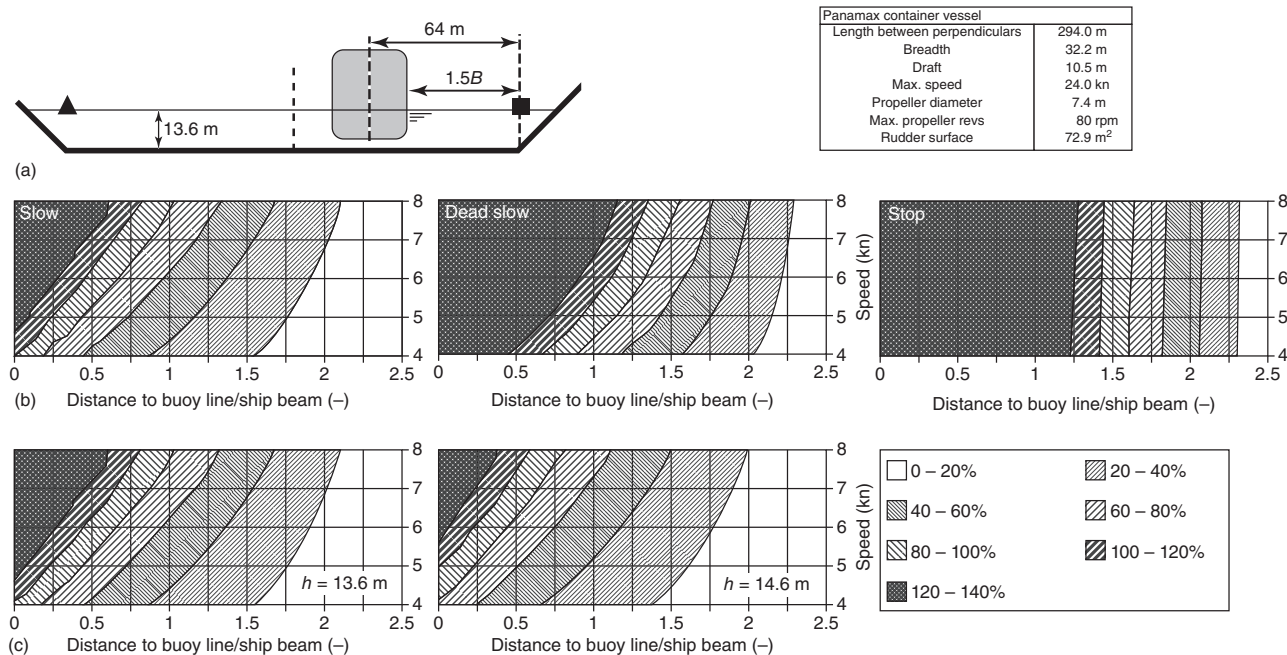


**Figure 5.** Panamax container vessel sailing on her meeting line in the Gaillard Cut. (a) Ship and canal geometry. (b) Required rudder capacity at different propeller rates as a function of ship speed and distance to buoy line. (c) Required rudder capacity: effect of canal deepening. (Reproduced with permission from Eloot, Verwilligen, and Vantorre, 2007. © Marc Vantorre, 2007.)

*dead slow*, and 85% with the propeller stopped. A comparison is also made with an enhanced situation after channel deepening. For a ship with engine *slow*, the required rudder capacity drops from 38% to 25% if the depth is increased to 14.6 m, due to the high sensitivity of the bank-induced forces with respect to UKC variations.

### 3 EFFECT OF MUDDY BOTTOMS

#### 3.1 Nautical bottom

Due to sedimentation, permanent maintenance dredging works are required to keep many ports accessible for deep-drafted vessels. In case of hard bottoms (rock, clay, and sand), the depth can be measured unambiguously by means of echo-sounding techniques. If the bottom is covered with soft mud layers, however, the boundary between water and bottom may be hard to define, as the survey results will depend on the applied ultrasonic frequency: while high-frequency echoes (e.g., 210 kHz) reflect at the mud–water interface, lower frequency signals (e.g., 33 kHz) penetrate deeper into the mud. The difference between both signals may vary from a few decimeters to even 3–4 m. While the upper part of this layer may be fluid (black water), the density and the rheological properties (viscosity and yield stress) of the layer gradually increase with depth.

In this case, the *nautical bottom* concept has to be introduced, defined by PIANC (1997) as *the level where physical characteristics of the bottom reach a critical limit beyond which contact with a ship's keel causes either damage or unacceptable effects on controllability and maneuverability*. The application range of this definition is not limited to muddy bottoms. In case of a hard bottom (e.g., rock), bottom contact will cause damage, while contact with a muddy bottom will rather result in unacceptable ship behavior.

The nautical bottom concept was introduced in the 1970–1980s in a few West-European harbors. It is a common practice to select a critical density as a criterion for the nautical bottom, typically around 1.2 ton/m<sup>3</sup>, because this characteristic can be measured *in situ* in a relatively easy and unambiguous way. However, the rheological behavior of fluid mud is not directly related to sediment density, but also depends on the mud composition. Eventually, mud rheology is more important than density, because it is the rheology that determines whether mud behaves like a fluid or like a solid material. Due to the complexity of mud rheology, it is up till now not feasible to use a rheology-related criterion for

determining the nautical bottom, although several measuring systems are under development.

Maintenance-dredging problems in harbors have led to on-going research on mud sedimentology, and also on behavior of ships navigating with decreased or even negative UKC with respect to the mud–water interface (further denoted UKCi). Model test research was performed in the 1970s and 1980s at MARIN for investigating the access of deep-drafted tankers to the port of Rotterdam, at SOGREAH in the light of sedimentation problems in French harbors, and at Flanders Hydraulics Research (FHR, Antwerp). More recently, a comprehensive captive maneuvering program executed at FHR led to the development of mathematical maneuvering simulation models (Delefortrie, Vantorre, and Eloot, 2005) to determine new access criteria for the port of Zeebrugge. Besides model tests, full-scale experiments were conducted in Rotterdam, Nantes–Saint-Nazaire, and Zeebrugge in the 1970s and 1980s, and more recently in the port of Delfzijl (Verwilligen *et al.*, 2014).

#### 3.2 Physical phenomena

Ship behavior may be affected by the presence of mud due to two phenomena:

- the mud rheology, which is of particular importance if contact occurs between the mud layer and the ship's keel;
- the generation of undulations (*internal waves*) in the water–mud interface, which may not only affect the flow around a ship in contact with the mud layer, but also when a ship is moving with limited UKCi.

The internal wave pattern depends on the ship's forward speed. At very low speed, the interface remains practically undisturbed. At intermediate speed, an interface sinkage is observed under the ship's entrance, which at a certain section changes into an elevation. This internal hydraulic jump is perpendicular to the ship's longitudinal axis, and increases in magnitude while moving toward the stern with increasing speed (second speed range). At higher speeds, the interface jump occurs behind the stern (third speed range), with increasing angle between the ship's heading and the propagation direction of the jump (Figure 6).

The occurrence of these speed ranges can be explained by means of a simplified theory, assuming that both water and mud are ideal, inviscid fluids. For a ship moving at low speed above a mud layer, dynamic equilibrium leads to both a sinking and a rising of the water–mud interface, while only a sinking is feasible for speeds exceeding a critical value  $U_{crit}$



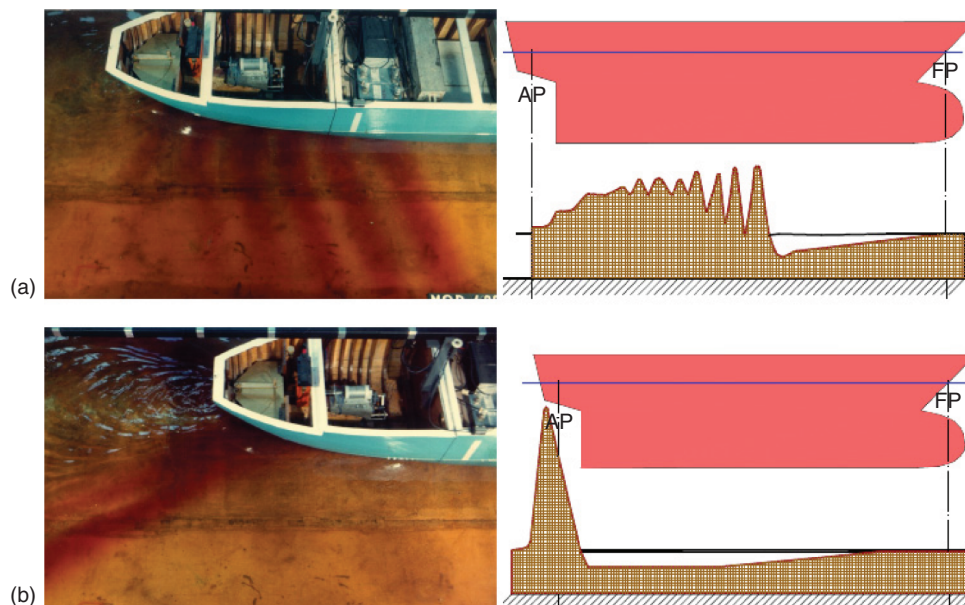


**Figure 6.** Mud–water interface undulations: second speed range (a) and third speed range (b). (Reproduced with permission from Vantorre, Laforce, and Delefortrie, 2006. © Marc Vantorre, 2006.)

(Vantorre, 1991):

$$U_{\text{crit}} = \sqrt{\frac{8}{27}gh_1 \left(1 - \frac{\rho_1}{\rho_2}\right)} \quad (4)$$

$h_1$  being the depth of the water layer, and  $\rho_1$  and  $\rho_2$  denoting water and mud densities, respectively. Figure 7 shows that critical speeds are situated in the usual range at which harbor approach takes place.

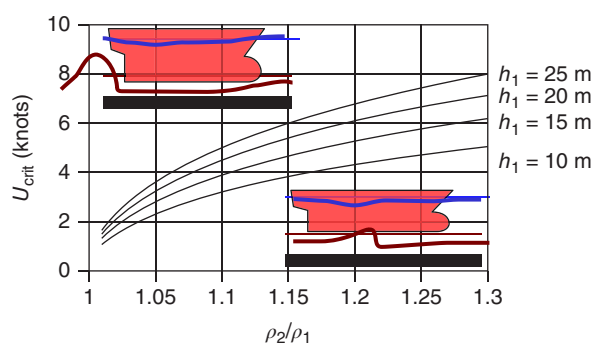


**Figure 7.** Critical speed separating second and third speed ranges as a function of mud–water density ratio for different water depths. (Reproduced with permission from Vantorre, Laforce, and Delefortrie, 2006. © Marc Vantorre, 2006.)

### 3.3 Hydrodynamic forces on a maneuvering ship

#### 3.3.1 Hull forces

The following trends are of interest for understanding ship maneuverability in muddy areas:

- Hydrodynamic inertia terms increase significantly with decreasing water depth and increasing mud density and viscosity, see Figure 8. If the ship's keel penetrates deep into the mud, very large values are observed, but even when no contact occurs, the layer characteristics have an important effect. For a constant UKCi, the shallow-water effect is lessened with increasing layer thickness and decreasing mud density and viscosity. No abrupt transition is observed at zero UKCi.
- The drift-induced lateral force and yawing moment increase significantly with decreasing water depth. However, this increase appears to stagnate when the keel touches the interface. For a given positive UKCi, the presence of a mud layer appears to minimize the shallow-water effects, especially for layers with low density and viscosity. On the other hand, for a given UKC relative to the hard bottom, a mud layer always has an adverse effect.
- The yaw-induced lateral force follows the tendencies described in Section 1.3 for small and negative UKCi;

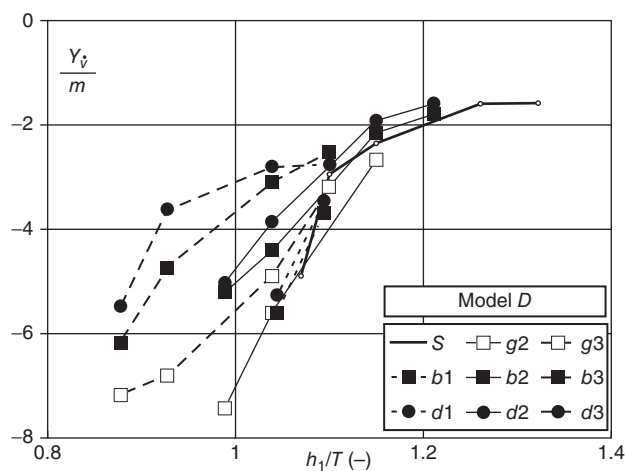


**Figure 8.** Effect of bottom characteristics and UKCi on the sway-added mass of a container carrier:  $S$ =solid bottom;  $g/b/c/d$ =mud density 1.25/1.18/1.15/1.10 ton/m<sup>3</sup>; 1/2/3: increasing layer thickness. (Reproduced with permission from Delefortrie, 2007. © Guillaume Delefortrie, 2007.)

the resulting lateral force even becomes centripetal. The transition from centrifugal to centripetal action takes place at a larger UKCi when the mud density and viscosity increase and the layer thickness decreases. Therefore, this effect is not typical for muddy areas, but should rather be considered as a (very) shallow water effect. Moreover, the yaw-induced yaw moment increases with increasing density and decreasing UKCi.

### 3.3.2 Rudder forces

The forces caused by rudder action depend on the axial flow into the rudder. This flow is a function of the forward speed, propeller rate, and rudder wake factor. The latter is significantly affected by the bottom condition and the UKCi: the wake factor decreases and, consequently, the flow to the rudder improves with increasing mud density and increasing UKCi. When the ship penetrates deep into soft, low density mud layers, however, the inflow to the rudder is affected unfavorably.

At near-zero UKCi values, due to interface undulations the ship's keel touches both water and mud, which may cause rudder instability: small rudder angles sometimes induce unexpected effects.

### 3.3.3 Propeller-induced forces

The longitudinal force acting on the ship due to propeller action depends on the propeller thrust, but also on the thrust-deduction factor. A larger value for the latter—which implies a smaller longitudinal force for a given thrust—is

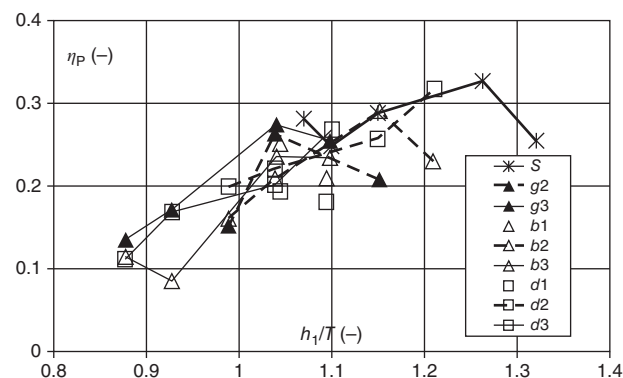


**Figure 9.** Overall propeller efficiency of a container carrier model: effect of bottom characteristics and UKCi. Symbols: see Figure 8. (Reproduced with permission from Delefortrie, 2007. © Guillaume Delefortrie, 2007.)

obtained at positive UKCi with high-density mud layers; at negative UKCi, on the other hand, the thrust deduction factor is larger for the lowest densities.

The propeller thrust is determined by the propeller rate and the axial inflow velocity. The latter depends on the ship's forward speed, but also on the wake factor: a larger value for this factor implies a smaller inflow velocity and, therefore, a higher propeller loading. The wake factor is clearly affected by the bottom conditions: it increases when navigating above or through low-density mud layers, while a significant decrease is observed in contact with high-density mud layers.

Figure 9 shows the effect of mud on the overall propeller efficiency: compared to a solid bottom, a significant loss of efficiency is observed, especially at negative UKCi.

## 3.4 Ship performance and maneuverability

### 3.4.1 Speed and propulsion

The relationship between forward speed and propeller rate clearly illustrates the effect of interface undulations on a ship's propulsive performance. In the second speed range, as defined in Section 3.2, a given propeller rate results in a significantly lower speed above a muddy bottom; a similar effect was observed recently during full-scale observations (Verwilligen *et al.*, 2014). An increased effort is required to reach the third speed range, where the mud effect practically disappears. The transition between both ranges is very clear at 10–20% UKCi, but is smoothened at negative UKCi.

This effect is not caused by increased resistance, but rather by obstruction of the flow to the propeller due to internal waves. Deeper penetration into mud layers, however, leads to a significant resistance increase.

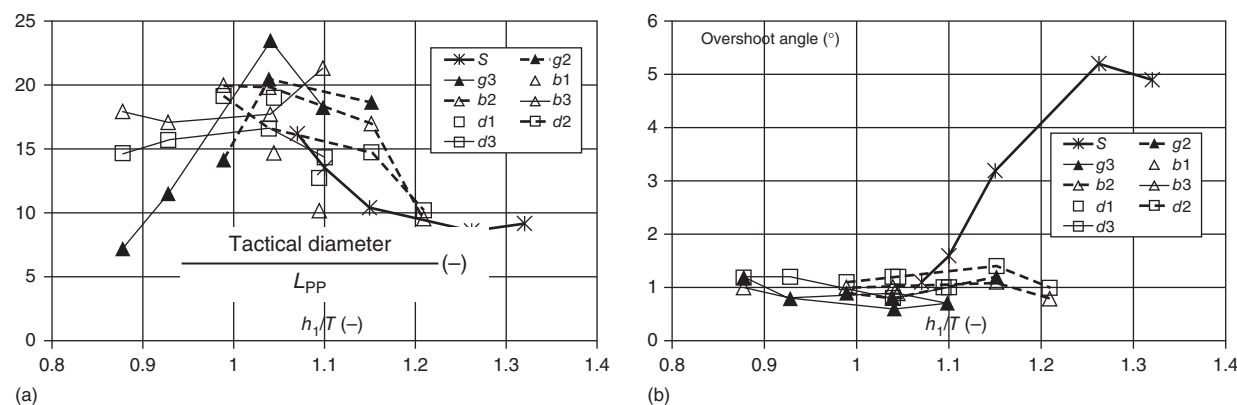


**Figure 10.** Tactical diameter (a) and first overshoot angle for 20/20 zigzag (b) for a container carrier model: effect of bottom characteristics and UKCi. (Reproduced with permission from Delefortrie, 2007. © Guillaume Delefortrie, 2007.)

### 3.4.2 Standard maneuvers

Simulated turning circles show that a ship's turning ability generally decreases when a fluid mud layer is present. The tactical diameter appears to reach a maximum at a very small positive UKCi, but decreases once the keel penetrates the mud layer and, in high density mud layers, even becomes smaller than above a solid bottom (Figure 10). The drift angles during turning-circle maneuvers are very small above and in mud.

With respect to zigzag tests, the first overshoot angle takes much smaller values above and in mud layers compared to a solid bottom condition, see Figure 10.

### 3.4.3 Actual practice

In several ports, the introduction of the nautical bottom concept has resulted in navigation with reduced UKCi; in case of mud layers with important thicknesses, even navigating through the mud layer is a common practice. In particular, in the port of Zeebrugge, a maximum penetration of 7% of draft into the mud layer is commonly accepted as a safe limit. Even larger penetration depths are applied in the port of Emden, where the mud is permanently fluidized.

Pilots and captains, however, have to account for a modified ship behavior, for example, by anticipating the increased inertia, strict speed limitations, and sufficient tug assistance. Not only the nautical bottom level has to be known, but also the position of the interface is of importance. In general, a slight negative UKCi results in a more stable and predictable behavior compared to a small positive UKC. Contact with consolidated mud layers, however, may lead to uncontrollable speed and heading, and should be avoided.

## 4 SHIP-SHIP INTERACTION

### 4.1 Types of ship-ship interaction

One of the problems interfering with navigation in restricted channels is the hydrodynamic interaction between ships. Four types of interaction will be considered:

- interaction between ships advancing at parallel courses: during overtaking, ships are sailing in the same direction, while encountering (meeting, reciprocal, or head-on passing) occurs with ships sailing in opposite directions;
- interaction with a moored ship;
- interaction between ships advancing at approximately equal forward speed in parallel and in close proximity to each other, which occurs during lightering and underway replenishment (UNREP) maneuvers;
- interaction of tugs with ships.

### 4.2 Ships moving on parallel courses

#### 4.2.1 Encountering

In general terms, the interaction effects (Figure 11) begin to be felt when the bows of both ships are pushed away from each other, which is accompanied by a slight increase in speed. As the ships pass, the bow-out yaw moment turns to bow-in and the repulsion reduces. The bow-out moment then returns as passing continues but is now stronger and may cause the ships to sheer away from each other once they have passed. A reduction in speed may also be felt. Finally, a weak bow-in moment accompanied by a repulsion may

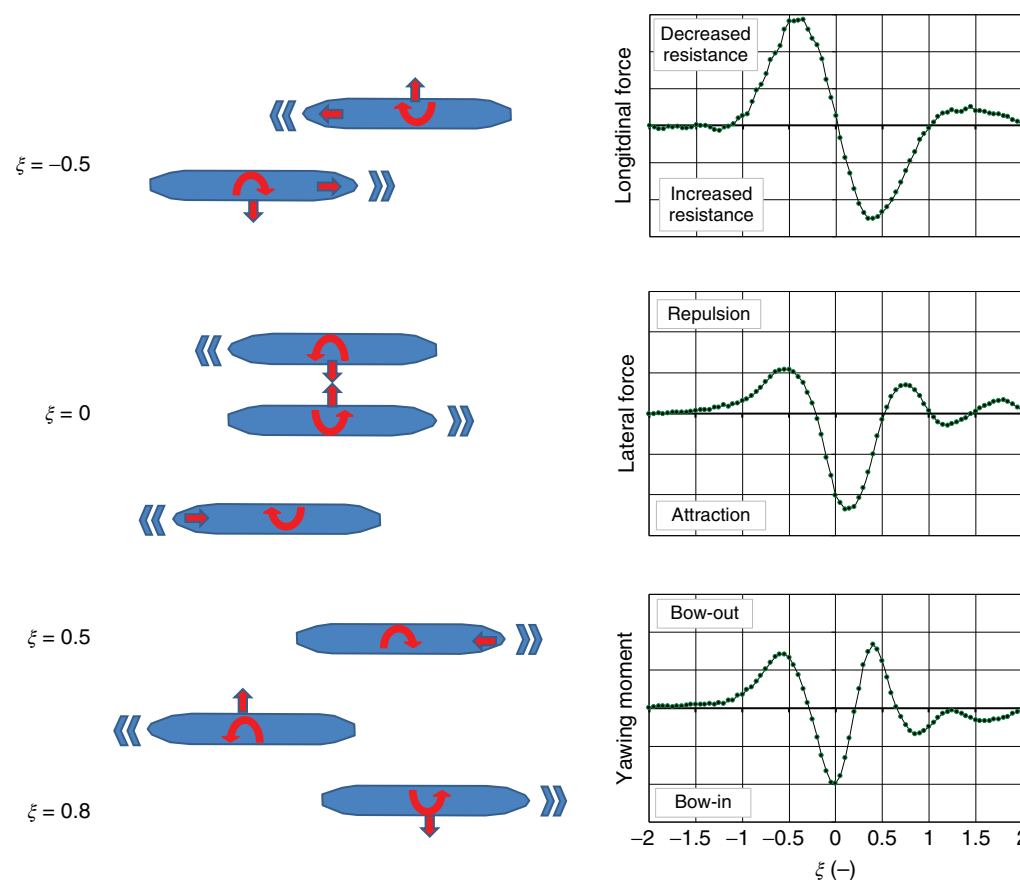


**Figure 11.** Graphical indication of the horizontal interaction effects during encountering maneuvers,  $\xi$  being a nondimensional notation for the longitudinal separation between both midships sections (FHR).

be felt (Dand, 1995; Vantorre, Verzhbitskaya, and Laforce, 2002). Similarly, the varying pressure distributions around the ships affect the sinkage and trim of both vessels.

From an interaction point of view, passing on reciprocal courses has the merit of happening quickly so that the ship often does not have time to react to the various interaction forces and moments she feels. Usually, the dominant effects are the bow-out moments as the ships begin to pass and the stronger bow-out moments once passing is almost over.

#### 4.2.2 Overtaking

Typical interaction forces are shown in Figure 12 for both ships involved. As the overtaking vessel overhauls the other vessel, a bow-in moment is first experienced by the fastest vessel. The overtaken ship will then experience a strong bow-out moment followed by a bow-in moment. The sway force on the overtaken ship is characterized by a sequence of repulsion, attraction, and repulsion, comparable to encounter maneuvers. The overtaken ship first experiences a resistance increase but when the overtaking ship gets in front of the

overtaken ship, a resistance decrease causes speeding up of the overtaken ship, whereas the overtaking ship slows down; this renders overtaking more difficult (*trapping*).

As the relative velocity during overtaking may be low, interaction has time to take effect. A collision scenario is shown in Figure 13a and is caused when the overtaken ship turns across the bows of the overtaking ship, which may perversely turn toward her. If a collision does not occur and the overtaking vessel moves past the other, both ships will feel powerful bow-out moments together with a mutual attraction. This may cause both ships to “fly apart” and their sterns to collide, as shown in Figure 13b (Dand, 1995).

#### 4.3 Interaction with moored ships

Ships moored in harbors experience hydrodynamic forces due to other ships passing nearby, see Figure 14, as well as vertical motions. The passing vessel induces forces on the moored vessel that are associated with the low-frequency



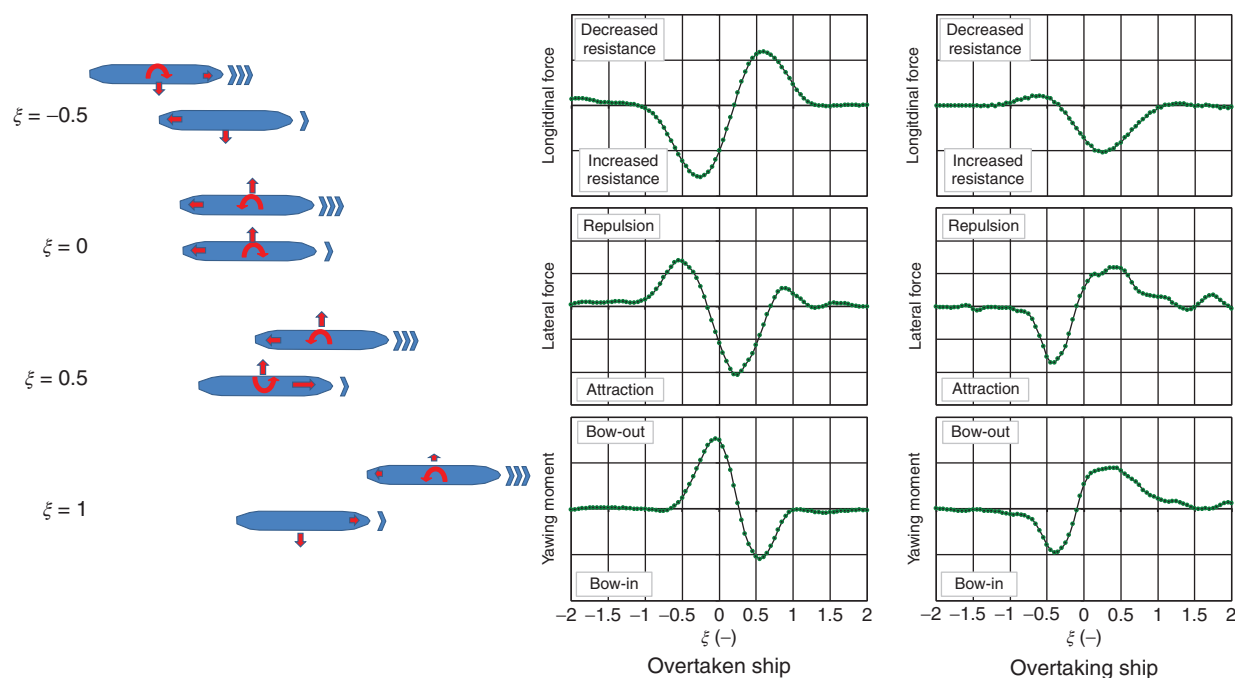


**Figure 12.** Graphical indication of the horizontal interaction effects during a typical overtaking maneuver (FHR).

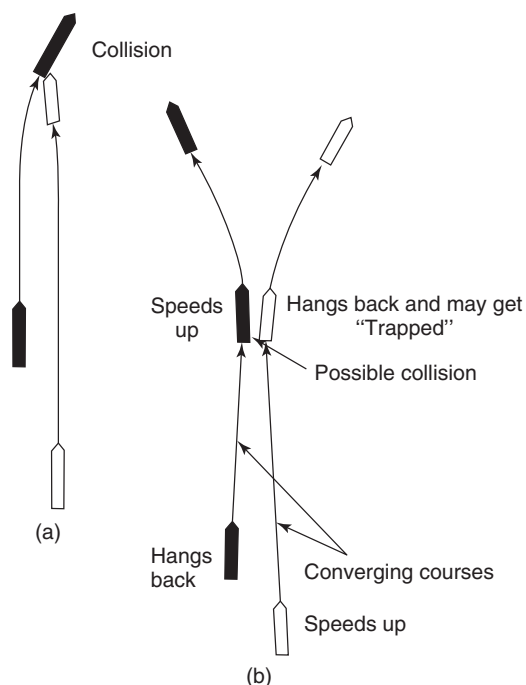


**Figure 13.** (a,b) Possible collision situations during an overtaking maneuver. (Reproduced with permission from Dand, 1995. © BMI Ltd, 1995.)

primary pressure system and forces that are associated with the higher-frequency secondary pressure system. The low-frequency (suction) forces are more significant for

the moored ship at low speeds, while wash waves become important at near-critical or supercritical speeds (Pinkster, 2004; Van Der Molen *et al.*, 2011).

The interaction forces induce motions of the moored ship that may hinder (un)loading operations or cause damage to the mooring system. Even though the sway force is larger than the surge force, the latter often causes high loading in mooring lines because of the lower surge damping. The disruption that passing ships cause to moored ships can often be reduced by paying close attention to the vessels' mooring. Alternative measures are reducing passing ship speeds (which is not always possible as a minimum speed may be required to maintain maneuverability), greater passing distances, or deepening the channel and berth area. As the sizes and speeds of vessels have increased over the years, so have the interaction forces.

Quite logically, the interaction forces on the moored ship increase as the lateral passing distance and UKC decrease and the size and speed of the passing vessel increase (Talstra and Blik, 2014). Experiments have shown that the forces on a moored ship due to a passing ship are proportional to the passing speed squared, provided the speeds are relatively low. The forces can be significantly larger for larger Froude numbers as the forces significantly divert from the square law assumption roughly for a depth-related Froude number  $Fr_h > 0.25$  (Van Der Molen *et al.*, 2011).

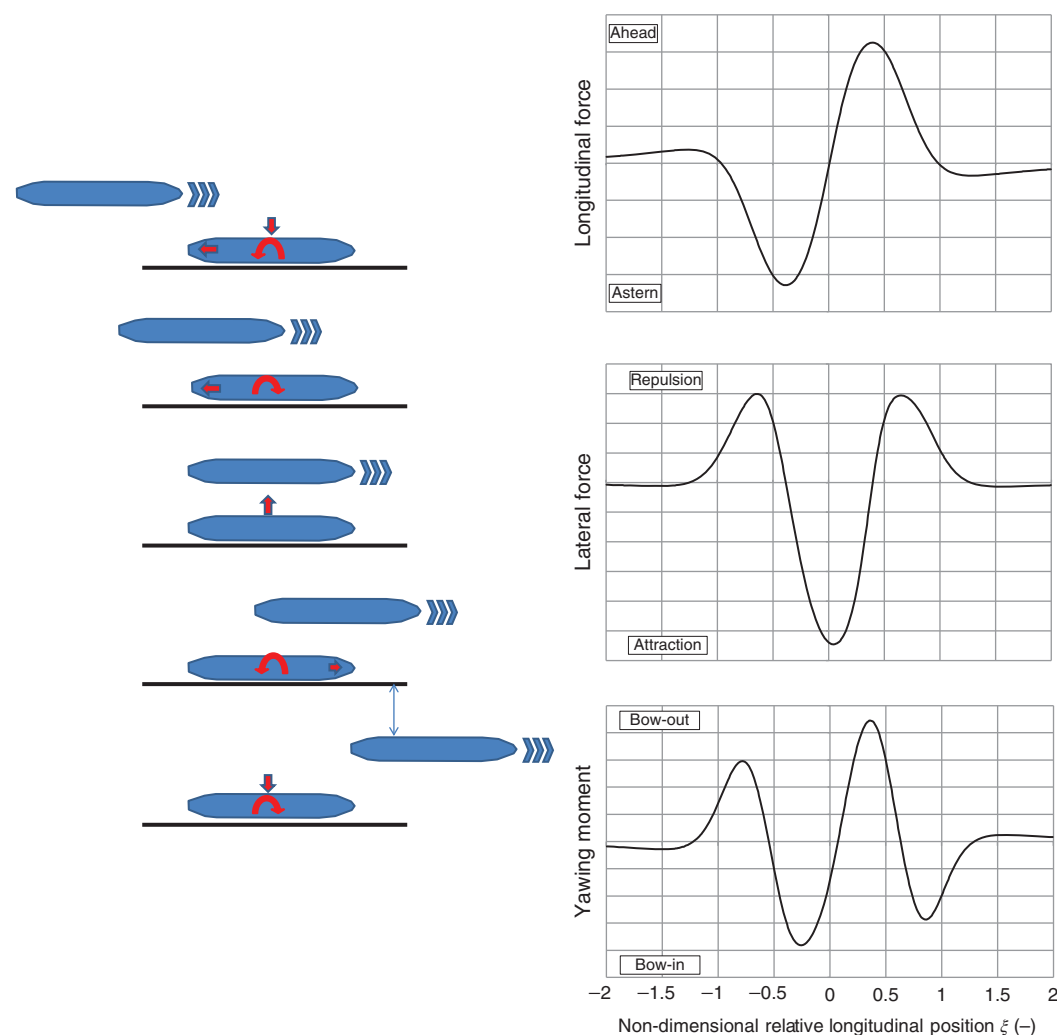


**Figure 14.** Graphical indication of the interaction forces on a moored ship due to a passing ship (results from ROPES software).

#### 4.4 Lightering and underway replenishment

Ship-to-ship transfer of oil or gas is commonly defined as a lightering operation, which usually involves two vessels that are distinctively different in size. The larger ship is referred as a *ship to be lightered (STBL)*, while the smaller ship is named a lightering or a service ship. The operation can be performed in sheltered or open and deep waters. For operations that take place in sheltered waters, the two involved ships are mostly at anchor and moored together, and this situation will not be discussed; attention is paid to lightering operations that involve two ships advancing in parallel side by side at low forward speeds. The situation is similar to a replenishment at sea (RAS) operation, or UNREP, carried out by warships.

The maneuvering requirements for the lightering ship change as she passes through different stages. The lightering ship usually starts her approach from behind, on the starboard side of the STBL. In order to accomplish the lightering operation, that is, the abeam transfer position, the lightering ship must match the speed and heading of the STBL, and the transversal and longitudinal distance relative to this ship has to be monitored continuously. Once the mentioned requirements are fulfilled, both advancing ships are moored together, by using fenders that ensure a lateral separation of up to 5 m in diameter (Skejic and Berg, 2009).

Potentially hazardous collision situations may develop because of the presence of hydrodynamic interaction between loads when two ships operate in close proximity.

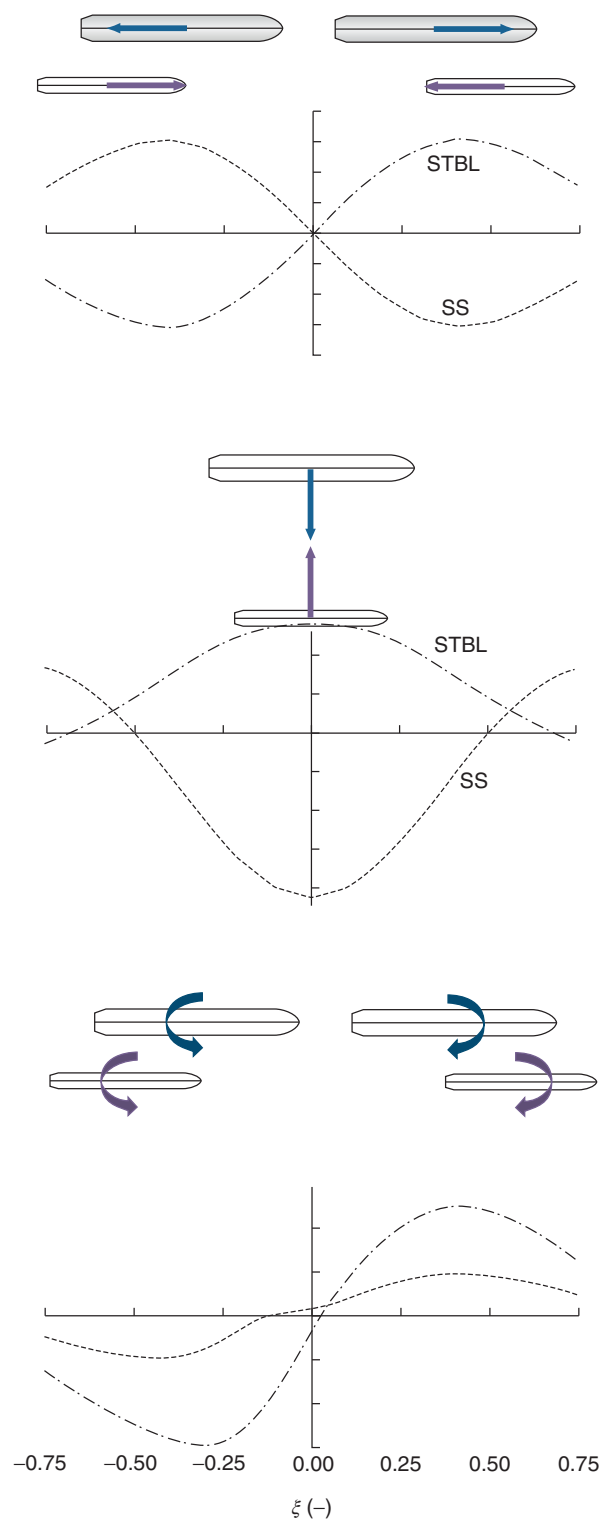


**Figure 15.** Interaction forces during lightering maneuver as a function of relative longitudinal position of both ships (based on Lataire *et al.*, 2012): longitudinal force (up), lateral force (middle), and yawing moment (down). (Reproduced with permission from Lataire *et al.*, 2012. © Elsevier, 2012.)

The interaction forces depend on speed, lateral separation, and relative longitudinal position, as indicated in Figure 15.

#### 4.5 Tug–ship interaction

Due to their tasks, tugs have to come close to the ships they assist and sometimes at relatively high speeds, which implies that the interaction forces can be high. To avoid accidents, a good understanding of the interactions between ships and tugs is therefore important for both ship and tug operators (Dand, 1975).

The tug is generally much smaller than the ship it is assisting and while a given depth of water may be deep for the tug, it may well be shallow for the ship. This means that the ship will have a large interactive effect on the tug and the tug will have virtually no effect on the ship (Dand, 1995). In particular, a sway force, a surge force, and a yawing moment will be induced due to the asymmetry of the flow. As usual, these interaction forces will intensify if the flow becomes more two-dimensional (Geerts *et al.*, 2011).

Figure 16 shows diagrammatically the sort of interaction forces and moments conventionally powered (and steered) tugs will typically experience when they come alongside. When the tug is near the stern of the ship, an increase in its velocity may occur due to the flow velocity from the aft of the ship. In close proximity to the ship hull, a low pressure starts moving the tug in the ship's direction. For ships in ballast condition, or ships having particular overhanging stern, the tug risks damage to its hull or superstructure. Going forward and near the hull, the tug experiences an important suction force in the direction of the ship hull and a bow-out yaw moment. When the tug is attracted by the ship, it is in general difficult to recover her course. When the tug is further forward near the side of the bow, she enters high-pressure area and the bow-out yaw moment is growing, which must be compensated by the appropriate use of the rudder and propeller. Finally, when the tug is near the bow, a strong sway force acting on the stern brings the tug to the front and under the bow with the risk of capsizing. This has caught a number of conventional tugs unawares over the years with disastrous consequences, largely due to the sudden changes in the interaction forces and moments acting on the vessel as it alters its fore and aft position alongside the bigger ship. Such variations are larger if the assisted ship has pronounced shoulders (Dand, 1995).

The tug may approach safely in the vicinity of midships where the longitudinal interaction force helps in station-keeping. Some areas near the bow and stern are best avoided because the control that the rudder exerts adds to, rather than subtracts from, the effects of interaction.

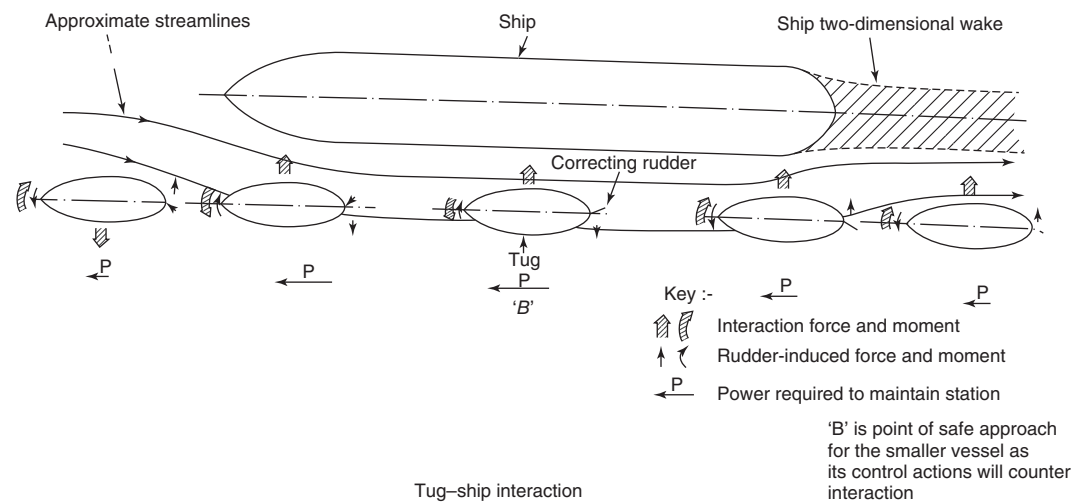


**Figure 16.** Interaction forces on tugs. (Reproduced with permission from Dand, 1995. © BMI Ltd, 1995.)

## NOMENCLATURE

$a, b$	coefficients in weight distribution function $w(y, z)$	$V_{crit}$	critical speed in a canal (m/s)
$a_H$	multiplication factor for $Y_R$ to obtain rudder-induced lateral force acting on the hull	$w(y, z)$	weight distribution function for calculating distance to bank parameter $d2b$
$B$	ship beam (m)	$Y$	lateral force (N)
$d2b$	non-dimensional distance to bank parameter	$y_{B3}$	non-dimensional ship-bank distance parameter
$Fr_h$	depth-related Froude number	$y_p$	lateral distance at port side from ship's centerline to bank at bottom level (m)
$g$	acceleration of gravity ( $m/s^2$ )	$y_{p3}$	distance from ship's centerline to bank at port side at half draft (m)
$h$	water depth (m)	$Y_R$	lateral force component (in ship's coordinate system) acting on rudder (N)
$h_1$	depth of water layer (in muddy areas) or water depth on flooded bank (m)	$y_S$	lateral distance at starboard side from ship centerline to bank at bottom level (m)
$h_{avg}$	average water depth (m)	$y_{s3}$	distance from ship's centerline to bank at starboard side at half draft (m)
$k$	bank slope factor	$Y_v$	added mass for sway (kg)
$L$	ship length (m)	$\beta$	drift angle ( $^\circ$ )
$L_{pp}$	length between perpendiculars (m)	$\chi$	integral of weight distribution function $w(y, z)$ over a specified domain mentioned in subscript
$m$	ship mass (kg) or blockage factor	$\eta_0$	non-dimensional ship-bank distance at free surface
$m_{eq}$	equivalent blockage factor	$\eta_B$	non-dimensional ship-bank distance at bottom
$N$	yawing moment ( $kg\ m^2/s^2$ )	$\eta_P$	overall propeller efficiency
$N_f$	added moment of inertia for yaw ( $kg\ m^2$ )	$\rho_1$	water density ( $kg/m^3$ )
$r$	yawing rate ( $1/s$ )	$\rho_2$	mud density ( $kg/m^3$ )
$\dot{r}$	yaw acceleration ( $1/s^2$ )	$\xi$	non-dimensional stagger (longitudinal distance between ships on parallel courses)
$T$	draft (m)	$\dot{\alpha}$	time derivative of $\alpha$ ( $1/s$ )
$u$	longitudinal ship speed component (m/s)	ITTC	International Towing Tank Conference
$\ddot{u}$	ship acceleration in longitudinal direction ( $m/s^2$ )	PIANC	The World Association for Waterborne Transport Infrastructure (originally Permanent International Association of Navigation Congresses)
$U_{crit}$	critical speed for navigation above fluid mud, as defined in Equation 4 (m/s)		
UKC	under keel clearance		
UKCi	under keel clearance with respect to the water-mud interface		
$v$	lateral ship speed component (m/s)		
$\dot{v}$	ship acceleration in lateral direction ( $m/s^2$ )		
$V$	ship speed (m/s)		

RAS	replenishment at sea
STBL	ship to be lightered
TEU	twenty feet equivalent unit
UNREP	underway replenishment

GLOSSARY

Bank effect	Forces and moments acting on a ship due to a motion that has a mainly parallel orientation with respect to a bank.
Blockage	Ratio between the cross-sectional area of a ship and the cross-sectional area of a canal.
Critical speed	(of a ship in a waterway) maximum speed for which a steady solution for the sinkage and the return flow can be found.
Critical speed	(in channels with muddy bottoms) maximum speed at which a rising of the water-mud interface under a ship navigating above the mud layer is possible.
Froude number	Speed of the ship made non-dimensional by division by the square root of the gravitational acceleration multiplied with a characteristic dimension (usually ship length; water depth in case of depth-related Froude number).
Lightering	Operation during which cargo is transferred between two ships.
Nautical bottom	The level where physical characteristics of the bottom reach a critical limit beyond which contact with a ship’s keel causes either damage or unacceptable effects on controllability and maneuverability.
Ship-ship interaction	Hydrodynamic forces and moments induced by the relative speed between two ships, especially when the ship’s courses are (nearly) parallel.
Under-keel clearance	Vertical distance between a ship’s keel and the bottom of the navigation area.

REFERENCES

Briggs, M., Vantorre, M., Uliczka, K., and Debaillon, P. (2009) Prediction of squat for underkeel clearance, in *Handbook of Coastal and Ocean Engineering* (ed. Y.C. Kim), World Scientific, Singapore.

Ch’ng, P.W., Doctors, L.J., and Renilson, M.R. (1993) A method of calculating the ship–bank interaction forces and moments in restricted water. *International Shipbuilding Progress*, **40** (412), 7–23.

Crane, C.L. (1979) Maneuvering trials of a 278 000-DWT tanker in shallow and deep waters. *SNAME Transactions*, **87**, 251–283.

Dand, I.W. (1975) *Some Aspects of Tug Ship Interaction*. Proceedings of the Fourth International Tug Convention, New Orleans, LA, USA, pp. 61–80 (Paper A5).

Dand, I.W. (1995) Interaction. Squat, Interaction, Manoeuvring, The Nautical Institute, Humberside Branch Seminar, pp. 1–20.

Delefortrie, G. (2007) Manoeuvring behaviour of container vessels in muddy navigation areas. Ph.D. thesis, Ghent University.

Delefortrie, G., Vantorre, M., and Eloot, K. (2005) Modelling navigation in muddy areas through captive model tests. *Journal of Marine Science and Technology*, **10** (4), 188–202.

Eloot, K. (2006) Selection, experimental determination and evaluation of a mathematical model for ship manoeuvring in shallow water. Ph.D. Thesis, Ghent University. ISBN 90-8578-092-6. XIV, 398 pp.

Eloot, K., Vantorre, M. and Delefortrie, G. (2006) *Prediction of Ship Manoeuvrability of an 8000 TEU Containership in Deep and Shallow Water: Mathematical Modelling and Captive Model Testing*. Marine Simulation and Ship Manoeuvrability: Proceedings of the International Conference MARSIM 2006, Terschelling, The Netherlands, 25–30 June 2006. pp. M-3-1–M-3-9.

Eloot, K., Verwilligen, J. and Vantorre, M. (2007) A Methodology for Evaluating the Controllability of a Ship Navigating in a Restricted Channel. *Hydronav 2007, Seventeenth International Conference on Hydrodynamics in Ship*, Polanica Zdrój, Poland, September 2007, pp. 114–125.

Geerts, S., Vantorre, M., Eloot, K., Huijsmans, R. and Fierens, N. (2011) *Interaction Forces in Tug Operations*. Second International Conference on Ship Manoeuvring in Shallow and Confined Water: Ship to Ship Interaction, Trondheim, Norway, R.I.N.A., pp. 153–163.

ITTC (2002) *The Manoeuvring Committee—Final Report and Recommendations to the 23rd ITTC*. Proceedings of the 23rd ITTC, Vol. I, pp. 153–234.

Lataire, E. (2014) Experiment based mathematical modelling of ship–bank interaction. Ph.D. thesis, Ghent University.

Lataire, E. and Vantorre, M. (2008) *Ship–Bank Interaction Induced by Irregular Bank Geometries*. Proceedings 27th Symposium on Naval Hydrodynamics, Seoul.

Lataire, E., Vantorre, M., Delefortrie, G., and Candries, M. (2012) Mathematical modelling of forces acting on ships during lightering operations. *Ocean Engineering*, **55**, 101–115.

Norrbin, N. (1974) *Bank Effects on a Ship Moving through a Short Dredged Channel*. 10th ONR Symposium on Naval Hydrodynamics, Cambridge, MA.

Norrbin, N. (1985) *Bank clearance and optimal section shape for ship canals*. 26th PIANC International Navigation Congress, Brussels, Section 1, Subject 1, pp. 167–178.

PIANC (1992) Capability of ship manoeuvring simulation models for approach channels and fairways in harbours. Report of Working Group no. 20 of Permanent Technical Committee II, Supplement to PIANC Bulletin No. 77, 49 pp.

- PIANC (1997) Approach channels—a guide for design. Supplement to PIANC Bulletin 95, 108 pp.
- PIANC (2014) Harbour approach channels design guidelines. Maritime Navigation Commission, Report No. 121.
- Pinkster, J.A. (2004) The influence of a free surface on passing ship effects. *International Shipbuilding Progress*, **61** (4), 313–338.
- Rijkswaterstaat (2011) Waterline Guidelines 2011. Directorate-General for Public Works and Water Management, 177 pp.
- Skejic, R. and Berg, T.E. (2009) *Hydrodynamic Interaction Effects during Lightering Operation in Calm Water—Theoretical Aspects*. MARSIM '09 Conference, Proceedings, Panama City, Panama, Panama Canal Authority, International Marine Simulator Forum, pp. M-8-1–M-8-9.
- Talstra, H. and Blik, A.J. (2014) *Loads on Moored Ships Due to Passing Ships in a Straight Harbour Channel*, PIANC World Congress, San Francisco, USA.
- Van Der Molen, W., Swiegers, P., Moes, J., and Vantorre, M. (2011) *Calculation of Forces on Moored Ships due to Passing Ships*. Second International Conference on Ship Manoeuvring in Shallow and Confined Water: Ship to Ship Interaction, Trondheim, Norway, R.I.N.A., pp. 369–374.
- Vantorre, M. (1991) *Ship Behaviour and Control at Low Speed in Layered Fluids*. Proceedings International Symposium on Hydro- and Aerodynamics in Marine Engineering (HADMAR), BSHC, Varna.
- Vantorre, M., Verzhbitskaya, E., and Laforce, E. (2002) Model test based formulations of ship–ship interaction forces. *Ship Technology Research*, **49** (3), 124–141.
- Vantorre, M., Laforce, E., and Delefortrie, G. (2006) A novel methodology for revision of the nautical bottom, in *Seminar: Flanders, a Maritime Region of Knowledge (MAREDFlow)* (eds Y. Peeters, N. Fockedey, J. Seys, and J. Mees), Vlaams Instituut voor de Zee (VLIZ), Oostende, pp. 15–34.
- Verwilligen, J., Vantorre, M., Delefortrie, G., Kamphuis, J., Meinsma, R., and Van Der Made, K.-J. (2014) *Manoeuvrability in Proximity of Nautical Bottom in the Harbour of Delfzijl*, PIANC World Congress, San Francisco.
- Yasukawa, H. and Kobayashi, E. (1995) *Shallow Water Model Experiments on Ship Turning Performance*. Mini Symposium on Ship Manoeuvrability, 26 May 1995, Fukuoka, Japan, pp. 71–83.

## Appendix C: Hose Length Calculations



Hose String Component	SMOG	OCIMF
Bow to center of manifold	545 FT.	545 FT.
Hawser	180 FT.	180 FT.
Hawser elongation	48 FT.	48 FT.
Freeboard (Ballast)	67 FT.	67 FT.
½ Beam	112 FT.	-
Chafe Chain	8 FT.	8 FT.
76mm Mooring Chain	8 FT.	8 FT.
Manifold Height	5 FT.	5 FT.
Hose Rail to Manifold	18 FT.	18 FT.
Center – Aft Manifold	-	15 FT.
Buoy R (hawser lug)	-	16 FT.
Teardrop allowance	-	40 FT.
<b>TOTAL HOSE LENGTH REQUIRED</b>	<b>991 FT.</b>	<b>950 FT.</b>

## Hose Length in SPM System

Required Overall Length of floating hose string can be designed as per the following formula:-

$$TL = C + (R \times (1+E)) + (B/2) + L + H + M + G$$

WHERE:

TL: REQUIRED OVER ALL LENGTH

R : LENGTH OF MOORING HAWSER

E : MAX. ELONGATION OF MOORING ROPE

L : DISTANCE BETWEEN BOW AND MANIFOLD

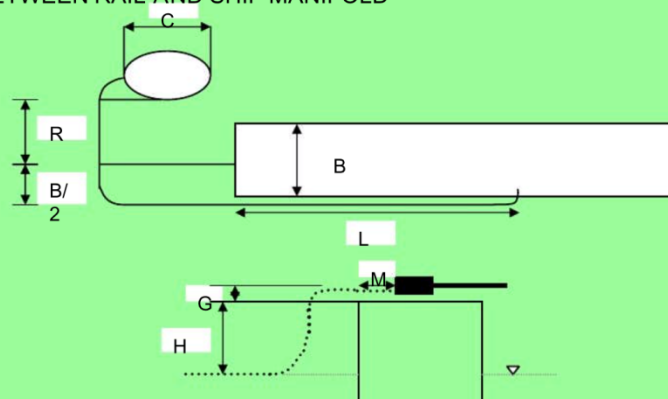
M : DISTANCE BETWEEN RAIL AND SHIP MANIFOLD

C : DIAMETER OF BUOY

B : BEAM OF TANKER

H : MAXIMUM FREEBOARD

G : HEIGHT OF MANIFOLD FROM DECK





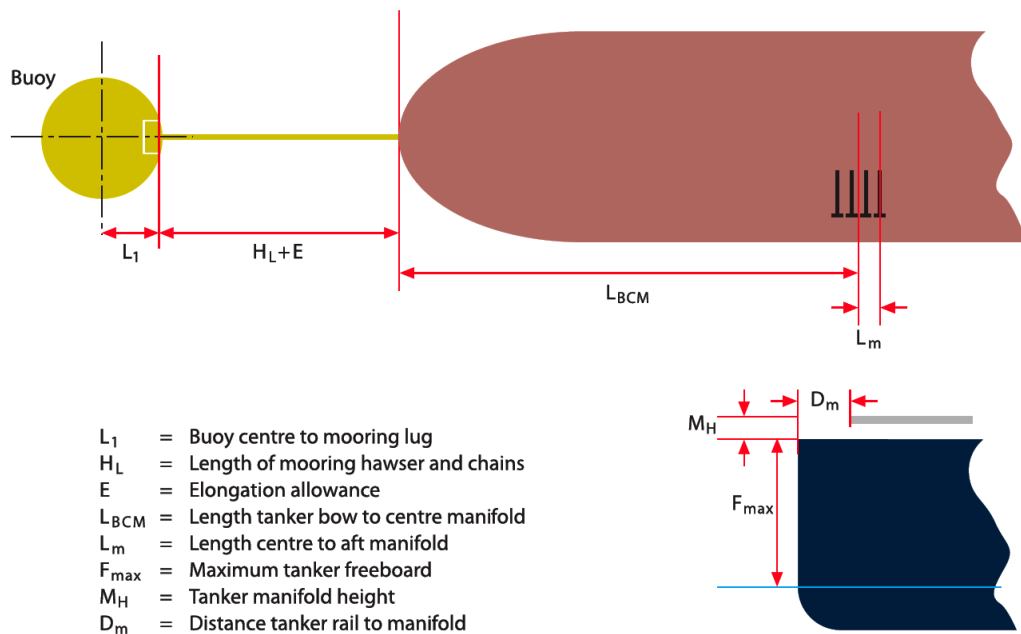


**Figure 2.6:** Calculation of length of catenary anchor leg mooring floating hose string

There are a number of ways to calculate the optimum hose string length, one example is set out below:

$$\text{Total length (TL)} = L_1 + (H_L + E) + (L_{BCM} + L_m) + F_{max} + M_H + D_m + \text{teardrop allowance}$$

# Appendix D: ABS Guidance notes on Qualifying New Technologies



Guidance Notes on

## **QUALIFYING NEW TECHNOLOGIES –**

### **Applied to Texas GulfLink conceptual Vapor Recovery System**

---

These Guidance Notes describe the ABS approach for qualification of new technologies to confirm their ability to perform intended functions in accordance with defined performance requirements. This document introduces a systems engineering approach to qualification that allows for systematic and consistent evaluation of new technologies as it matures from a concept through confirmation of operational integrity in its intended application.

The marine and offshore industries regularly develop new technologies that have no service history in the proposed application or environment. Often, governing industry codes and regulations do not develop at the same pace. These new technologies have little or no precedent and may be so different from existing designs that the requirements contained in class Rules may not be directly applicable. Marine vessels and offshore units which contain new technological features or designs that are not currently governed by Rules, Guides and existing industry standards may still be qualified and/or approved by ABS through the process described in these Guidance Notes.

A new technology for the purpose of these Guidance Notes is defined as any design (material, component, equipment or system), process or procedure which does not have prior in-service experience, and/or any classification rules, statutory regulations or industry standards that are directly applicable. It is possible to categorize the type of “novelty” in one of four categories with vapor recovery at an offshore Deepwater Port falling under category ii:

- ii.) Existing design/process/procedures in new or novel applications

New Technology Qualification (NTQ) process could be applicable in the following case

- i.) To qualify new technology that may need to be classed or certified at a later date

As the proposed vapor recovery system will be a new process at an offshore SPM facility, the system will have to be certified design by a Certifying Entity, and then proven operational during a tanker loading operation before receiving USCG final approval.

### **New Technology Qualification Process**

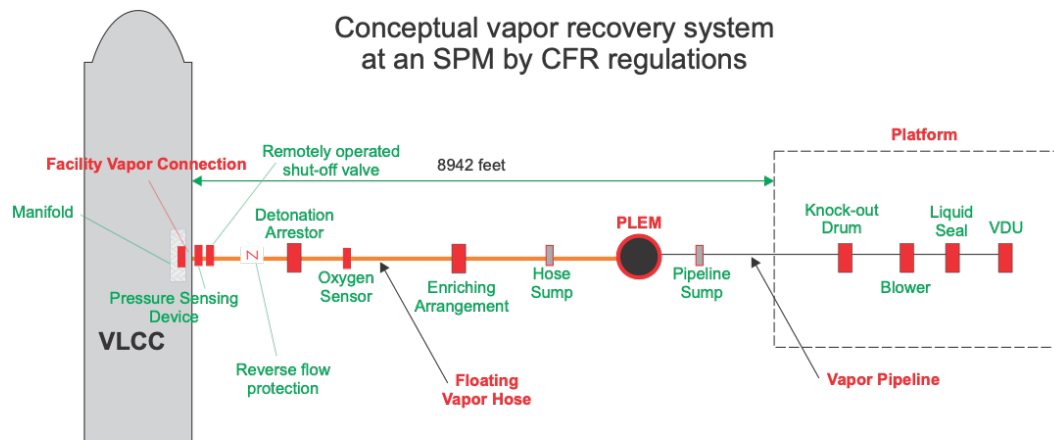
The NTQ process confirms the ability of a new technology to perform its intended functions in accordance with defined performance requirements. The process starts with a

comprehensive description of the technology to be qualified, followed by a screening of the technology to reveal the new or novel features that the qualification should focus on.

### **Vapor Recovery System description**

A vapor recovery system at an offshore Deepwater Port, in unprotected waters is a new concept. The proposed vapor recovery system will attempt to capture vapor emissions from a crude oil tanker loading at a CALM Buoy style SPM and process the vapors on a manned platform nearby. The system will be operated by a SCADA architecture control system from the shoreside control room by an Oil Movement Controller (OMC). The vapor pathway from the tanker to the platform will be by floating hoses, subsea pipelines, SPM swivel, subsea riser hoses, PLEM, and vapor pipelines. Vapor destruction units, enriched with propane, will destroy the vapors at the platform. The location of the facility vapor connection should be the manifold vapor connection on the tank vessel as this would reduce the hazards associated with the 985 ft of floating vapor hose. A facility vapor connection assigned to the CALM Buoy would not protect the hazards associated with the 985 ft of floating hose and would not be close to the tank vessel. The location of the facilities vapor connection is important because it serves as a reference for the positioning of several devices such as detonation arrestors, automatic vapor valves, pressure sensing devices, and others. The offshore Deepwater Port SPM operation is difficult to matchup to the definition in 33 CFR §154.2001 but the intent is to be as close as possible to the tank vessel and protect against the hazards associated with the hose. The only location to be considered the facility vapor connection is the vapor hose connection at the tank ship manifold. The system will be composed of the following items:

1. SCADA network monitor stations
2. Shoreside Control Room- SCADA control
3. Vapor destruction unit (VDU)
4. Knockout drum or condensate removal system
5. Detonation Arrestor (DA)
6. CALM Buoy swivel connection
7. Vapor Enrichment system (propane)
8. Floating vapor hoses: 985 ft
9. Subsea riser vapor hoses: 160 ft
10. Pipeline End Manifold (PLEM)
11. Oxygen & Remote Pressure and Temperature Sensors
12. Subsea vapor pipeline: 7595 ft
13. Vapor blower or compressor and pressure control system
14. Drain sump on subsea pipeline



**Facility vapor connection:** 33 CFR §154.2001 Definitions. Facility vapor connection means the point in a facility's vapor collection system where it connects to a vapor collection hose or the base of a vapor collection arm and is located at the dock as close as possible to the tank vessel to minimize the length of the flexible vapor collection hose, thus reducing the hazards associated with the hose.

**Blower or Compressor:** 33 CFR §154.2100 Vapor control system, general.

(a) Vapor control system (VCS) design and installation must eliminate potential over pressure and vacuum hazards, overfill hazards, sources of ignition, and mechanical damage to the maximum practicable extent.

**Check-valve:** 33 CFR §154.2101 Requirements for facility vapor connections.

(h) A vapor collection system, fitted with a gas injection system that operates at a positive gauge pressure at the facility vapor connection, must be fitted with a means to prevent backflow of vapor to the vessel's vapor collection system during loading.

**Oxygen Sensor:** §154.2105 Fire, explosion, and detonation protection.

The oxygen analyzer required by paragraph (a)(1) can be located 4 meters (13.1 feet) downstream of the detonation arrestor.

**Pressure Sensing Device:** 33 CFR §154.2103 Facility requirements for vessel vapor overpressure and vacuum protection.

(g) If a facility draws vapors from a vessel with a vapor-moving device, the facility vapor connection must have a pressure-sensing device, independent of the device used to activate the alarm required by paragraph (e) of this section, which closes the remotely operated cargo vapor shutoff valve required by 33 CFR 154.2101(a) when the vacuum at the facility vapor connection is more than the higher (lesser vacuum) of the following:

**Detonation Arrestor:** §154.2105 Fire, explosion, and detonation protection.

The total pipe length between the detonation arrestor and the facility vapor connection must not exceed 18 meters (59.1 feet) and the vapor piping between the detonation arrestor and the facility vapor connection must be protected from any potential internal or external ignition source

§154.2106 Detonation arrestors installation

(b) On either side of a detonation arrestor, line size expansions must be in a straight pipe run and must be no closer than 120 times the pipe's diameter from the detonation arrestor unless the manufacturer has test data to show the expansion can be closer.

**Enriching System:** 33 CFR §154.2107 Inerting, enriching, and diluting systems.

(b) A VCS that uses an inerting, enriching, or diluting system must be equipped, except as permitted by 33 CFR §154.2105(a), with a gas injection and mixing arrangement located as close as practicable to the facility vapor connection and no closer than 10 meters (32.8 feet) upstream from the vapor processing unit or the vapor-moving device that is not protected by a detonation arrestor required by 33 CFR §154.2108(b). The total pipe length between the arrangement and the facility vapor connection must not exceed 22 meters (72.2 feet).

**Hose Sump:** 33 CFR §154.2100 Vapor control system, general.

(h) The VCS must be equipped with a mechanism to eliminate any liquid condensate from the vapor collection system that carries over from the vessel or condenses as a result of an enrichment process.

**Pipeline Sump:** 33 CFR §154.2100 Vapor control system, general.

(h) The VCS must be equipped with a mechanism to eliminate any liquid condensate from the vapor collection system that carries over from the vessel or condenses as a result of an enrichment process

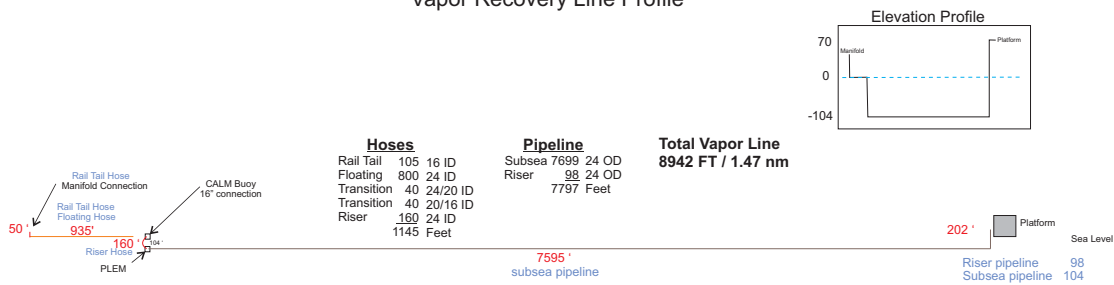
**Remote Operated shut-off valve:** §154.2101 Requirements for facility vapor connections.(a) A remotely operated cargo vapor

shutoff valve must be installed in the vapor collection line between the facility vapor connection and the nearest point where any inerting, enriching, or diluting gas is introduced into the vapor collection line, or where a detonation arrestor is fitted.

All operational aspects of the vapor recovery system will be monitored, controlled, and operated by the OMCs. The SCADA system will also have monitoring display stations located on the platform. The technicians and operators on the platform will assist the OMCs as needed to perform local tasks and report on the status of the platform equipment. The Mooring Master will report on operational information of the Vapor Recovery system onboard the tanker to the Oil Movement Controller. The Chief Mate, Mooring Master, Vessel Traffic Controller and Oil Movement Controller will all monitor a common UHF channel for communications.

The tankers will load crude oil at a maximum rate of 85,000 bph with an average rate of 65,000 bph. The anticipated frequency will be 15 VLCC tankers per month. The tankers will not vent any tank vapor emissions out their mast riser or pressure/vacuum relief valves as all vapor emissions will be passed through the vapor manifold when loading. The tankers will arrive at the Deepwater Port with cargo tanks inert with an oxygen content below 8%. The facility vapor connection will be located at the tanker's manifold vapor connection by 33 CFR§154.2001 regulations. A 24-inch, floating vapor hose 985 feet in length will connect to the tanker's vapor manifold by a 16-inch flanged connection. The floating hose will connect to the base of the CALM Buoy, then a pipeline connection will pass over the top of the CALM Buoy and down into the swivel. The CALM Buoy will have three connections, two for outbound crude oil hoses and the other for an inbound vapor hose. On the underside of the CALM Buoy swivel a 24-inch subsea vapor riser hose, 160 feet in length will connect the CALM Buoy to the PLEM anchored on the seabed floor. A 7595 feet, 24-inch pipeline will be buried three feet into the seabed and run between the PLEM and the base of the platform. The subsea pipeline will terminate at the meter deck at 98 feet above sea level. In all, the emission vapors from the tanker's manifold must travel 8942 feet to reach the platform VDU units. A drain and sump system will be required at the PLEM to address liquid drop-out in the subsea vapor pipelines. The liquid drop-out in the floating cargo hoses must also be addressed. Modeling shows as much as 30% restriction may occur in the vapor lines from liquid condensation drop-out. A blower or compressor will have to generate a substantial vacuum to allow the flow of cargo tank vapors to reach the platform given the pressure drop in the line. Modeling shows that in the winter months while loading at 30,000 bph a vacuum as much as -11.8 psig may be required. The additional safety measures to operate at this vacuum level will be substantial. Once the vapors reach the platform it will pass through a detonation arrestor then into a knock-out drum to remove the liquid drop-out. A propane vapor enriching system will be used to enrich the vapors to above the upper flammability limit of the vapors and to support combustion and a blower to move the vapors from the tanker into the VDUs. Anticipated propane requirement will be 1,500 gallons per tanker loading. A 32,000-gallon propane storage tank will be required with propane deliveries by portable bottles. There will be no means to measure, monitor, or drain the floating vapor hose after each load.

Texas GulfLink Deepwater Port  
Vapor Recovery Line Profile

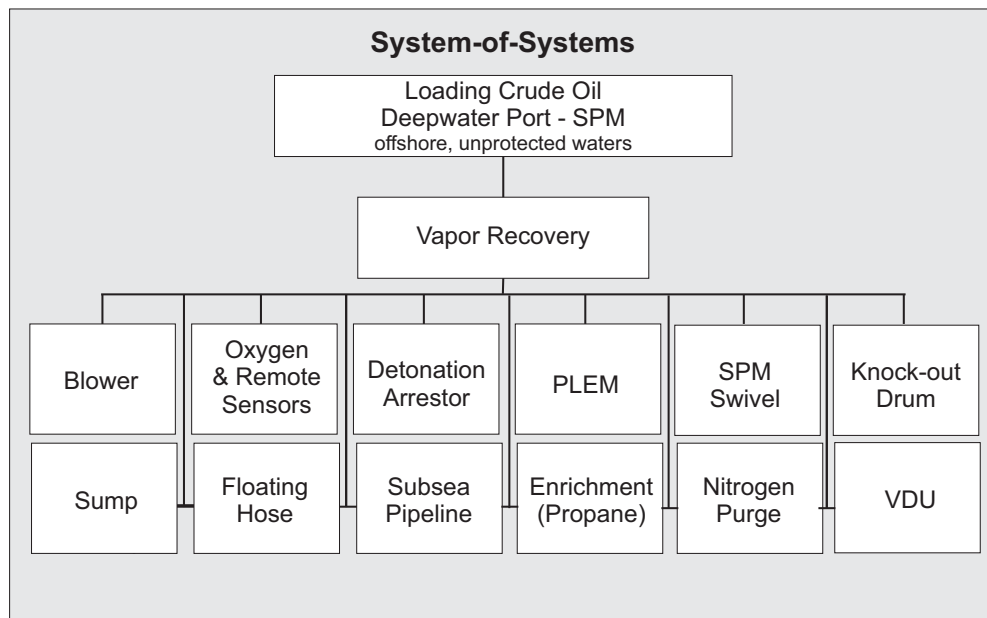


LEGEND	DRAWN BY: Captain Dan Harris		TEXAS GULFLINK PROJECT	
	DATE:	30 Sep 2019	PROFILE VAPOR LINES	
	DWG NAME: Profile VR			
	SHEET of		REV: 01	REV DATE: 29 Apr 2020
			SENTINEL MIDSTREAM	

**System-of-Systems:**

System-of-Systems (SoS) refers to the larger system with which integration of the new technology could occur. The asset becomes a novel concept if the incorporation of any new technology appreciably alters its service scope, functional capability, and/or risk profile.

Vapor Recovery at a Deepwater Port, offshore, in unprotected water, through a SPM buoy is a novel concept. It will alter the established practice of offshore SPM loading operations. SPM crude oil loading throughout the world takes place without vapor recovery at the facility. The concept is new technology with associated risks to personnel and the tankers loading.

**Goals:**

Design, test, and certify a VCS to the approval of the USCG and Certifying Entity. The goal of the vapor recovery system is to safely and effectively capture all vapors from a tanker loading at the SPM and destroy the vapors at the facility. Provide a safe working environment for personnel and allow for the protection of the environment. The system must not subject the tanker to any increased risk of over pressurization or excessive vacuum. Additionally, the VCS cannot add any additional hazards of fire or explosion to a similar loading system without vapor control. This system must follow all industry established guidelines and CFR regulations for safe operations.

**Functional requirements which must be meet:**

- Designed to address liquid drop-out in the vapor hoses and pipelines
- Designed to overcome the pressure drop of the 8,942 feet vapor line when moving vapors between the tanker and the terminal.



- Follow established industry guidelines
- Achieve a level of safety one magnitude greater than a Deepwater Port w/o vapor recovery using submerged loading and VOC management techniques.
- Provide a safe working environment for personnel on the tanker and the platform
- Operate in unprotected, offshore waters
- Allow for a safe-port-design concept
- Not unduly obstruct critical mooring operations with the additional vapor hose string
- Eliminate potential overpressure and vacuum hazards to the maximum practicable extent.
- Any pressure, flow, or concentration indication required must provide a remote indicator for safe operation and controls
- Allow for safe storage, resupply and use of propane on a manned platform.
- Provide protection from mechanical damage to the vapor hose
- Obtain USCG or Certifying Entity approval
- Meet all the requirements of 33CFR§154Subpart P requirements
  - Detonation arrestor
  - Excessive vacuum
  - Oxygen sensor
  - Level of safety
  - Remote pressure and temperature sensors
  - Check valve
  - Hose kinking and support
  - Remote shut-off valve
  - Liquid removal from lines and hoses

**Performance requirements which must be meet:**

- Capacity to process the tanker's maximum loading rate of 85,000 bph plus the vapor growth for the cargo.
- Provide a means to continuously remove excessive liquid drop-out from the vapor hoses and pipelines.
- Not subject the tanker or its crew to consequences of pressure spikes in the cargo tanks, operating range is between 1.4 and 1.6 psi
- Effectively destroy 95% of the VOC emissions
- Operate safely up to port established operating limits

**Design Conditions:**

The system design conditions describe all applicable loading requirements under the environmental and operating conditions. The Gulf of Mexico offers some challenging weather conditions, unlike most SPM installations located near shore and inshore.

- VLCC loading to a maximum rate of 85,000 bph, 2.2 M bbls
- Offshore (more than 3nm off the shoreline)
- Unprotected waters (not shelter or lee side of effects of winds and seas)
- Gulf of Mexico sea conditions (winter/summer seasons, hurricanes)
- Operating conditions to 14 feet seas, 40 knots wind
- Manned platform
- Provide mechanical protection for floating hose
- SPM moorings (weathervane)
- VLCC class tankers (320,000DWT)
- CALM Buoy designed for GOM operations based on metocean data
- Hoses designed for vapor use in rough sea conditions.

#### **System Interfaces:**

The system interface requirements define all internal and external physical and functional interfaces relevant to the new technology. The Texas GulfLink new technology vapor recovery system would include:

1. Blower or Compressor: The blower will be designed to create a additional motive force to crude oil vapors which will allow them to overcome the line pressure drop and effectively move the vapors from the tanker to the platform VDU without exceeding the pressure and vacuum limitations of the tank vessel . The amount of vacuum required to draw the vapors from the tank vessel to the platform will be significant due to the distance of the tank vessel to the suction side of the vapor blower at the platform. Flow modeling has indicted this vacuum level may reach -11.8 psig (or 2.9 psia) in the winter months while loading at 30,000 bph. A blower or compressor will have to generate a substantial vacuum to allow the flow of cargo tank vapors to reach the platform given the pressure drop in the line. This pressure drop in the vapor line includes additional losses due to the anticipated condensation of liquid in the vapor hose.
2. Knock-out Drum: The knock-out drum will be used to remove liquid from the emissions stream prior to the VDU unit. The knock-out drum will have a mechanism to determine liquid level and a high-level alarm. However, it will not remove any carry over moisture which drops-out in the floating cargo hoses or subsea pipeline as liquid. That liquid will need to be removed by other methods.

3. Detonation Arrestor: The DA is designed to protect the tank vessel from any flame propagation originating from the VCS and platform through the vapor piping and to the VLCC. The DA is a fail-safe device to protect the tank vessel from fire or explosion hazards. It should be located as close to the tank vessel as possible to provide maximum protection, less than 59 feet. It is not possible to install a DA to meet this requirement. The DA will have to be located on the platform 8942 feet away from the facility vapor connection. The vapor hoses will not be protected from a DA located on the platform. The floating vapor hoses are subject to mechanical damage from the support boats and unauthorized fishing boats as there is no means to shield them.
4. Pigging system: A pigging system will be provided to clear the subsea vapor pipelines after each load. The subsea vapor line between the platform and the PLEM will be pigged by a looped pipeline. The dual pipeline vapor system should allow pigging without significant engineering challenges. There is no means to conduct pigging of the floating vapor hoses. A nitrogen purge could be used on the vapor pipelines, but the vapor hoses would present a problem.
5. Floating Hoses: The 985 feet floating vapor hose will move the vapors from the tank vessel to the SPM. The tank vessel's vapor manifold will be a 16-inch connection and the main line vapor hose will be 24-inch with a 16-inch rail tail. The floating hoses will have to bend 90 degrees over the tank vessel's hose rail to align with the manifold connection. The floating hoses are subject to movement from the seas and weathervane motion. The hose will conform to the crests and troughs of the seas. The hoses are floating in sea water and heat transfer will occur between the surrounding sea temperature and the vapor temperature. Any liquid drop-out occurring in the floating hose will have to be removed to prevent liquid slugs from forming in the bottom of the hoses. The vapor hose will be electrically insulated from the vessel vapor connection. The use of a floating hose to transfer vapors to an offshore facility is a new concept. Lightering operations uses short lengths of flexible hoses to balance vapors with the shuttle tanker, but the hoses are suspended between the tank vessel above the sea.
6. Reverse Flow Prevention: A backflow check valve can be fitted to prevent backflow of vapor from the VCS to the vessel's vapor collection system during loading. It is required to be located at the facility vapor connection. Optionally, a differential pressure sensor can be used to detect reverse flow through an orifice or the DA. If a reverse flow is sensed, the control system will automatically shut down the VCS and isolate the VCS from the VLCC

7. Propane Enriching System: Propane will be injected into the vapor emission stream to render the vapor above the upper flammability limit. Additionally, the enrichment gas increases the heating value of the waste vapors to facilitate meeting the destruction efficiency requirements of the vapor destruction unit. The enriching arrangement will be capable of at least two system volume exchanges. The enriching should take place as close as possible to the facility vapor connection, not exceeding 22 meters. The early stages of loading will be mostly inert gas mixtures, which will require enrichment. The vapor stream will be constantly sampled to determine the hydrocarbon level with propane injected as needed. A remotely operated cargo vapor shutoff valve will be installed between the facility vapor connection and the enrichment arrangement. Propane will be stored on the platform and delivered by support boats. The propane storage will have to be located at least 75 feet from the living quarters. Propane deliveries will be by support boat in various sea conditions.
8. Remote Cargo Vapor Shut-off Valve: A remote controlled cargo vapor shut-off valve is required between the facility vapor connection and rest of the VCS. By regulation the enriching arrangement must be within 22 meters of the facility vapor connection. This would require the remote shut-off valve to be in the vapor hose string. This shutoff valve will require an exemption from the USCG for its location.
9. Oxygen sensor: A remote oxygen sensor or analyzer is required nearby the facility vapor connection to measure and confirm the oxygen content of the vapor stream. The sensor or analyzer is used to confirm that the vapors from the vessel are properly inerted. The maximum requirement is 19.7 feet between the oxygen sensor and the facility vapor connection. It is not possible to install an oxygen sensor as required. This will preclude any sampling of the oxygen content of the vapor stream until it reaches the platform. This oxygen sensor will require an exemption from the USCG for its location.
10. CALM Buoy: The CALM Buoy will provide the vapor pathway for the vapor emissions between the floating hoses and subsea riser hoses. A swivel connection with a dual product swivel will be fitted. One for vapor and the other for crude oil. The Buoy will allow the tank vessel to weathervane in a secure mooring. Telemetry on the buoy will relay data to the platform including: Tank vessel location, hawser strain, current, leak detection, and valve position. Dual product swivels for

liquid cargoes are in use in many locations throughout the world today. A vapor connection will be a new concept.

- 11.Subsea Riser Hoses: The riser hose will connect the PLEM to the underside of the CALM Buoy. A Chinese lantern configuration will be use to allow for movement of the buoy in the seas. The curved hose arrangement will act as a shock absorber to the vertical movement of the buoy. A 160 feet, 24-inch vapor hose will be used. The Chinese lantern configuration is commonly found in similar water depths.
- 12.Vapor Destruction Units: Three VDUs will be required to destroy VOCs at the maximum loading rate and allow for 25% vapor growth. The VDUs will use propane as a supplemental fuel to the waste vapor stream and support a 1200 deg. F combustion zone temperature. Unlike a platform-based vapor recovery system, shoreside VDU units are not located near living quarters.
- 13.Sump: A sump will have to be fitted at the low point in the subsea pipeline. The tank and pumping arrangement will have to be buried below the pipeline, which is 3 feet below the seafloor. A means to monitor the sump liquid level and pump out the liquid will be required. A sump located near the PLEM would have to be pumped back to the platform 1.25nm away. The lift height from the sea floor to the platform 98-foot level would be 202 feet and may require a second sump at this location.
- 14.Subsea vapor pipeline: The pipeline will run 7595 feet between the PLEM to base of the platform, then a vertical run for 202 ft. The line will be buried 3 feet below the sea floor. The line will be grounded and electrically continuous.

#### **Human System Integration Requirements:**

Human factors play an important role for the system to work safely and effectively in achieving required functions and goals, and should be considered throughout the design life of the new technology.

Vapor recovery during cargo loading operations on tankers has been around since the early 90's. A STCW dangerous cargo endorsement as PIC is required for Chief Officers and covers vapor recovery knowledge and training. Shoreside terminals in the US have required facility vapor recovery as far back as 1991. The experienced deck officer on a tanker is familiar with vapor recovery operations and has ample exposure to it. Vapor recovery at an offshore SPM will be similar to a shoreside system as far as the tanker's role is concerned. However, possible pressure spikes from a restricted vapor hose would be a new element of concern. The tanker will have a continuous manifold watch on duty.

Interfacing with the tanker, the control of the vapor recovery will be from the shoreside control room. The technical challenges and safety concerns of operating an SPM vapor recovery system will be addressed by the facility. As in shoreside terminals, the cargo tanks are protected from over pressurization by mechanical and liquid p/v arrangements. The Oil Movement Controllers and Mooring Masters will be given training in vapor recovery and cargo loading operations as stated in the facility operations manual. During cargo loading operations the tanker PIC, Mooring Master, and Oil Movement Controller will be continuously on duty and work closely to monitor the flow of the vapor emissions. The terminal PIC, the Port Superintendent, must also be at the Deepwater Port for any loading operations. On the platform, a platform operator and a platform technician will also be on duty to address any local needs on the platform. Portable radios with microwave boosting will keep the tanker PIC, Mooring Master, Vessel Traffic Controller, Oil Movement Controller, Platform Operator, and Platform Technician in constant communications with each other throughout the loading operation. All personnel involved in cargo loading operations will be subject to OPA90 work hour limits.

**Safety and Environment:** Safety and environmental requirements applicable to eliminating or minimizing hazards related to people, environment, and asset.

The full EPA response document covers in detail all areas of safety concerns and hazards. There are several areas of concern when looking at a safe operation with minimal risk. An outline of the safety concerns would include:

1. Location of Detonation Arrestor (fail-safe device)
2. Excessive vacuum hazards
3. Potential sources of ignition
4. Over pressurization of cargo tanks (pressure spikes)
  - a. Vapor exposure to deck crew including H<sub>2</sub>S exposure
  - b. Full cargo vapor loss from liquid breaker activating
  - c. Structural damage to cargo tanks
5. Kinking vapor hoses
6. Protection of the vapor hoses from mechanical damage
7. Oxygen sensor location
8. Remote vapor shut-off valve location
9. Protection of floating vapor hoses

**Risk Assessment Requirements:**

For a new technology requesting qualification through the NTQ process, a risk assessment is to be performed/updated at each stage as applicable. The risk assessment within the NTQ process will vary from qualitative to quantitative depending on the maturity level and information available at that stage. The primary objective of the risk assessment is to identify technical risks and uncertainties associated with the proposed design and document all foreseeable hazards, their causes, consequences, and potential risk control measures considering the new technology in its proposed

application and operating environment. All possible interfaces, and known integrations are to be evaluated as part of this assessment.

The Texas GulfLink team has submitted technical documents to the EPA detailing the risks associated with vapor recovery at an SPM. The White Paper, Case-by-Case document and four in-person presentations have been undertaken as a method of presenting a risk assessment evaluation to the EPA.

#### **Engineering Evaluation:**

Engineering evaluations are used to verify and validate that the new technology is capable of performing acceptably with respect to intent and overall safety according to the requirements of each stage.

Texas GulfLink performed process modeling to simulate hypothetical vapor recovery situations for the proposed offshore loading operations. The vapor recovery modeling was executed using the Aspen HYSYS Hydraulics sub-flowsheet. An independent third-party engineering firm was utilized.

Simulation Results: The isothermal steady state case was evaluated at the maximum expected flow rate for both the winter and summer cases. With no heat transfer or water condensation, the required platform suction pressures for the winter and summer cases

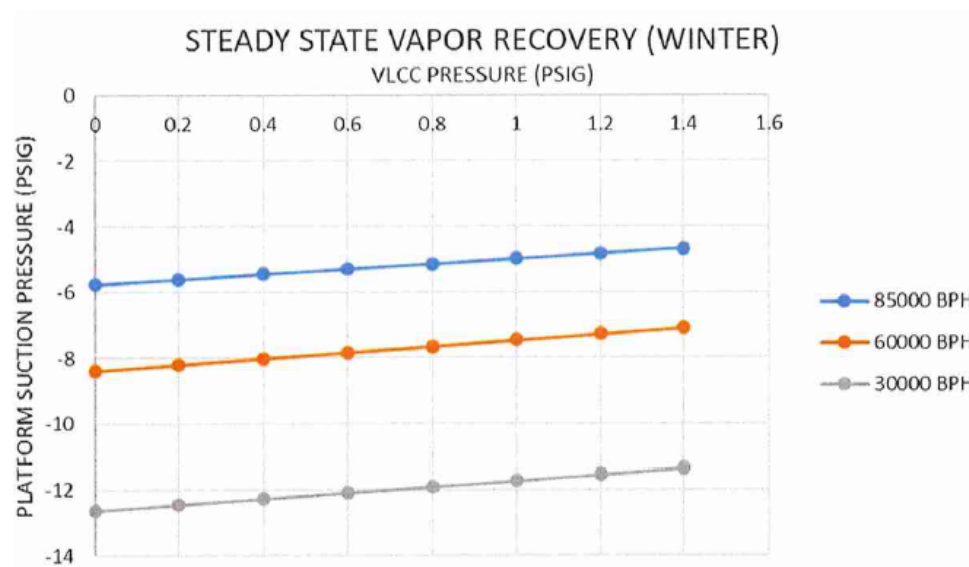
Case	Vapor Temp	VLCC Pressure	VLCC Flow Rate	Platform Suction Pressure	Platform Flowrate	
	°F	PSIG	ACFS	PSIG	ACFS	SCFS
85000 BPH Winter	70	1.4	132.6	-0.64	159.8	142.7
85000 BPH Summer	100	1.4	132.6	-0.51	157.6	135.1

at a VLCC fill rate are -0.64 psig and -0.51 psig, respectively. See the results below

However, once heat transfer and vapor condensation were considered, the winter steady state case resulted in the lowest platform suction pressures. Significant liquid hold-up resulted in reduced vapor flow area and two-phase, slug flow of the condensate and vapor. The condensate reduced the cross-sectional area of the flow path by 30%, thus generating increased pressure drop in the vapor piping sections.

The steady state results show that, as the vapor flow rate is reduced, the vacuum pressure required at the flow platform suction increases because the condensate accumulates within the floating vapor hose. At lower flow rates and velocities, less condensate is able to be swept away in stable two-phase flow, resulting in increased liquid hold-up and a slugging flow regime. At the 30,000 BPH filling rate, the minimum required vacuum at the platform suction steady state condition is -11.37 psig. The HYSYS simulation did not

converge in the steady state for any case at the 15,000 BPH fill rate, indicating excessive pressure drop resulting from liquid accumulation in the hose and piping. See the table below:



## Feasibility Stage

A new technology considered for qualification in the Feasibility stage is at an early concept maturity level, where basic research and development activities to identify engineering principles are complete; and a concept formulated along with its functional requirements. A high-level design analysis is performed to verify the concept in the intended application and that the overall proposed level of safety is comparable to those established in Rules, Guides, other recognized industry standards and recommended practices.

### Vapor Recovery engineering principles

Vapor recovery at a shoreside facility is common place in the US. The technology is well established with effective VOC reduction rates. These facilities mostly use rigid chiksan (aka vapor arms) vapor connections or a single length vapor hose, vapor pipelines are elevated or trussed, detonation arrestors are USCG compliant, drop-out legs are provided, excessive vacuum conditions are avoided, VDU or VCU are provided or the VOCs are burned as a fuel source. There are numerous vendors with proven vapor recovery systems in operation at shore side facilities.

Vapor recovery at an offshore manned platform is entirely new application. The proposed vapor recovery system looks to take existing onshore design, process, and procedures and apply it to a new application. Successful facility vapor recovery was conducted at the Gaviota facility and the Exxon OST operation in the Santa Barbra channel in the 80's and 90's, but dedicated, specially equipped tankers were required. On the US West Coast offshore marine facilities, like the North Sea Norway facilities, dedicated shuttle tankers fitted with onboard vapor processing units are used to capture VOC emissions when



loading. Offshore, unprotected water, and SPM moorings are a new application for facility vapor processing.

The process required to allow the tank vessel's vapor emissions to travel from the individual cargo tanks to the platform's facility VDU has engineering obstacles with foreseeable hazards. The table below breaks down the individual components as technically possible, based on similar shoreside units, questionable as a new application, or in direct violation of a CFR requirements.

Vapor recovery conceptual design at Texas Gulfink's offshore facility with SPM moorings in unprotected waters compared to a shoreside facility that process emissions at the facility.

Component	Shoreside Facility	Offshore Facility
Vapor Destruction Unit at facility	In use most terminals	Possible
Compliant detonation arrestor	All facilities with vapor recovery	Non-compliant 33CFR§2105 (a) (2) due to the 18-meter distance requirement
Compliant oxygen analyzer	All facilities with vapor recovery	Non-compliant 33CFR§2105 (a) (1) due to the 6-meter distance requirement
Gas injecting and mixing arrangement	All facilities with vapor recovery	Non-compliant 33CFR§2107 (b), propane use due to the 10 meter distance requirement
Vapor pipeline trussed	All facilities with vapor recovery	Not possible to support the vapor piping above the water level from the platform to the VLCC.
Vapor pipeline submerged	None	Possible
Knock-out drum	All facilities with vapor recovery	Possible
SPM swivel connection	None	Possible
Floating hoses	None	Questionable liquid drop-out issues. No proven technology other than excessive vapor blower suction pressures to remove condensation between the CALM buoy and the VLCC.
Nitrogen purge system	Some terminal	Possible
Drains and drip legs	All facilities with vapor recovery	Sump possible on vapor pipeline
Blower or Condenser	In use most terminals	Questionable – excessive vacuum, -11.4 psig
Subsea riser hose	None	Questionable – vacuum issues
PLEM	None	Possible
Remote vapor shut-off valve	All facilities with vapor recovery	Questionable – location in hose string. No plot space available at the VLCC loading header. In water installation is not possible
Vapor pathway: tank vessel to VDU	No issues at shoreside facilities	Questionable – pressure drop, hose size, ~9000ft



**Detailed explanation and evaluation of questionable design issues:**

1. **P-Trap:** There is a p-trap between the tank vessel's vapor manifold header (46 ft avg) and the CALM Buoy (16 ft) where liquid drop-out will accumulate. A p-trap is a section of pipeline or vapor hose that forms a "U" shape, trapping liquid in the bottom of the "U" shape until sufficient pressure can overcome the vertical rise of the second leg to force the liquid out. The approximate pressure to lift any liquid over the CALM Buoy would be 6.9 psi, well above the structural damage pressure of the tank vessel at 3.6 psi. The accumulation of liquid drop-out in the vapor hose would be cumulative as the vapor hose cannot be drained between subsequent loads.

A simple calculation using the common unit conversation of 2.3067 ft wc = 1 psi.  
i.e. (16 feet) / (2.307 ft wc/psi) = 6.9 psi

**Calculation to show pressure required to overcome p-trap**

Unitized hydrostatic pressure of a liquid column:

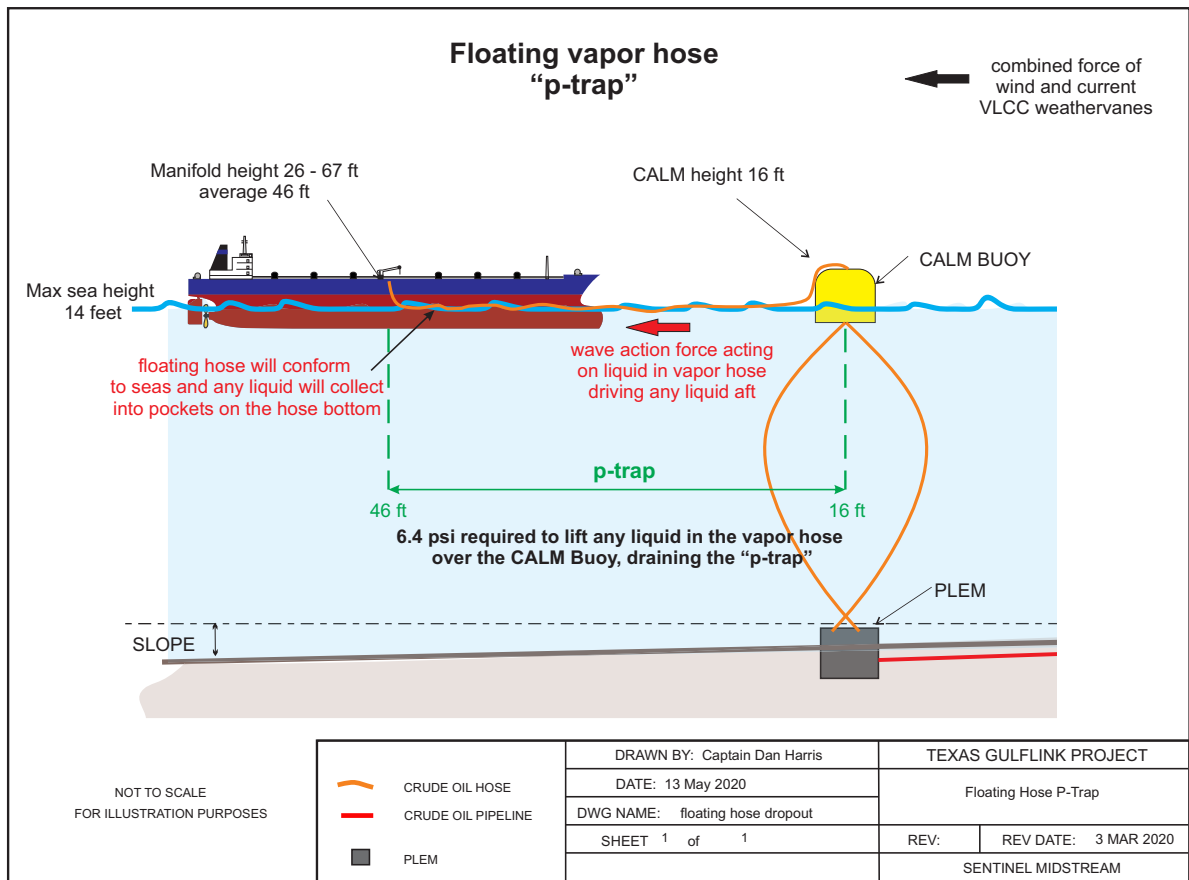
$$P = \frac{F}{A} = \frac{m \cdot a}{g_c \cdot A} = \frac{\rho \cdot V \cdot a}{g_c \cdot A}$$

- P (Fresh Water Density) = 62.43 lb<sub>m</sub>/ft<sup>3</sup>
- V = 1 ft<sup>3</sup>
  - Unitized (per foot of elevation) by putting in as V = 1 ft<sup>3</sup> / ft
- a = 32.164 ft/s<sup>2</sup>
- g<sub>c</sub> = 32.164 lb<sub>m</sub> · ft / lb<sub>f</sub> · s<sup>2</sup>
- A = 1 ft<sup>2</sup>

$$\begin{aligned} P \text{ (per foot of elevation)} &= \frac{\left(62.43 \frac{\text{lb}_m}{\text{ft}^3}\right) \cdot \left(1 \frac{\text{ft}^3}{\text{ft}}\right) \cdot \left(32.164 \frac{\text{ft}}{\text{s}^2}\right)}{\left(32.164 \frac{\text{lb}_m \cdot \text{ft}}{\text{lb}_f \cdot \text{s}^2}\right) \cdot (144 \text{ in}^2)} = \frac{(62.43) \cdot \left(\frac{1}{\text{ft}}\right) \cdot (1)}{\left(\frac{1}{\text{lb}_f}\right) \cdot (144 \text{ in}^2)} \\ &= \frac{62.43 \text{ lb}_f}{144 \text{ in}^2 \cdot \text{ft}} = 0.4335 \frac{\text{psi}}{\text{ft}} \end{aligned}$$

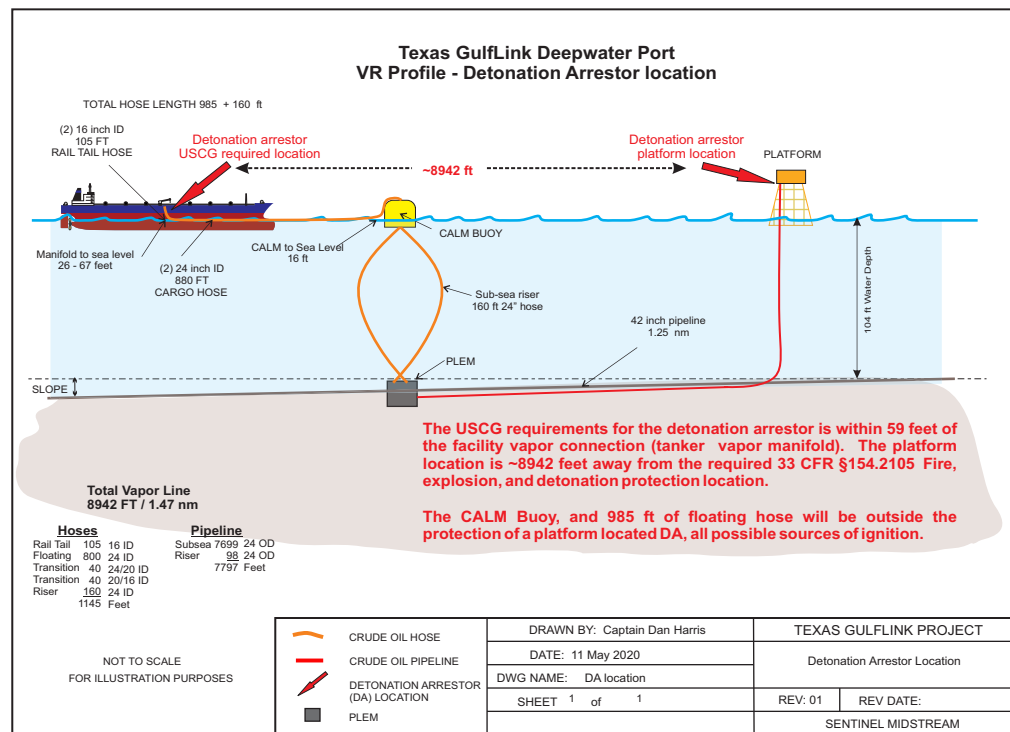
Height of 16 ft, at the buoy

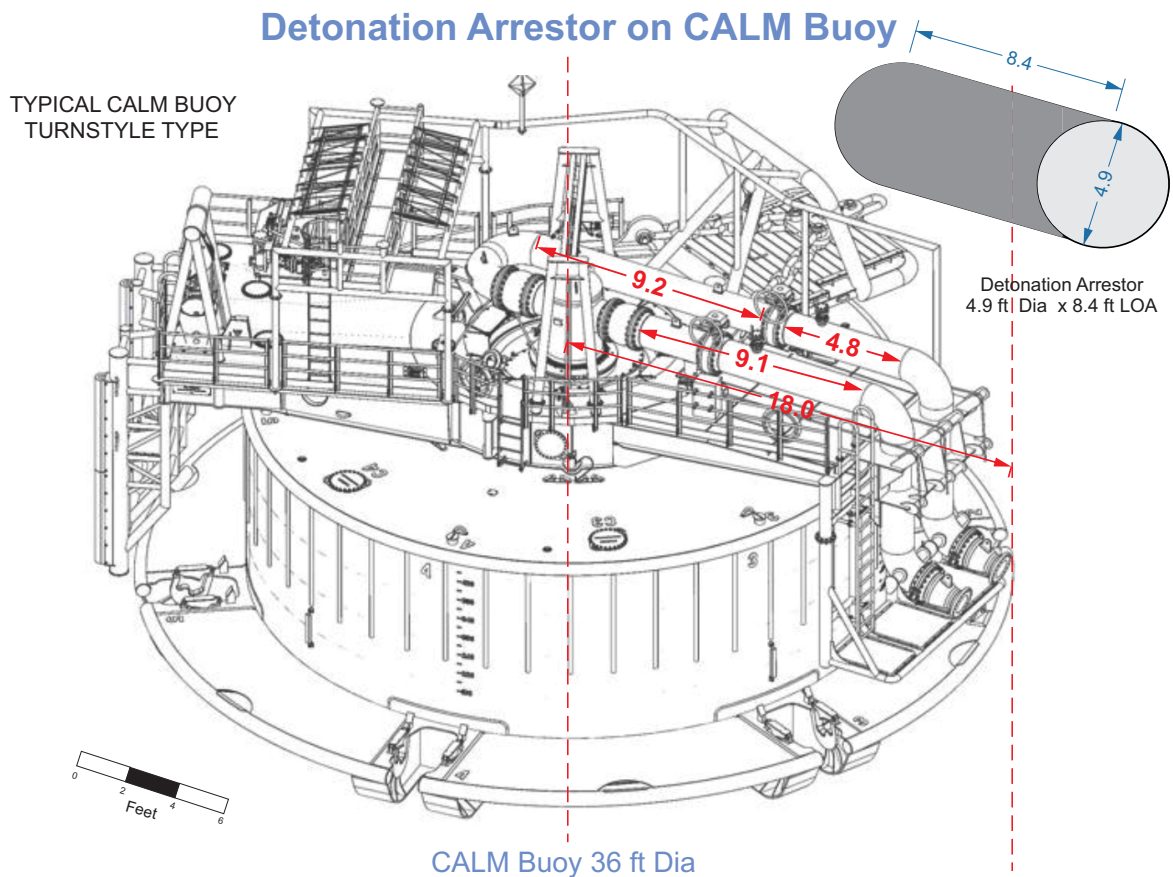
$$P = P \text{ (per foot of elevation)} \cdot h = \left(0.4335 \frac{\text{psi}}{\text{ft}}\right) \cdot (16 \text{ ft}) = 6.937 \text{ psig}$$



2. **Vapor Line total Length 8942 ft:** The combined length of vapor pipe and hoses between the VDU and the tank vessel's vapor manifold present a unique regulatory challenge because of safety and engineering considerations to draw vapors at this length through subsea lines and floating hoses. The vacuum required by the platform blowers or compressors is excessive and near impossible to overcome due to the pressure drop. Modeling shows as much as -11.4 psig could be required at times. The 1.25 nm SPM distance is essential for safe port operations design.
3. **Detonation Arrestor (DA):** The platform location of the detonation arrestor is 8942 ft from the facility vapor connection. DA is a fail-safe device to protect the tank vessel from flame propagation. By regulation 33CFR § 154. 2105 the maximum distance allowed is 59 ft. The CALM Buoy swivel seals and flange connections could be under a vacuum and are subject to leaking, a leak will allow fresh air intake and possible a static charge (perfect fire triangle) and possibly compromise the oxygen content of the inerted vapors. Any sump to address liquid drop-out in the subsea vapor pipelines and hoses will be outside of a platform DA. The DA placed anywhere but immediately alongside the tanker will put the tanker and its crew at risk. There is inadequate room on the tanker's manifold deck area which to place a

DA unit. Manifold connections are made over the tanker's fixed drip pan. The space between the manifold drip pan and hose rail is limited and the cargo hoses, lifting gear, snubbing chains, and hose end floats are located within this space. There is no room to place a DA on the deck of the tanker, so this leaves either the SPM or platform as possible locations. A DA located at the CALM Buoy will face operational reliability issues, liquid condensation drop-out issues, inspection & cleaning access issues, and be exposed to salt water. The CALM Buoy's overall diameter is 12 meters leaving little space to install a compliant DA. A typical 24-inch DA would be 4.9 feet in diameter, 8.4 ft in length, and weigh 4 tons. The space between the center well vapor pipeline connection and the connection to the vapor hoses has minimal horizontal space to fit a DA. There are no SPMs fitted with DA available from the vendors we have spoken with. The platform is the only physical location to place the DA at.





CALM Buoy with (2) two crude oil lines and DA for 24" vapor hose

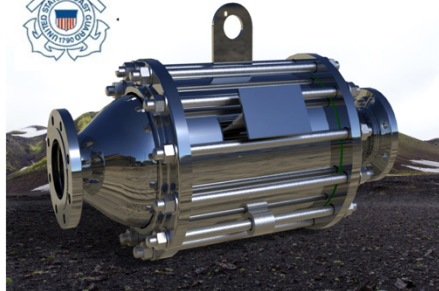
The above picture of a CALM Buoy is not showing the third line for the vapor emissions. The additional line for the vapor emissions will not allow for sufficient space to install a DA on the CALM Buoy as the diameter of the DA is 4.9 feet. Additionally, a DA located on the CALM Buoy will not protect the 985 feet floating vapor hoses. The floating vapor hoses are not protected from possible mechanical damage.



Examples of a turn style CALM Buoy with (3) pipeline connections



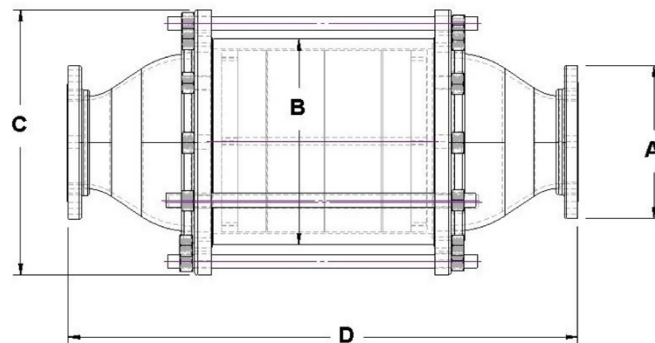
## Detonation Flame Arrestor Series C



*The Paradox Detonation Flame Arrestor*, represents the best technology for value in flame arrestor protection. They prevent flame propagation by absorbing heat and dissipating supersonic pressure waves, using multiple spiral wound crimped ribbon flame cells staged with turbulent creating screen sections.



## Series C-Detonation Flame arrester Specifications



USCG  
Approved



Model	A 150# AN-SI Conn. Size in. (mm)	B Housing Size In. (mm)	C Outside Di- ameter In. (mm)	D Overall Length In. (mm)	Initial Pressure Rating Group D (-2 psia for Group C)	Approx. Weight Lb. (Kg.) Grp D (Grp C&B +15% to 20%)
*C-24C	24 (600)	48 (1200)	59.50 (1511)	101.00 (2565)	22.7 psia (1.54 bar)	8400 (3810)

Notes: This Paradox DA is only used as a typical example of the size and weight of a USCG approved DA. Other approved DAs are available but are of similar size and weight.



4. **Low point in vapor pipeline:** A sump device will have to be designed to address liquid drop-out in the vapor pipelines near the PLEM. The reliability and operation of the sump system at 104 ft water depth will be an engineering challenge for service, inspection and reliability. The sump would have to be buried below the pipelines to collect the liquid and pump to the platform for processing. Access to the sump chamber for inspection, repairs, and maintenance will be difficult.

5. **3<sup>rd</sup> Floating Hose - vapor hoses**

**Combination of Vapor and Cargo Hoses in a three-hose string configuration:**

The vapor hose would be the third hose connection on the CALM Buoy. The handling of the two cargo hoses and one vapor hose will be accomplished by a single support boat. Typical SPM operations have the line boat handling only two cargo hoses. The cargo hose will be filled with crude oil while the vapor hose will have a gas mixture. The buoyancy forces on the two different hoses will be mismatched. The vapor hose will float much lighter on the water compared to the cargo hoses. The lighter vapor hose will have a tendency to ride up over the deeper cargo hose and can become fouled easily when moving the hose string for mooring and unmooring operations. Mooring and unmooring are critical operations and a fouled hose string will stop all operations until they can be cleared. When departing the SPM in moderate seas, a tangled hose string can't be pulled clear of the tanker by the support boat when fouled. This forces the tanker to back fully clear of the hose string (1100ft) before maneuvering clear around the SPM, which could put the tanker dangerously close to the platform when the stern is aligned with the platform.



Typical SPM hose arrangement with (2) two liquid filled cargo hoses with matched buoyancy. Note the width and general layout of the surface area of the hose string with two hoses.



In contrast, note the spread and general layout profile when adding a third hose to the hose string. The surface area of the hose string is significantly increased. The make-up of the hoses on the support boat will be complicated and extremely difficult to maneuver. Here, all hoses have equal buoyancy forces.





This picture gives a good representation of the length and mass of the hose string when adding a third hose. Unlike a combination of cargo and vapor hoses, these hoses are all floating with equal buoyancy. A single support boat will have to control all three of these hoses, with the vapor hose, floating lighter and riding over the cargo hoses when pulled laterally.



LOOP Loaded is shown with a single hose.



Typical hose string with two matched hoses.

6. **Liquid Drop-out:** Liquid drop-out will accumulate and have to be addressed. The tanker's inert gas system inherent design will saturate the vapor content in cargo tanks with moisture. The temperature differential between the vapors and the surrounding seas will cause liquid drop-out. Multiple dips in the floating hoses

when conforming to seas (operating conditions to 14 ft sea) will contribute to pocketing of liquid along the 985 ft length. The weathervane motion of the tanker around the SPM will allow the sea motion to drive the liquid in the floating hose aft, towards the stern of the ship. Undulations between dips in low points in the hose will occur causing reduction in throughput capacity and total blockage at times. Pressure surges in the vapor line will impact the tanker and the VCS as this occurs. In the latter stages of loading this could be significant. Modeling has indicated liquid drop-out in the vapor lines. In the winter months when loading at 30,000 bph this drop-out could restrict 30% of the vapor flow. There is no method for draining, pigging, or monitoring any liquid in the floating hoses. Subsequent loads will experience a cumulative effect from the liquid drop-out. The tanker will be operating between 70% and 80% (1.4 psi – 1.6 psi) pressure setting of the pressure vacuum (p/v) valves (2.0 psi), leaving little room for pressure spikes before lifting ( $\frac{1}{2}$  psi).

7. **Blower/Compressor Vacuum:** Pressure drop in the 8942 ft vapor line from tanker will require a substantial vacuum to pull vapors from tanker. The maximum 20-inch CALM Buoy swivel connection and 16-inch rail tail floating hoses will factor into this equation. Regulation 33CFR§154.2103 Facility Requirements for vessel overpressure and vacuum protection address this. Vacuum hazards must be taken into consideration and avoided. Modeling has indicated that a maximum vacuum of -11.8 psig may be required at times. A system operated at this vacuum level would need significant safety measures installed to safeguard the vapor pipeline and tankship.
8. **CALM Buoy:** The CALM Buoy will be a 12 meters turntable type buoy with two 24-inch cargo connections and one 20-inch vapor connection. It will be designed for forty years life with twelve compartments. The turntable will be designed and constructed to safely transmit all mooring forces from the tanker into the turntable-bearing assembly. It will be designed as a rigid, one-piece unit with internal members as required to support the applied loads. The turntable will be outfitted with a balance arm, ballast box, piping, valves, air winch, overhead framework, locking device, and mooring lugs for attachment of the hawser and bridle assembly. There will be (6) six catenary anchor leg moorings bored into the seabed. The CALM Buoy will be in a constant state of motion from the forces of the seas. CALM Buoys are successfully used throughout the world with multiple product swivels. Vendors SOFEC, Bluewater, IMODCO, and Wartsila are unaware of any CALM Buoys with a vapor connection.

The flanges and swivel connection of the vapor line in the CALM Buoy could be leak sources which may be in a vacuum state. Fresh maritime air will be drawn in making small leaks difficult to detect, but dangerous, as the fresh air will mix with the hydrocarbon vapors present in the lines. Additionally, the introduction of air into the vapor header could compromise the oxygen level of the inerted vapor. The

maritime air is high in moisture and water droplets could have static charge. An explosion at the CALM Buoy would instantly rupture the cargo and vapor hoses igniting a large fire. A ruptured vapor hose will supply hydrocarbon vapors to the fire until the tanker's crew can close off the manual vapor header valve at the manifold. Cargo oil will be escaping from the ruptured cargo hoses until the flow can be stopped.

#### 9. Propane:

The VOC emissions from tanker loading will require enriching to support combustion in the VDU unit. This is especially true for the early stages of loading. Propane is a volatile energy source to use as an enrichment gas in a VDU at an offshore platform. As compared to natural gas, which is mostly methane, and a low reactivity fuel, propane is a medium reactivity fuel. The delivery, storage, and use of propane on a manned platform presents more hazards than found at a shoreside terminal or refinery. Some concern with the use of propane include:

- Frequent deliveries by support boat – the unloading of the portable propane bottles will be conducted in various sea conditions. The work deck of a support boat is a dynamic platform to offload propane bottles from with any rolling or pitching motion adding an element of risk.
- Storage capacity required would be ~ 32,000 gallons of propane – as per OSHA 1910 subpart H, the minimum distance to any living quarters, or nearest important building (control room, labs, and MCC) will be 75 feet. As offshore platforms have limited space, this requirement is difficult to meet without building a second platform at considerable expense.
- Proximity of VDU and propane enrichment process to the living quarters – unlike shoreside facilities and refineries, an offshore platform will have an inherent risk to the personnel living on the platform.
- Volatility of propane – propane is a medium reactivity fuel source. Commercial propane is composed of about 95% propane and propylene gas. Propane explosions are expected to result in overpressures that are about 40% higher than that of a natural gas explosion under identical conditions
- Propane gas is heavier than air – any leaking propane will tend to concentrate on the work decks of the platform.

Proceedings of the 5<sup>th</sup> International Symposium on Fire Investigation Science and Technology

#### **EXPLOSION SEVERITY: PROPANE VERSUS NATURAL GAS**

Alfonso Ibarreta, Ph.D., PE, CFEI, Timothy Myers, Ph.D., PE, CFEI, CFI, James Bucher, Ph.D., CFEI and Kevin Marr, Ph.D., CFEI Exponent, USA

“However, propane explosions have been shown to produce higher overpressures in unconfined explosion tests when compared to methane.”

“In vapor cloud explosion modeling, methane is considered to be a “low” reactivity fuel, while propane is listed as a “medium” reactivity fuel.”

“Although the maximum laminar burning velocity associated with propane is only about 15% higher than that associated with methane, commercial propane explosions are expected to result in overpressures that are about 40% higher than that of a natural gas explosion under identical conditions with a perfectly-mixed near- stoichiometric fuel-air mixture, based on empirical correlations.”

**Table 1 Fuel parameters**

FUEL	K <sub>G</sub> <sup>a</sup> (bar-m/s)	Specific Gravity	Maximum Burning Velocity <sup>b</sup> (cm/s)	Flame Temperature (K)	Expan. Ratio	MJ per kg of fuel	MJ per m <sup>3</sup> of mixture
<b>Natural Gas</b>	55	0.60	40	2148	7.4	51.2	3.46
<b>Commercial Propane</b>	100	1.52	46	2198	7.6	49.9	3.75

The table shows how natural gas and commercial propane have very different gas densities, with natural gas being lighter than air, and propane being heavier than air.

OSHA 1910 subpart H

1910.110(b)(6)(ii)

Each individual container shall be located with respect to the nearest important building or group of buildings in accordance with Table H-23.

Table H-23

Water capacity per container	Minimum distances		
	Containers		Between above-ground containers
	Under-ground	Above-ground	
Less than 125 gals(1).....	10 feet.....	None.....	None.
125 to 250 gals.....	10 feet.....	10 feet.....	None.
251 to 500 gals.....	10 feet.....	10 feet.....	3 feet.
501 to 2,000 gals.....	25 feet(2)..	25 feet(2)..	3 feet.
2,001 to 30,000 gals.....	50 feet.....	50 feet.....	5 feet.
30,001 to 70,000 gals.....	50 feet.....	75 feet(3)..	
70,001 to 90,000 gals.....	50 feet.....	100 feet(3)..	

## SUMMARY

The conceptual design of a Vapor Recovery system at an offshore SPM is clearly a novel technology. Using the ABS guidance notes on Qualifying New technologies as a template the conceptual vapor recovery system was evaluated. Throughout the document numerous components and elements showed technical failures to perform their intended function or could not meet regulatory requirements. Several safety issues were also raised. The floating vapor hose is not protected from mechanical damage and this places the tank ship and crew in danger. The modeling of the vapor emissions from the tanker to the platform vapor destruction unit provides solid engineering analysis to show a VCS designed to meet shoreside requirements of USCG outlined in 33 CFR 154 Subpart P system cannot currently pass a verification process required by ABS.

Our conclusion is that the current, proven technology and regulations of land-based VCS are not adequate for the safe design, installation and operation of an offshore based vapor recovery system using an SPM, floating hoses, subsea pipelines, platforms, PLEMS and a safe-port-design concept.

# Appendix E:

## Detonation Arrestor



## E. Detonation Arrestor

### Detonation Arrestor – USCG approved

24” Size - ~ 4.9 feet dia      x      8.4 ft length



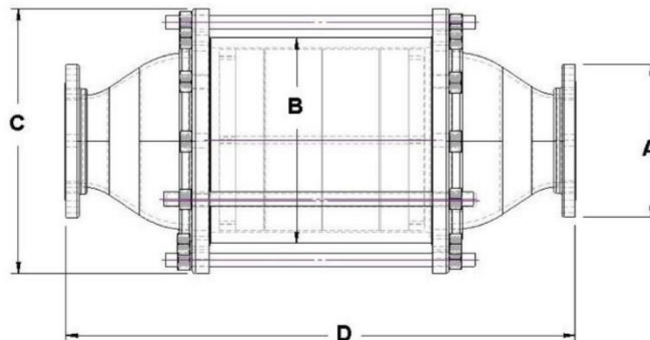
### Detonation Flame Arrestor Series C



*The Paradox Detonation Flame Arrestor*, represents the best technology for value in flame arrestor protection. They prevent flame propagation by absorbing heat and dissipating supersonic pressure waves, using multiple spiral wound crimped ribbon flame cells staged with turbulent creating screen sections.



### Series C-Detonation Flame arrester Specifications



USCG  
Approved



Model	A 150# AN- SICConn. Size in. (mm)	B Housing Size In. (mm)	C Outside Di- ameter In. (mm)	D Overall Length In. (mm)	Initial Pressure Rating Group D (-2 psia for Group C)	Approx. Weight Lb. (Kg.) Grp D (Grp C&B +15% to 20%)
*C-24C	24 (600)	48 (1200)	59.50 (1511)	101.00 (2565)	22.7 psia (1.54 bar)	8400 (3810)

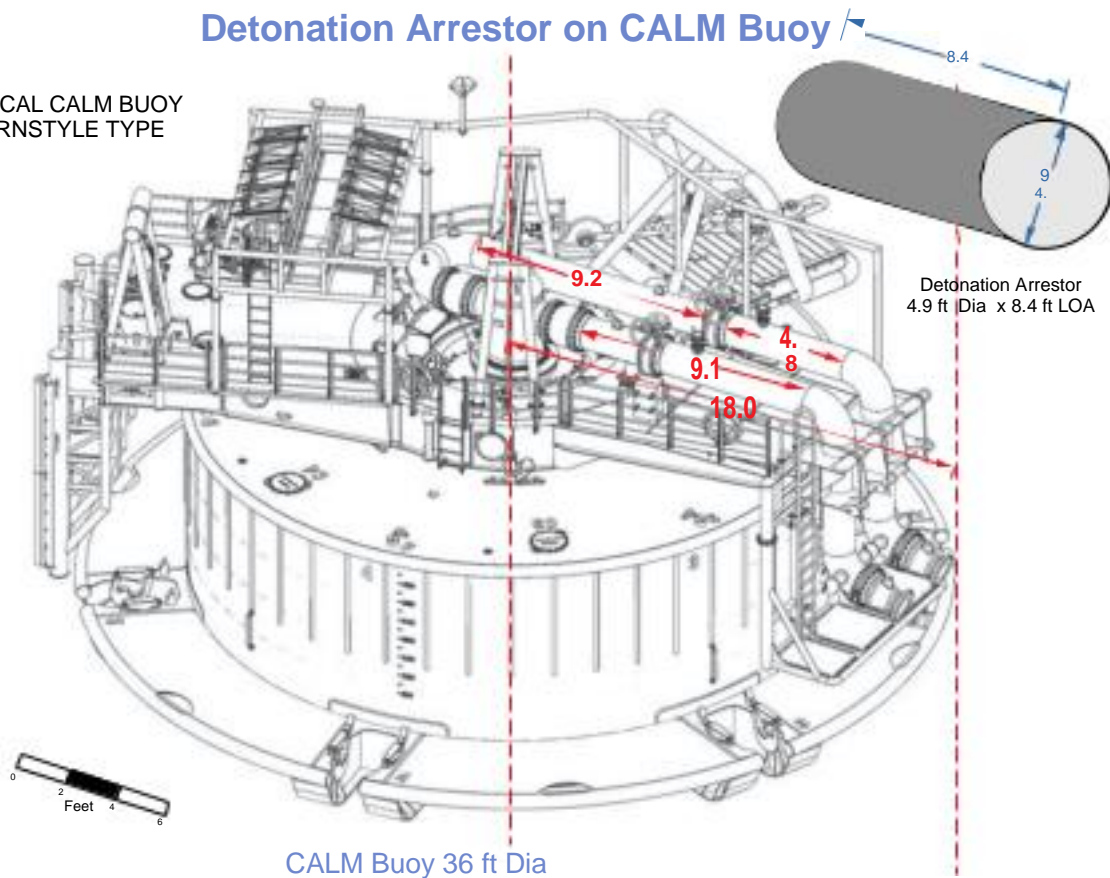
# Appendix F:

Detonation Arrester on a CALM Buoy



## Detonation Arrestor on CALM Buoy

TYPICAL CALM BUOY  
TURNSTYLE TYPE



CALM Buoy with (2) two crude oil lines and DA for 24" vapor hose

The above picture of a CALM Buoy is not showing the third line for the vapor emissions. The additional line for the vapor emissions will not allow for sufficient space to install a DA on the CALM Buoy as the diameter of the DA is 4.9 feet. Additionally, a DA located on the CALM Buoy will not protect the 985 feet floating vapor hoses. The floating vapor hoses are not protected from possible mechanical damage.

# Appendix G: USCG Policy Letter 2-16



16715  
CG-ENG Policy Letter  
No. 02-16  
June 2, 2016

From:  B. J. Hawkins, CAPT  
COMDT (CG-ENG)

To: Distribution

Subj: CLARIFICATION AND GUIDANCE FOR IMPLEMENTATION OF MARINE  
VAPOR CONTROL SYSTEMS (VCS); EXEMPTION AND CERTIFICATION,  
DETONATION ARRESTORS, AND ANTI-FLASHBACK BURNERS

Ref: (a) Title 33 Code of Federal Regulations (33 CFR) Part 154, Subpart P

1. Purpose. This policy letter provides guidance on the implementation and interpretation of the final rule for the design and operation of new and existing Marine Vapor Control Systems (VCS) designed and installed in accordance with reference (a) . Specifically, this policy letter interprets requirements for line size expansion, liquid seals and anti-flashback burner compliance.
2. Directives Affected. None.
3. Background. The marine VCS regulations were first published in 1990 and updated on July 16, 2013 (78 FR 42596-42651) to promote maritime safety and marine environmental protection. The revisions promoted safe VCS operation in an expanded range of activities that are subject to Federal and State environmental requirements. They reflected industry advances in VCS technology and codified standards for the design and operation of a VCS at tank barge cleaning facilities. These regulations came into effect for new systems on August 15, 2013 and will become effective for existing systems on August 16, 2016.

In accordance with 33 CFR 154.107 and 108, the Hazardous Materials Division in the Office of Design and Engineering Standards (CG-ENG-5) receives and reviews requests for exemptions or alternative arrangements as facilities implement system upgrades to ensure compliance with the updated VCS regulations. This policy has been developed to address the regulatory citations that are most frequently the subject of requests for exemptions, interpretations or alternative arrangements.

4. Discussion.
  - a. Exemption and Certification of VCSs

Subj: CLARIFICATION AND GUIDANCE FOR IMPLEMENTATION OF MARINE VAPOR CONTROL SYSTEMS (VCS); EXEMPTION AND CERTIFICATION, DETONATION ARRESTORS, AND ANTI-FLASHBACK BURNERS

- i. Certifying Entities (CEs) will continue to certify marine VCSs in accordance with reference (a). This policy will enable their certification to incorporate the two exemptions addressed herein in accordance with 33 CFR 154.2025 (1).
- ii. Commandant (CG-ENG-5) will continue to consider requests for exemptions not described by this policy letter on a case-by-case basis as described in 33 CFR 154.108.

b. Definitions:

The following definitions are not provided in 33 CFR 154.2001, but may be helpful in interpreting 33 CFR Part 154, Subpart P.

*Facility Vapor Connection Detonation Arrestor (FVC DA)* - means the detonation arrestor required by 33 CFR 154.2105 (a-i). It is nearest to the facility vapor connection, and is the last detonation arresting device before the facility vapor connection.

*Excluded Detonation Arresters (EDA)* - means any detonation arrestor not specifically required by 33 CFR 154.2105 excluding 33 CFR 154.2105 (j), (i.e., every detonation arrestor which is not the FVC DA).

c. Detonation Arresters Installation

For facilities collecting vapors of flammable, combustible, or non-high flash point liquid cargoes, 33 CFR 154.2106(b) requires that line size expansions on either side of a detonation arrestor, be installed in a straight pipe run and no closer than 120 times the pipe diameter from the detonation arrestor unless the manufacturer has test data to show the expansion can be closer.

Detonation arresters are required in several sections of 33 CFR Part 154 (e.g. 154.2105 and 154.2109) and good engineering practice occasionally suggests additional detonation arresters be incorporated in the VCS arrangement. The installation of detonation arresters above and beyond what is required by the regulations does not present additional safety hazards; in fact, they provide additional levels of safety. Therefore, their presence does not trigger the need for safety mediation as prescribed by 33 CFR 154.2106 (b). However, in order to be excluded from 33 CFR 154.2105 as an EDA the following conditions must be met:

- 1) The system must have at least one FVC DA installed in the system in accordance with 33 CFR 154.2106; and
- 2) Be located as close as practical to the source of ignition it is installed to arrest, regardless of the location of a pipe expansion.

Furthermore, line size expansions on the vessel side (or upstream) of the FVC DA do not affect the FVC DA's ability to protect the FVC and, subsequently, the vessel. Therefore, with verification by the CE, as part of the CE Certification documentation, the line size



Subj: CLARIFICATION AND GUIDANCE FOR IMPLEMENTATION OF MARINE VAPOR CONTROL SYSTEMS (VCS); EXEMPTION AND CERTIFICATION, DETONATION ARRESTORS, AND ANTI-FLASHBACK BURNERS

expansions between the FVC and the FVC DA may alternatively comply with 33CFR 154.2106 by meeting the following conditions:

- 1) A FVC DA is installed within 18 meters or 59.1 feet from the FVC;
- 2) All piping between the FVC and the FVC DA is fully protected from external mechanical damage; and
- 3) No internal or external ignition sources are installed between the FVC and the FVC DA.

d. Liquid Seal replaced by Anti-Flashback Burner §154.2109 (b)(3)(i)

In accordance with 46 CFR 154.2109(b)(3)(i), anti-flashback burners may be used instead of liquid seals provided they are accepted by the Commandant. In the past acceptance of anti-flashback burners has been given through the course of plan review on an individual, case-by-case, site specific basis. However, to reduce the administrative burden on industry and the Coast Guard for submission and review of anti-flashback burners for site specific installations, CG-ENG-5 will post a list of Coast Guard accepted anti-flashback burners on Homeport ([www.homeport.uscg.mil](http://www.homeport.uscg.mil)). All previously issued acceptances for anti-flashback burners will remain in effect.

An anti-flashback burner acceptance request need only be requested once per anti-flashback model number. An anti-flashback burner installation will be considered acceptable provided the conditions below and any conditions listed in the Coast Guard acceptance letter are met. A list of model numbers for Coast Guard accepted anti-flashback burners will be posted on Homeport alongside all other VCS approved lists. Requests for anti-flashback burner acceptance should be directed to Commandant (CG-ENG-5) at the address listed above.

Conditions for anti-flashback burner acceptance:

1. The anti-flashback burner is proven to have greater ability than a liquid seal to prevent flame flashback, (i.e., passing a longer endurance burn test than a liquid seal as per manufacturer's specifications or claims).
2. A thermocouple is securely installed upstream of each anti-flashback burner so that the temperature of the anti-flashback burners can be measured continuously throughout the entire VCS operation. The thermocouple is installed within ten feet of the burner or within six inches of the burner stack/shell.
3. Any thermocouple penetration in the flare or vapor piping is sealed to prevent flame from entering the VCS piping.
4. The thermocouple activates the emergency shutdown system required by 33 CFR 154.550 and VCS shutdown systems required by 154.2109(d) when the temperature

Subj: CLARIFICATION AND GUIDANCE FOR IMPLEMENTATION OF MARINE  
VAPOR CONTROL SYSTEMS (VCS); EXEMPTION AND CERTIFICATION,  
DETONATION ARRESTORS, AND ANTI-FLASHBACK BURNERS

measured by the thermocouple rises above a shutdown set point. The set point shall be 250°F or less for cargoes with an auto-ignition temperature equal to or higher than 300°F, or it shall be 50°F lower than the auto-ignition temperature for cargoes with an auto-ignition temperature lower than 300°F.

5. A differential pressure transmitter or other suitable method that activates a means to prevent backflow is installed in conjunction with the detonation arrester in the combustion system inlet to prevent vapor backflow.
6. The purge cycle required by 33 CFR 154.2107(a) provides enough enriching gas downstream of the injection point such that the vapor collection line achieves a minimum of two-volume exchanges of enriching gas prior to receiving cargo vapor with extra precaution for startup and purging conditions which may exceed burner heat capacities.

5. Applicability. This policy is applicable to all facilities subject to 33 CFR Part 154, Subpart P regulations.

6. Disclaimer. While the guidance contained in this document may assist the industry, public, Coast Guard, and other Federal and State regulators in applying statutory and regulatory requirements, the guidance is not a substitute for applicable legal requirements nor is it a regulation itself. Thus, it is not intended to nor does it impose legally binding requirements on any party outside the Coast Guard.


7. Changes. This policy letter will be posted on the web at [www.homeport.uscg.mil](http://www.homeport.uscg.mil) Changes to this policy will be issued as necessary. Suggestions for improvements of this policy should be submitted in writing to Commandant (CG-ENG-5) at the address listed above.

#

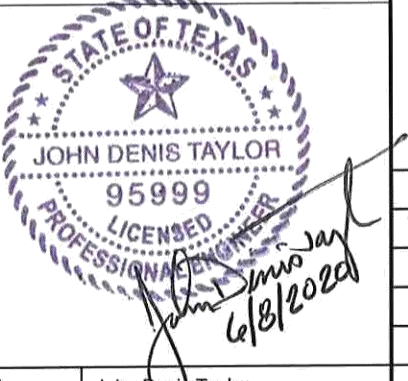

Distribution: CG-FAC  
CG-CVC  
CG-OES  
CG-MSD  
All Area/District (p)(r)(cc)  
All Sectors/MSUs/MSDs (p)(r)(cc)

# Appendix H:


## Modeling

 <b>audubon</b> 111 VETERANS BLVD, SUITE 1200 METAIRIE LA 70005 TX REG. NO. 8696	<b>ENGINEERING ASSESSMENT</b>  <b>TEXAS GULFLINK</b> <b>VAPOR RECOVERY MODELING</b>	Doc. No.:	021599001-AE-TE-PE0001
		Project No.:	021599-001
		File Loc.:	021599001.600.110
		Rev. No.:	2
		Rev. Date:	06/08/2020

**ENGINEERING ASSESSMENT**  
  
**021599001-AE-TE-PE0001**  
  
**VAPOR RECOVERY PROCESS MODELING**  
  
**FOR**  
  
**ABADIE-WILLIAMS**  
  
**CLIENT AFE: TBD**  
  
**TEXAS GULFLINK TERMINAL**

<b>Engineering Seal</b> 							
		<b>Revisions</b>					
<b>Rev</b>	<b>Date</b>	<b>Description</b>	<b>By</b>	<b>Chk'd</b>	<b>App'd</b>		
0	05/22/20	For Information	MTM	CAC	JDT		
1	06/03/20	Issued Final	CAC	MTM	JDT		
2	06/08/20	Reissued Final	MTM	CAC	JDT		
P.E. Name: John Denis Taylor							
License No.: TX95999							
This Document is solely for the use of the contractual Client and Audubon and its affiliates (Audubon). Audubon assumes no liability to any other party for any representations contained in this Document.							



 <b>audubon</b> 111 VETERANS BLVD, SUITE 1200 METAIRIE LA 70005 TX REG. NO. 8696	<b>ENGINEERING ASSESSMENT</b>  <b>TEXAS GULFLINK</b> <b>VAPOR RECOVERY MODELING</b>	Doc. No.:	021599001-AE-TE-PE0001
		Project No.:	021599-001
		File Loc.:	021599001.600.110
		Rev. No.:	2
		Rev. Date:	06/08/2020

## 1.0 INTRODUCTION

The purpose of this engineering evaluation is to document the vapor recovery process modeling for the proposed Texas GulfLink Terminal (TGL). The TGL will temporarily store crude oil onshore to pump offshore to Very Large Crude Carriers (VLCCs). The crude oil will be transferred via a 42" pipeline, which will flow through an offshore platform, through a SPM and on to a VLCC. No vapor recovery is intended for the process; however, the vapor recovery process model was generated to support the EPA Case by Case MACT Analysis (112(g)).

## 2.0 BASIS AND METHODS

### 2.1 Compositions

The following flue gas compositions were utilized. The vapor was assumed to be water saturated for all simulation cases.

**TABLE 1: FLUE GAS COMPOSITION**

COMPONENT	VOL %
N <sub>2</sub>	83
CO <sub>2</sub>	12
O <sub>2</sub>	4
Other Gases	Trace

### 2.2 AMBIENT CONDITIONS


The following ambient conditions were considered in the evaluation:

**TABLE 2: AMBIENT CONDITIONS**

CASE	Water Temperature	Air Temperature	Water Flowing Speed	Wind Speed
Winter	60°F	60°F	3 FT/S	25 FT/S
Summer	85°F	85°F	3 FT/S	25 FT/S

### 2.3 Simulation Methods

The vapor recovery modeling was executed using the Aspen HYSYS Hydraulics sub-flowsheet. The length, elevation, and heat transfer properties for each piping segment were specified per the client-supplied model diagram and equipment details (see Attachment 1). A flow schematic of the HYSYS sub-flowsheet

 <b>audubon</b> 111 VETERANS BLVD, SUITE 1200 METAIRIE LA 70005 TX REG. No. 8696	<b>ENGINEERING ASSESSMENT</b>  <b>TEXAS GULFLINK</b> <b>VAPOR RECOVERY MODELING</b>	Doc. No.:	021599001-AE-TE-PE0001
		Project No.:	021599-001
		File Loc.:	021599001.600.110
		Rev. No.:	2
		Rev. Date:	06/08/2020

is shown in Attachment 2. All horizontal and inclined piping segments were modeled using the Beggs & Brill 1979 flow correlation. The vertical 24" Riser section was modeled using the Aziz et al flow correlation.

Two steady state simulations were generated. The first model assumed isothermal flow through the vapor recovery line. The purpose of the isothermal case was to establish the ideal boundary conditions for the system. The second simulation considered thermal heat transfer and water condensation in the vapor recovery line. Only the ambient conditions that generated the worst case operating conditions (i.e., the conditions that required the lowest platform suction pressure) were considered.

For each simulation, the flow and pressure at the VLCC were specified in order to calculate the required platform suction pressure in steady state operation. The required flow was based upon the actual volume displaced by crude oil filling the VLCC. Four filling rates were considered: 15,000 BPH, 30,000 BPH, 60,000 BPH, and 85,000 BPH. Case studies were utilized to determine the required suction pressure at the platform for various VLCC operating pressure at constant flow rate.


### 3.0 SIMULATION RESULTS

The isothermal steady state case was evaluated at the maximum expected flowrate for both the winter and summer cases. With no heat transfer or water condensation, the required platform suction pressures for the winter and summer cases at a VLCC fill rate are -0.64 psig and -0.51 psig, respectively. See the summary of results below:

**TABLE 3: ISOTHERMAL STEADY STATE RESULTS**

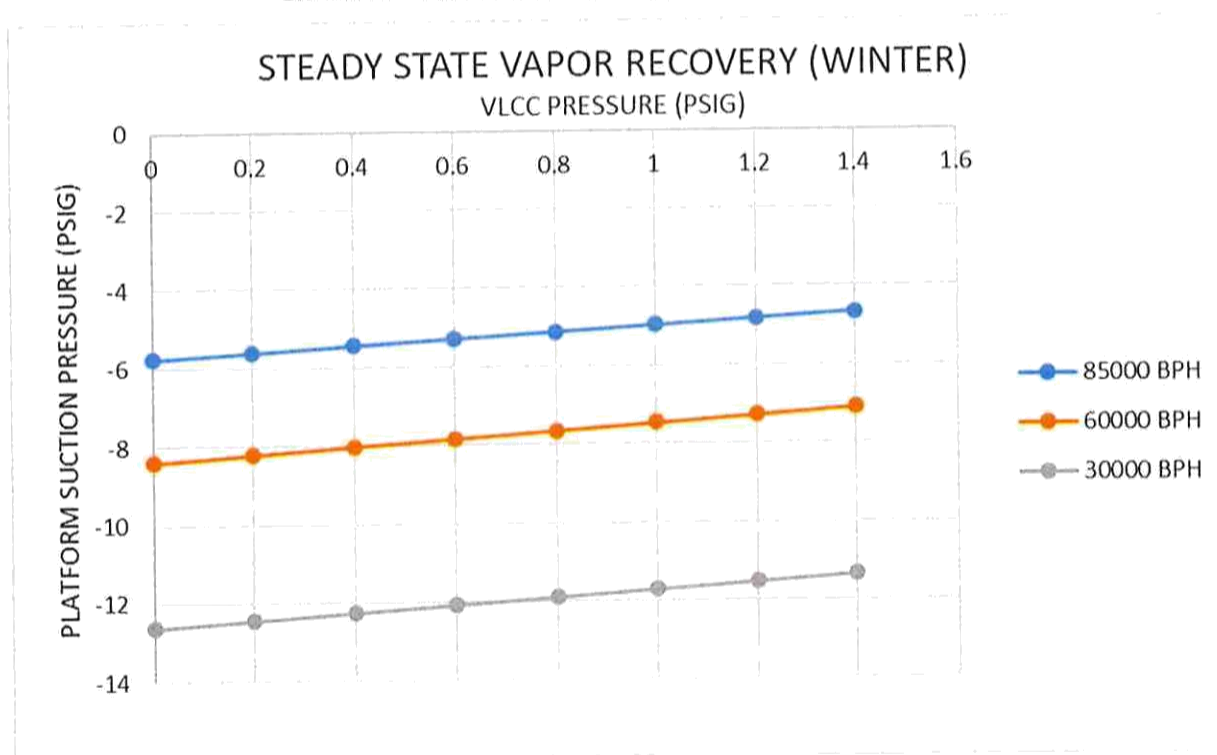
Case	Vapor Temp	VLCC Pressure	VLCC Flow Rate	Platform Suction Pressure	Platform Flowrate	
	°F	PSIG	ACFS	PSIG	ACFS	SCFS
85000 BPH Winter	70	1.4	132.6	-0.64	159.8	142.7
85000 BPH Summer	100	1.4	132.6	-0.51	157.6	135.1

Once heat transfer was considered, the winter steady state case resulted in the lowest platform suction pressures. Significant liquid hold-up in the lower section of the 24" riser resulted in reduce vapor flow area and slug flow, generating increased pressure drop in the piping sections. The steady state results show that, as the vapor flow rate is reduced, the vacuum pressure required at the platform suction increases. At lower flow rates and velocities, less condensate is swept away in stable two phase flow, resulting in increased liquid hold-up and a slugging flow regime. At the 30,000 BPH filling rate, the minimum required vacuum at the platform suction at steady state conditions is -11.37 psig. The HYSYS simulation did not converge in the steady state for any case at the 15,000 BPH fill rate, indicating excessive pressure drop resulting from liquid accumulation.

 <b>audubon</b> 111 VETERANS BLVD, SUITE 1200 METAIRIE LA 70005 TX REG. NO. 8696	<b>ENGINEERING ASSESSMENT</b>  <b>TEXAS GULFLINK</b> <b>VAPOR RECOVERY MODELING</b>	Doc. No.:	021599001-AE-TE-PE0001
		Project No.:	021599-001
		File Loc.:	021599001.600.110
		Rev. No.:	2
		Rev. Date:	06/08/2020

The minimum steady state liquid hold up occurs at a VLCC operating pressure of 1.4 psig and fill rate of 85000 BPH. At these conditions, the liquid hold up is approximately 22% of the cross sectional area up to an elevation of 8 ft from the base of the riser section. The maximum liquid hold up occurs at VLCC operating pressure of 0 psig and fill rate of 30000 BPH. At these conditions, the liquid hold up is approximately 35% of the cross sectional area at the base of the riser section and 30% at an elevation of 40 ft from the base of the riser. See the summary of results below:

**GRAPH 1: STEADY STATE WINTER SIMULATION RESULTS**




#### 4.0 CONCLUSIONS

When heat transfer from the vapor stream results in liquid condensation, the required suction vacuum at the platform increases significantly as liquid accumulates in the vertical piping sections of the vapor recovery line.

#### 5.0 ATTACHMENTS


Attachment 1: Client-Provided Model Diagram and Equipment Details

Attachment 2: HYSYS Hydraulics Sub-Flowsheet

 <b>audubon</b> 111 VETERANS BLVD, SUITE 1200 METAIRIE LA 70005 TX REG. NO. 8696	<b>ENGINEERING ASSESSMENT</b>  <b>TEXAS GULFLINK</b> <b>VAPOR RECOVERY MODELING</b>	Doc. No.:	021599001-AE-TE-PE0001
		Project No.:	021599-001
		File Loc.:	021599001.600.110
		Rev. No.:	2
		Rev. Date:	06/08/2020

Attachment 1: Client-Provided Model Diagram and Equipment Details

## Client-Provided Data

 Abadie-Williams 1 Galleria Blvd. Suite 1680 Metairie, LA 70001		TGL TERMINAL Vapor Recovery Process Modeling	Doc. No.:	General
			A-W Job No.:	1095AW01
			Client AFE No.:	
			Rev. No.:	A
			Rev. Date:	05/07/20
			File No.:	

## Model Diagrams

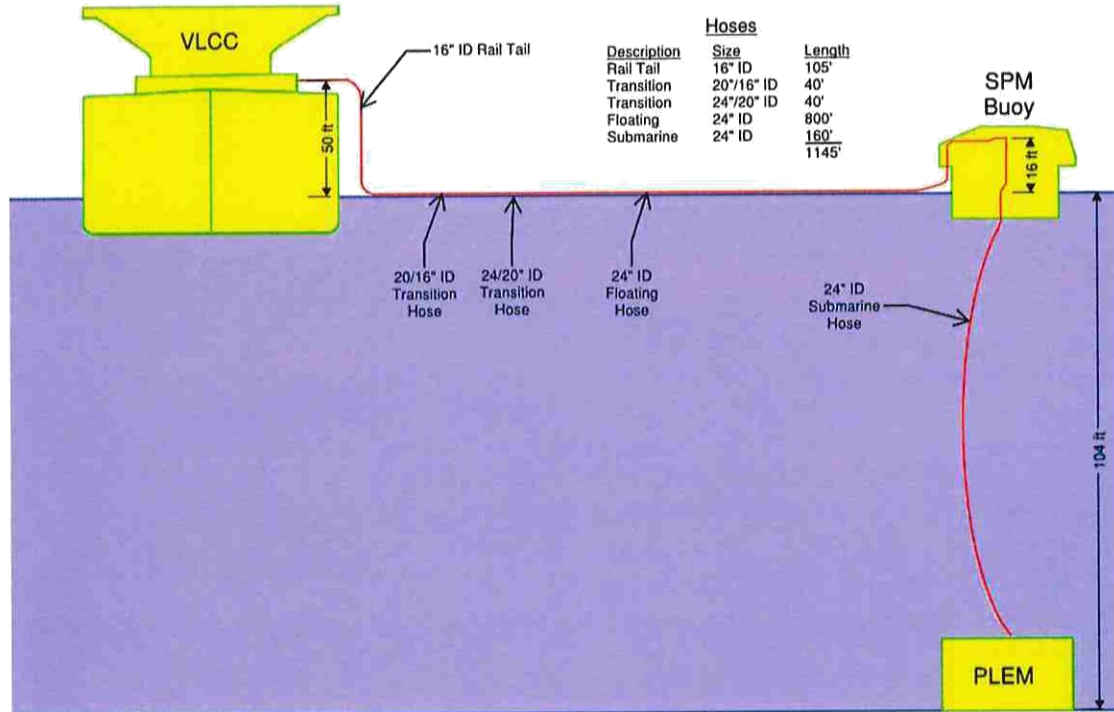


Figure 1: Layout overview of the hose connections from the VLCC to the PLEM. Lengths and Elevations of the hoses are shown.



## Client-Provided Data

 <b>Abadie-Williams</b> 1 Galleria Blvd. Suite 1680 Metairie, LA 70001	 <b>TEXAS</b> GulfLink	TGL TERMINAL Vapor Recovery Process Modeling	Doc. No.:	General
			A-W Job No.:	1095AW01
			Client AFE No.:	
			Rev. No.:	A
			Rev. Date:	05/07/20
			File No.:	

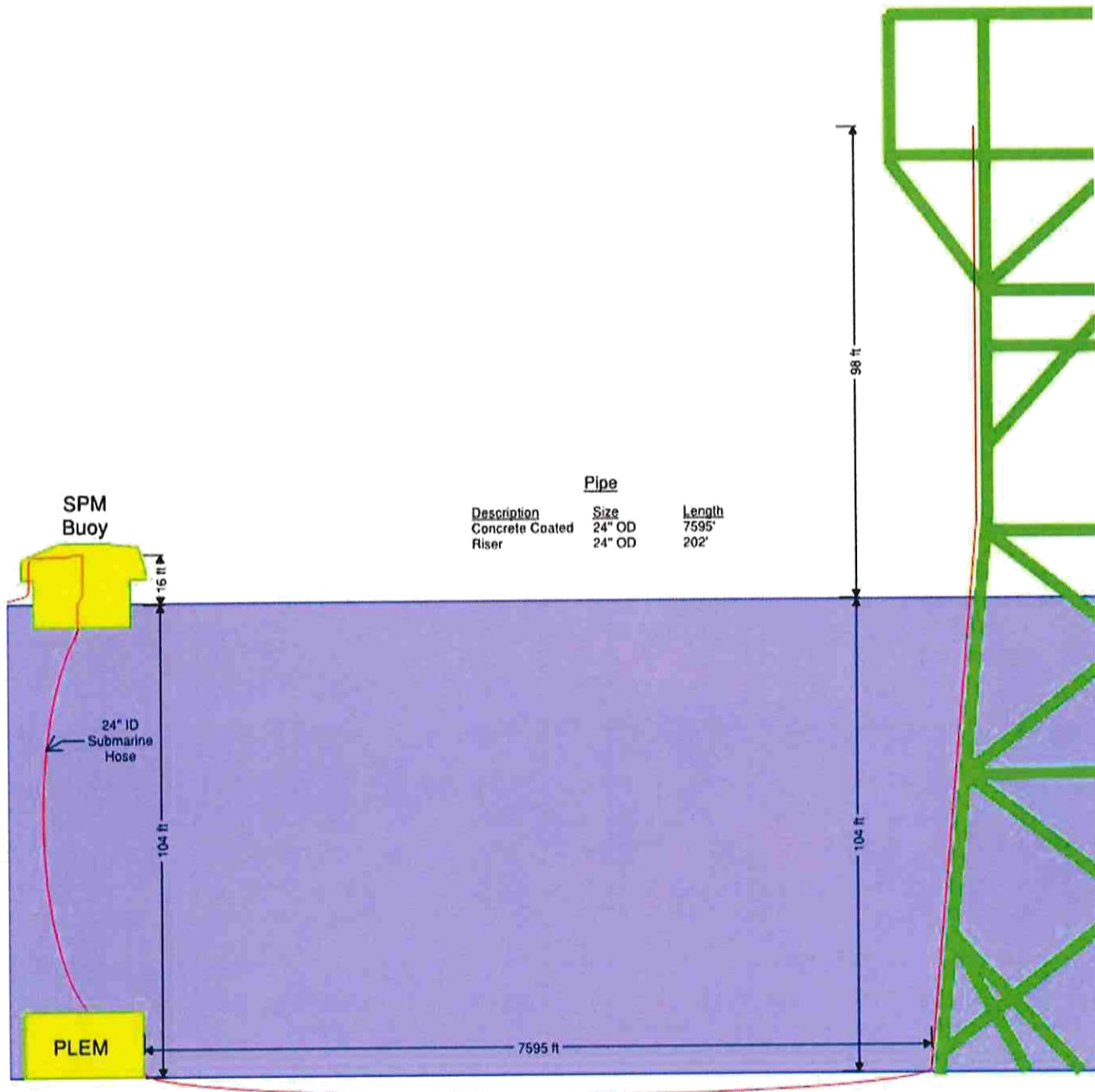


Figure 2: Continuation of Figure 1 layout. Shows the overview of the piping from the PLEM to the Platform elevation, where equipment could be placed.

### Client-Provided Data

 Abadie-Williams 1 Galleria Blvd. Suite 1680 Metairie, LA 70001		TGL TERMINAL Vapor Recovery Process Modeling	Doc. No.:	General
			A-W Job No.:	1095AW01
			Client AFE No.:	
			Rev. No.:	A
			Rev. Date:	05/07/20
			File No.:	

### Hoses and Piping

- VLCC to PLEM – Reference Figure 1

Hoses											
Description	O.D. (in)	I.D. (in)	W.T. (in)	Roughness (in)	Section Bending Stiffness (lb•ft <sup>2</sup> )	Average Heat Transfer Coefficient (BTU/hr•ft <sup>2</sup> •°F)	Section Length (ft)	# of Sections	Total Length (ft)	Starting Elevation (ft)	Ending Elevation (ft)
16" Rail Tail	28.00	16.00	6.00	0.000984	94,641.4	47.877	35	3	105	+50	0
20/16" Transition	31.83	19.27	6.28	0.000984	181,485.6	45.217	40	1	40	0	0
24/20" Transition	35.83	23.27	6.28	0.000984	319,414.7	43.089	40	1	40	0	0
24" Floating	35.83	23.27	6.28	0.000984	319,414.7	43.089	40	20	800	0	+3
24" Submarine	35.83	23.27	6.28	0.000984	319,414.7	14.363	40	4	160	-5	-100


Table 2: Hose details, as referenced in Figure 1. Note: SPM Buoy has an internal elevation of +16 ft.

- PLEM to Platform – Reference Figure 2

Piping									
Description	O.D. (in)	I.D. (in)	W.T. (in)	Roughness (in)	Concrete Coating Thickness (in)	Section Length (ft)	Starting Elevation (ft)	Ending Elevation (ft)	Depth of Cover (ft)
24" Pipeline	24.00	23.25	0.375	0.002402	3	7595	-104	-104	3
24" Riser	24.00	23.25	0.375	0.002402	0	202	-104	+98	N/A

Table 3: Pipe details, as referenced in Figure 2.

## Client-Provided Data

 Abadie-Williams 1 Galleria Blvd. Suite 1680 Metairie, LA 70001	 TEXAS GulfLink	TGL TERMINAL Vapor Recovery Process Modeling	Doc. No.:	General
			A-W Job No.:	1095AW01
			Client AFE No.:	
			Rev. No.:	A
			Rev. Date:	05/07/20
			File No.:	

## Equipment Details

### Vapor

- Vapor compositions to be evaluated:
  - Flue Gas by Volume:
    - N<sub>2</sub> = 83%
    - CO<sub>2</sub> = 12%
    - O<sub>2</sub> = 4%
    - Other Trace Gases
  - Case 1 (Winter)
    - 70°F
    - Water Vapor Saturated
  - Case 2 (Summer)
    - 100°F
    - Water Vapor Saturated

### VLCC

- Cargo Tanks
  - Starts empty
  - Total cargo volume = 2,000,000 bbl (84,000,000 gal) (11,229,170 ft<sup>3</sup>)
    - Fills to a maximum of 98%
  - Liquid fill rate into the VLCC Cargo Volumes
    - 85,000 BPH (59,500 gpm) (132.6 ACFS)
    - 60,000 BPH (42,000 gpm) (93.6 ACFS)
    - 30,000 BPH (21,000 gpm) (46.8 ACFS)
    - 15,000 BPH (10,500 gpm) (23.4 ACFS)
- Vapor leaving is displacement volume only, as the VLCC is filled with crude oil.
  - All tank vents are attached for equalization across tanks.
  - Vapor discharge pressure is dynamic, as the VLCC starts at +0.25 psig and has a target operating pressure of 1.4 to 1.6 psig.
    - Model should maintain the VLCC tank operating pressures at 1.4 psig
  - Discharge elevation is +50 ft
- Internal piping is equal to 16", Sch. Std, maximum of 590 ft equivalent length.



## Client-Provided Data


 Abadie-Williams 1 Galleria Blvd. Suite 1680 Metairie, LA 70001	 TGL TERMINAL Vapor Recovery Process Modeling	Doc. No.:	General
		A-W Job No.:	1095AW01
		Client AFE No.:	
		Rev. No.:	A
		Rev. Date:	05/07/20
		File No.:	

### SPM Buoy

- 24" connections, but restricts down to 20" internally
- Maximum Internal Elevation = +16 ft
  - Internal height forms a P-Trap.
- Inlet Elevation = +3 ft
- Outlet Elevation = -5 ft
- Internal piping is equal to 20", Sch. Std, 104 ft equivalent length.

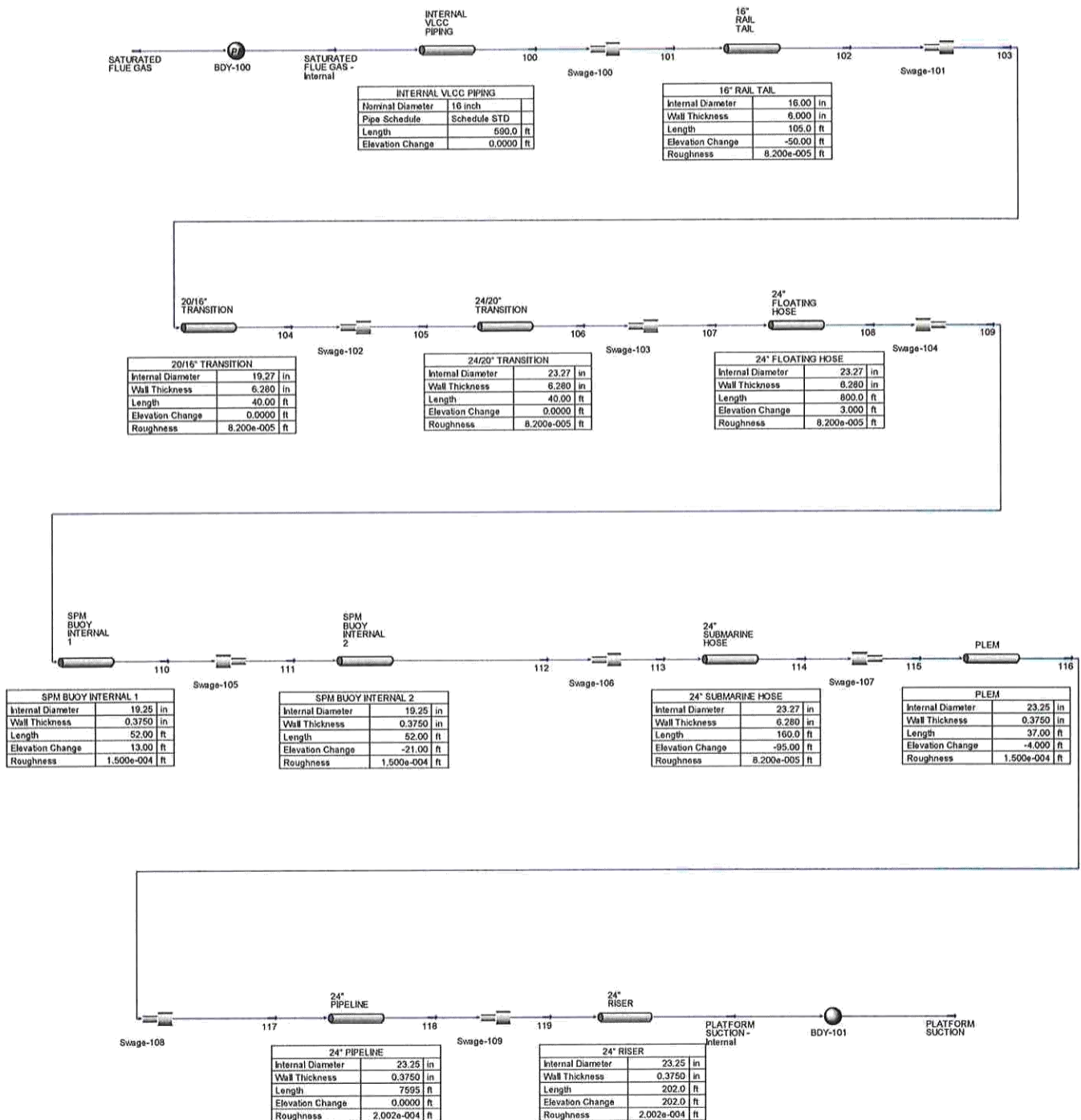
### PLEM

- Inlet Elevation = -100 ft
- Outlet Elevation = -104 ft
- Internal piping is equal to 24", Sch. Std, 37 ft equivalent length.

 <b>audubon</b> 111 VETERANS BLVD, SUITE 1200 METAIRIE LA 70005 TX REG. NO. 8696	<b>ENGINEERING ASSESSMENT</b>  <b>TEXAS GULFLINK</b> <b>VAPOR RECOVERY MODELING</b>	Doc. No.:	021599001-AE-TE-PE0001
		Project No.:	021599-001
		File Loc.:	021599001.600.110
		Rev. No.:	2
		Rev. Date:	06/08/2020

Attachment 2: HYSYS Hydraulics Sub-Flowsheet

# HYSYS Hydraulic Sub-Flowsheet Schematic



# Appendix I: Coast Guard Authorized Certifying Entities for Facility Vapor Control Systems

**Coast Guard Authorized Certifying Entities for Facility Vapor Control Systems**

(Revised: February 2020)

For additional information, contact Commandant (CG-ENG-5): (202) 372-1412  
hazmatstandards@uscg.mil

or 141

ABSG Consulting, Inc.  
16855 Northchase Drive  
Houston, TX 77060  
Contact Name: Mr. David Hua  
Phone: (281) 673-2744  
Fax: (281) 673-2798  
Email: dhua@absconsulting.com

Contact Names: Mr. Michael  
Flannigan/Mr. Amit Joshi  
Email: MJFlannigan@bei-  
us.com or amjoshi@bei-us.com

Brown and Root Industrial Services,  
LLC 8585 Archives Avenue Suite 210.

Baton Rouge, LA 70809

Contact Name: Mr. Michael H. Wink, P.E.  
Phone: (504) 468-3212 / (504) 452-1085  
Email: michael.wink@brownandroot.com

AECOM (formerly URS)  
1515 Poydras St. Suite 2700  
New Orleans, LA 70112-3587  
Contact Name: Mr. John Elmer, PE  
Phone: (504) 599-5214  
Fax: (504) 522-0554  
Email: john.elmer@aecom.com

Aura Engineering  
4801 W. Orange St.  
Pearland, TX 77581  
Contact Name: Mr. Gary Lawrence, P.E.  
Phone: (281) 485-1105  
Fax: (281) 582-5998  
Email: info@aura-eng.com  
www.aura-engineering.com

BEI Engineers  
12301 Kurland Dr. Suite  
250 Houston, TX 77034  
Main Office Number: (713) 475-2424 X 152

CB&I

14105 S. Route 59

Plainfield, IL 60544-8984

Contact Name: Mr. Jeffery Baker

Phone: (815) 439-6383

Email: jeffery.baker@cbi.com

Eichleay, Inc.

1390 Willow Pass Road, Suite  
600 Concord, CA 94520

Contact Name: Mr. John

Sakamoto Phone: (925) 689-7000

Fax: (925) 689-7006

Email: sakamoto@eichleay.com

Environmental Resources Management  
(ERM)

8550 United Plaza Blvd. Suite  
601 Baton Rouge, LA 70809

Contact Name: Mr. Matthew J.  
Skific, P.E. or Mr. Jeff Simmerman

Email: jeff.simmerman@erm.com

Phone: (225) 292-3001

Fax: (225) 288-7990

GHD Services, Inc.

1755 Wittington Place Suite

500 Dallas, TX 75234

Main Office Number: (972) 331-8500

Fax: (972) 331-8501

Contact Name: Dr. Suresh Raja Iyer

Email: Suresh.Iyer@ghd.com

Gulf States Engineering,

Inc. 4110 Moffett Road

Mobile, AL 36618

Contact Name: Mr. John T.  
Wade, P.E., F.P.E.

Phone: (251) 460-4646

Fax: (251) 460-4649

Email: tom.wade@gseeng.com

**Coast Guard Authorized Certifying Entities for Facility Vapor Control Systems**

(Revised: February 2020)

For additional information, contact Commandant (CG-ENG-5): (202) 372-1412

hazmatstandards@uscg.mil

Hess Engineering, Inc.

P.O. Box 1083

Calvert City, KY 42029

Contact Name: Mr. Daryl Hess

Phone: (270) 395-5248

Fax: (270) 395-5289

Email: dhess@ajhess.com

RJP Consulting

802 Hackberry Lane

Friendswood, TX 77546-3543 Contact Name:

Mr. Richard J. Pichler Phone: (832) 569-2127

Fax: (832) 569-2127

Cell: (281) 744-0319

Email: pichler@swbell.net

Lanier & Associates, Inc.

4101 Magazine Street

New Orleans, LA 70115

Contact Name: Mr. Thomas O'Keefe

Phone: (504) 895-0368

Fax: (504) 895-0566

Email: tokeefe@lanier-engineers.com

th

Norton Engineering

2750 Lake Villa Dr.

Metairie, LA 70002

Contact Name: Mr. Scott Haydel

Office: (504) 262-8060 x301

Cell: (504) 875-9662

Email: shaydel@nortonengr.com

or

277 Fairfield Road Suite

325 Fairfield, NJ 07004;

Contact Name: Dr. Rick Todd

Office: (973) 394-9330 x201 or x204

Cell: (973) 771-8479

Email: rtodd@nortonengr.com

RPMS Consulting Engineers

1 Rossmoor Drive

Suite 300

Monroe Township, NJ 08831

Contact Name: Mr. John

Warrington Phone: (609)

655-9292

Fax: (609) 655-5122

Email: johnwarr@rpmsengineers.com

Stantec Consulting Inc.

3010 W. Charleston Blvd. Suite 100

Las Vegas, NV 89102-1969

Contact Name: Mr. David C.

Rein, P.E. Cell: (925)

997-3591

Email: david.rein@stantec.com

S. T. Hudson Engineers,

Inc. 900 Dudley Ave

Cherry Hill, NJ 08002

Contact Name: Mr. Steven Gucciardi

Phone: (856) 342-6600

Fax: (856) 342-8323

Email: sgucciardi@sthe.com

Simpson Gumpertz & Heger (SGH)

500 12 Street Suite 270

Oakland, CA 94607

Contact Name: Mr. Luis Palacios

Phone: (510) 457-4458

Fax: (510) 457-4599

Email: lhpalacios@sgh.com

Spectrum Engineering &

Associates 6505 Mars Road

Cranberry Township, PA 16066

Contact Name: Mr. Eugene Miklaucic P.E.

Phone: (724) 776-6654

Fax: (724) 776-6630

Email: eugene@spectrummedical.com



**Coast Guard Authorized Certifying Entities for Facility Vapor Control Systems**

(Revised: February 2020)

For additional information, contact Commandant (CG-ENG-5): (202) 372-1412  
hazmatstandards@uscg.mil

**Technical Environmental**

Services 5133 Taravella Road  
Marrero, LA 70072

Contact Name: Angie Hendrix,  
MSPH or Robert Marrero, P.E.

Phone: (504) 348-3098

Fax: (504) 348-3043

Email: ahendrix@tesconsult.com  
or rmarrero@tesconsult.com

Warner Nicholson Consultants, PLLC  
(formerly Warner Nicholson Engineering  
Consultants, P.C.)  
PO Box 24<sup>th</sup>  
Wellborn, TX 77881

Contact Name: Mr. Jon W. Young,  
P.E. Phone: (918) 630-4473

Email: jyoung@vaporcontrol.com

**U.N.I. Engineering, Inc.**

156 Stockton Street

P.O. Box 1329

Hightstown, NJ 08520

Contact Name: Mr. David. M. Dileo, PE  
Phone: (609) 448-4633 X 304

Fax: (609) 448-5971

Email: ddileo@uni-eng.com

**Woodbridge Engineering**

LLC 4619 East 78 Street

Tulsa, OK 74136

Contact Name: Ms. Gayla Broostin, P.E.  
Phone: (918) 724-6893

Email: gbroostin@wb-eng.com

List of previous (but not current) CEs

(May appear on a facility's initial VCS Certification Letter):

Babet Engineering

D. Russell Associates, Inc.

Engineering Services, Inc. (ESI)

International Technology Corporation (IT)

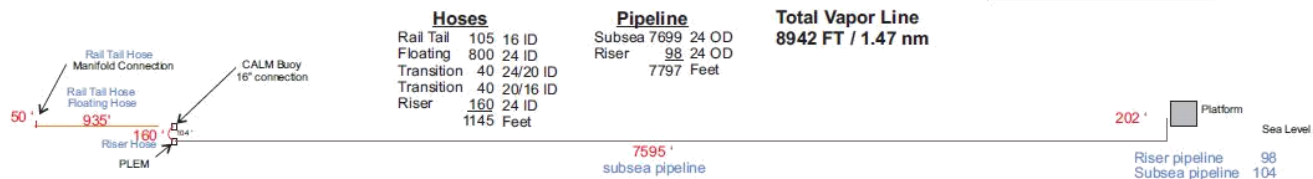
Miller-Remick Corporation

Orbital Engineering, Inc.

Parsons E&C Corp.  
Phoenix Engineering, Inc.  
Polo Corporation  
Preferred Engineering  
Process Automation Incorporated  
Process Systems International, Inc.  
Pyburn & Odom, Inc.  
S & B Engineers and Constructors, Ltd.  
Shaw Environmental  
S.I.P. Engineering, Inc.  
Walk, Haydel & Associates, Inc.  
Wink Engineering  
The WCM Group

<https://homeport.uscg.mil/missions/environmental/hazardous-materials-standards/marine-vapor-control-systems> 3

# Appendix J: Texas GulfLink Deepwater Port Vapor Recovery Line Profile



LEGEND	DRAWN BY: Captain Dan Harris	TEXAS GULFLINK PROJECT	
	DATE: 30 Sep 2019	PROFILE VAPOR LINES	
	DWG NAME: Profile VR		
	SHEET of	REV: 01	REV DATE: 29 Apr 2020
		SENTINEL MIDSTREAM	

# Appendix K: Correspondence

REDACTED

REDACTED

REDACTED



REDACTED

# Appendix L: Riverhead NY, United Riverhead Terminal Document

Riverhead NY, United Riverhead Terminal – VLCC loading crude w/o vapor recovery by exemption from DEC due cost of vapor recovery

The facility, located 80 miles east of New York Harbor on a 286-acre site in Suffolk County, New York, consists of 20 storage tanks, a truck transfer rack, and an off-shore barge/ship platform which is the only deepwater loading/unloading platform on the U.S. East Coast.



New York State Department of Environmental  
Conservation

Permit Review Report

Permit ID: 1-4730-00023/00030 Renewal Number:  
2 04/12/2016

Facility Identification Data

Name: UNITED RIVERHEAD TERMINAL Address: 212  
SOUND SHORE RD RIVERHEAD, NY 11901 Owner/Firm



Name: UNITED RIVERHEAD TERMINAL INC Address: 212 SOUND SHORE RD RIVERHEAD, NY  
11901, USA Owner Classification: Corporation/Partnership

#### Permit Description Introduction

The Title V operating air permit is intended to be a document containing only enforceable terms and conditions as well as any additional information, such as the identification of emission units, emission points, emission sources and processes, that makes the terms meaningful. 40 CFR Part 70.7(a)(5) requires that each Title V permit have an accompanying "...statement that sets forth the legal and factual basis for the draft permit conditions". The purpose for this permit review report is to satisfy the above requirement by providing pertinent details regarding the permit/application data and permit conditions in a more easily understandable format. This report will also include background narrative and explanations of regulatory decisions made by the reviewer. It should be emphasized that this permit review report, while based on information contained in the permit, is a separate document and is not itself an enforceable term and condition of the permit.

#### Summary Description of Proposed Project

This project consists of the renewal of the Title V permit issued to United Riverhead Terminal. There are no significant changes proposed to the existing petroleum bulk storage and transfer operations carried out at the facility as part of this renewal. In addition, the facility will continue to operate pursuant to its existing 6 NYCRR Part 229 VOC RACT variance for its offshore petroleum liquid loading operations.

United Riverhead Terminal was issued an air state facility permit to construct for a project related to the storage and handling of gasoline at the facility on June 11, 2014. United Riverhead Terminal has postponed the construction of the gasoline throughput project for the time being. Accordingly, this renewal does not incorporate any new applicable requirements related to gasoline throughput or storage. The facility is

required to apply for a Title V permit modification within one year of the commencement of operation of the emission sources included in the gasoline throughput project.

Emission unit U00005 - This emission unit includes the marine loading and unloading of petroleum and non-petroleum fuel liquids at an offshore platform. A variety of petroleum liquids including, but not limited to, crude oils, distillate oils, and residual oils are loaded and unloaded into marine vessels at the platform. The Department has granted a VOC RACT variance for the marine platform.

Process: DCK Petroleum liquids, including, but not limited to, crude oils, distillate oils, and residual oils are loaded and unloaded into marine vessels at the platform. Title V/Major Source Status

UNITED RIVERHEAD TERMINAL is subject to Title V requirements. This determination is based on the following information: United Riverhead Terminal is a major facility because the facility's potential to emit oxides of nitrogen hazardous air pollutants and volatile organic compounds exceeds the corresponding major facility threshold for those contaminants.

#### Program Applicability

The following chart summarizes the applicability of UNITED RIVERHEAD TERMINAL with regards to the principal air pollution regulatory programs:

#### Regulatory Program Applicability

PSD	NO
NSR (non-attainment)	NO
NESHAP (40 CFR Part 61)	NO
NESHAP (MACT - 40 CFR Part 63)	YES
NSPS	YES
TITLE IV	NO
TITLE V	YES
TITLE VI	NO
RACT	YES
SIP	YES

#### VOC RACT:

United Riverhead Terminal's potential to emit volatile organic compounds exceeds the applicable major facility threshold. Accordingly, the facility is subject to the VOC RACT requirements of 6 NYCRR Part 229. The facility has met these requirements for its petroleum bulk storage operations and the onshore loading of petroleum liquids.

United Riverhead Terminal also operates an offshore loading platform and dock located approximately one mile off the shore of Long Island. The operations performed on the platform are a source of VOC emissions, and therefore must be evaluated for VOC RACT applicability. The analysis conducted by the facility demonstrates that the cost of installing an appropriate control device on the platform exceeds the cost effectiveness threshold established by the Department's DAR-20 guidance document. According to

the Department has granted United Riverhead Terminal a variance from the VOC RACT requirements of 6 NYCRR Part 229 for the operations conducted on the offshore loading platform.

Previous versions of this permit contained a VOC RACT variance that restricted the throughput of petroleum liquids to less than 5,000,000 barrels per year. This limitation was based on a series of calculations developed several years ago based on the facility's typical operations at the time, and equates to approximately 341 tons per year of potential VOC emissions. In order to provide the facility with operational flexibility, the revised variance limits the VOC emissions from the loading of petroleum liquids with vapor pressure greater than 1.5 psia at the platform to less than 341 tons during each 12-month period. The facility is required to maintain records and submit periodic reports that demonstrate compliance with this limit. This limitation is approximately equivalent to the historical throughput limitation.

United Riverhead Terminal is required to re-evaluate the calculations and other considerations that make up its VOC RACT analysis as part of each permit renewal application. Should a future VOC RACT analysis demonstrate that the cost of controls is less than or equal to the cost effectiveness threshold established by DAR-20, United Riverhead Terminal will be required to install the appropriate controls.

# Appendix M:

API Flame Arresters

API I Flame Arrestors in piping systems - *API recommended practice*

## **Flame Arresters in Piping Systems**

API RECOMMENDED PRACTICE 2028  
THIRD EDITION, FEBRUARY 2002



**Helping You  
Get The Job  
Done Right.<sup>SM</sup>**

Safety & Fire Protection

API RECOMMENDED PRACTICE 2028

THIRD EDITION, FEBRUARY 2002

## 1.1 PURPOSE

This recommended practice is intended to inform industry about limitations of flame arresters installed in piping systems.

## 1.2 SCOPE

The scope of this recommended practice is the use and limitations of flame arresters installed in piping systems in the petroleum and petrochemical industries. It provides a general overview of flame arresters currently in use and some potential concerns or limitations.

## 5.2 PRESSURE CONCERNS AND MAINTENANCE

5.2.1 Typical flame arresters with elements will cause a pressure drop. Because of this pressure drop and the high surface area of the elements, condensation can readily occur.

Where condensation is a concern, it may be appropriate to install normally closed, valved drains on the housing of the flame arrester to enable draining of accumulated condensed liquids.

Some facilities install pressure gauges upstream and downstream of a flame arrester to monitor changes in pressure drop and facilitate determining if elements have become plugged.



# Appendix N: TGL Operating Weather Limits

## Texas GulfLink Deepwater Port – *weather limits*

### Weather Operating Limits of the Deepwater Port

#### Abort Conditions for Mooring Operations

- Sustained wind above 30 knots or wind gusts in excess of 40 knots
- Sea State above 9 feet
- Currents in excess of 3 knots
- Support Boats unable to safely operate (Support Boat Captain feels mooring conditions unsafe for their boat and crew)
- Reduced Visibility < ½ NM

#### Adverse Weather Alert

The Port will be under an Adverse Weather Alert whenever any of the following conditions exist:

- Sustained average winds are at least 35 knots.
- A front is approaching.
- A line of thunderstorms is approaching. Actions to be considered:
  - Make fast a support vessel to the stern of any moored Tanker, engine ready.
  - Commence towing if desired to equalize hawser strain.
  - Place moored Tanker's engines on short notice of 10 minutes or less.
  - Monitor hawser strain readings (33 tons high alarm and 65 tons high-high alarm).

#### Sever Weather Alert

The Port will be under a Severe Weather Alert whenever:

- Sustained average winds are 40 knots. Actions to be considered:
  - Commence towing if desired to equalize hawsers strain.
  - Engines on standby – engine room manned. Radar & Steering Systems running.
  - Monitor hawser strain readings. (33 tons high alarm and 65 tons high-high alarm).
  - Stop loading. Close the manifold valves.
  - Departing the buoy if hoses and hawsers can be safely disconnected.
  - Additional Crew available on deck.
  - Call out Mooring Master or Assistant Mooring Master.

#### Departing the SPM Moorings - Weather Limits & Conditions

When the present weather or sea conditions are above operational limits or forecasted to trend up beyond operational limits, or when the Tanker is unable to maintain its position behind the SPM the Tanker will make preparations to depart the SPM. The operations limits for departing the SPM are:

- Sustained wind > 40
- Knots Seas/Swell > 14 ft
- SPM Hawser Strain Gauge Monitor System is indicating repetitive upper limit high strain alarm condition.
- The mooring hawsers' motion is cycling up and down violently in a snapping motion subjecting the core of the hawser to heat buildup.

## Appendix O: El Segundo Marine Terminal, CA – San Pedro Vapor Barge

El Segundo Marine Terminal, CA - Vapor processing by 3<sup>rd</sup> party barge - San Pedro

San Pedro Vapor Barge

- **General**
  - **Vessel Name** : SAN PEDRO
  - **Operator** : FOSS MARITIME-PACIFIC SOUTHWEST
  - **Ships Type (ICST)** : Liquid Tank Barge (Other)
  - **Vessel Type** : Other Liquid Cargo Barge Not Elsewhere Included
  - **Construction** : Steel
- **Engine**
- **Location**
  - **City** : LONG BEACH
  - **STATE** : CA
- **Capacity**
  - **Net Tonnage** : 1048
  - **Full Load Capacity** : 2500 Short ton
- **Size**
  - **Register length** : 186 Feet
  - **Regular Breadth** : 46 Feet
  - **Overall Length** : 186 Feet
  - **Overall Breadt** : 46 Feet
  - **Load draft** : 15 Feet
  - **Light Draft** : 3 Feet
  - **Height** : 62 Feet
- **Other**
  - **Year** : 1981
  - **EQUIP2** : PUMP; BOOM
  - **EQUIP1** : DIESEL DEEP WELL
  - **Coast Guard Number** : 631605

The tank barge SAN PEDRO is a one of a kind third party vapor processing barge used at Chevron El Segundo marine terminal. The barge uses a cartridge-based system to process emission from other barges and small tankers loading at El Segundo. The San Pedro with limited canister capacity, moors alongside the loading tanker or barge and can process vapor emissions at a maximum of 15,000 bph. Mooring alongside requires favorable weather conditions and a conventional mooring system. The stationary mooring allows the barge to be made-fast alongside the tanker or barge with lines and fenders.

The terminal manual states that "Vapor lines should be drained hourly during loading operations." The draining is to address liquid condensation drop-out that will occur in the vapor hoses and pipelines between the cargo tanks and the San Pedro. A build-up of liquid in the vapor pipelines or vapor hose will cause a spike in the Tankers cargo tank pressure as the liquid forms slugs that reduces or stops the flow of vapors. Tankers must purge hydrocarbon vapors from their cargo tanks prior to arrival at El Segundo so that the VOC emissions can be processed by the San Pedro. In 2007 a deck hand, Piper Cameron, was killed on the tug boat handling the San Pedro when a line shifted and pinned the deckhand.

Barge vapor emission processing, like the San Pedro, is not possible at the Texas GulfLink Deepwater Port for the following reasons:

VLCCs coming from the GOLA lightering area to the Texas GulfLink Deepwater Port will not have the time to purge all their cargo tanks of hydrocarbons. Purging of all the cargo tanks on a VLCC to remove hydrocarbons below 2 % can take upward of two days. VLCCs discharging their cargoes at lightering will be prime candidates to back load US export crude oil at the Texas GulfLink Deepwater Port. The lightering area is only a few hours away. A requirement at El Segundo when using the San Pedro to capture and process vapor emissions is purging the hydrocarbons from the tanks before arrival. At the discharge port or lightering area a Tanker is required to conduct Crude Oil Washing by MARPOL regulations. Twenty-five percent of the cargo tanks must be wash at a minimum at each discharge. Some charterers require all tanks to be washed at the discharge to reduce ROB volumes. When the tanker crude oil washes the tanks, cargo oil is used to wash the tanks by fixed machines mounted in the tanks. This process generates VOCs and hydrocarbon vapors in the tank space to elevated levels.

The SPM is not a stationary mooring but weathervanes around the SPM. The Tanker will align itself with the combination of the forces of the wind and seas. At times, this will not be in the same direction of the wind or sea individually. The Tankers maximum draft will be 78 feet and the barges will be 15 feet. The current force in the water column will be acting differently on each hull. The Tanker may be aligned with a deep current in one direction and the barge with the surface current in another direction. The same holds true for the wind. The Tankers side shell sail area is massive compared to that of the barge and will react differently in the wind. A stationary mooring does not have these issues and is required to safely moor a barge alongside.

The required hourly draining of the vapor lines is not possible with the 985 ft floating hose string as required. Drain fittings or drop-legs are not possible to install on floating cargo hoses. Floating vapor hoses are subject to constant motion from the seas. The vapor hose string will run parallel to the cargo hose strings. The three hoses will be constantly contacting and rubbing against each other as a result of the sea motion. Any attempt to install a fitting projecting outward from the hose would be

quickly damaged as the three-hose strings interact. Any drain fitting could damage the integrity of the vapor hose as it is broken off from contact. The only other method to drain the liquid condensation from the vapor hose would require the hose to be disconnected, lowered onto to a support boat and pumped out by portable means. It is not feasible to stop the loading operations hourly, disconnect and drain the vapor hose, then reconnect it. The required hourly draining in the El Segundo Terminal manual would be impossible to meet.

Weather operational limits at the Texas GulfLink Deepwater Port exceed the operational limits of a barge. Mooring operational limits are 9 ft seas and 30 knots of wind, well beyond that of a barge. The maximum loading rate will be 85,000 bph at the Texas GulfLink Deepwater Port. The San Pedro's vapor processing capacity is 15,000 bph. This is about 18% of the capacity required to load at the 85,000 bph rate. The canister-based vapor processing system would require the barge to shut down and change out the canisters numerous times for a single VLCC load. Canister type vapor emission processing system have a limited amount of processing volume for each canister. Canister type systems are typically limited to Tankers under 50,000 DWT. A typical VLCC loading at the Texas GulfLink Deepwater Port would have 320,000 DWT or 6 times the size of a Tanker using a canister-based vapor processing system.